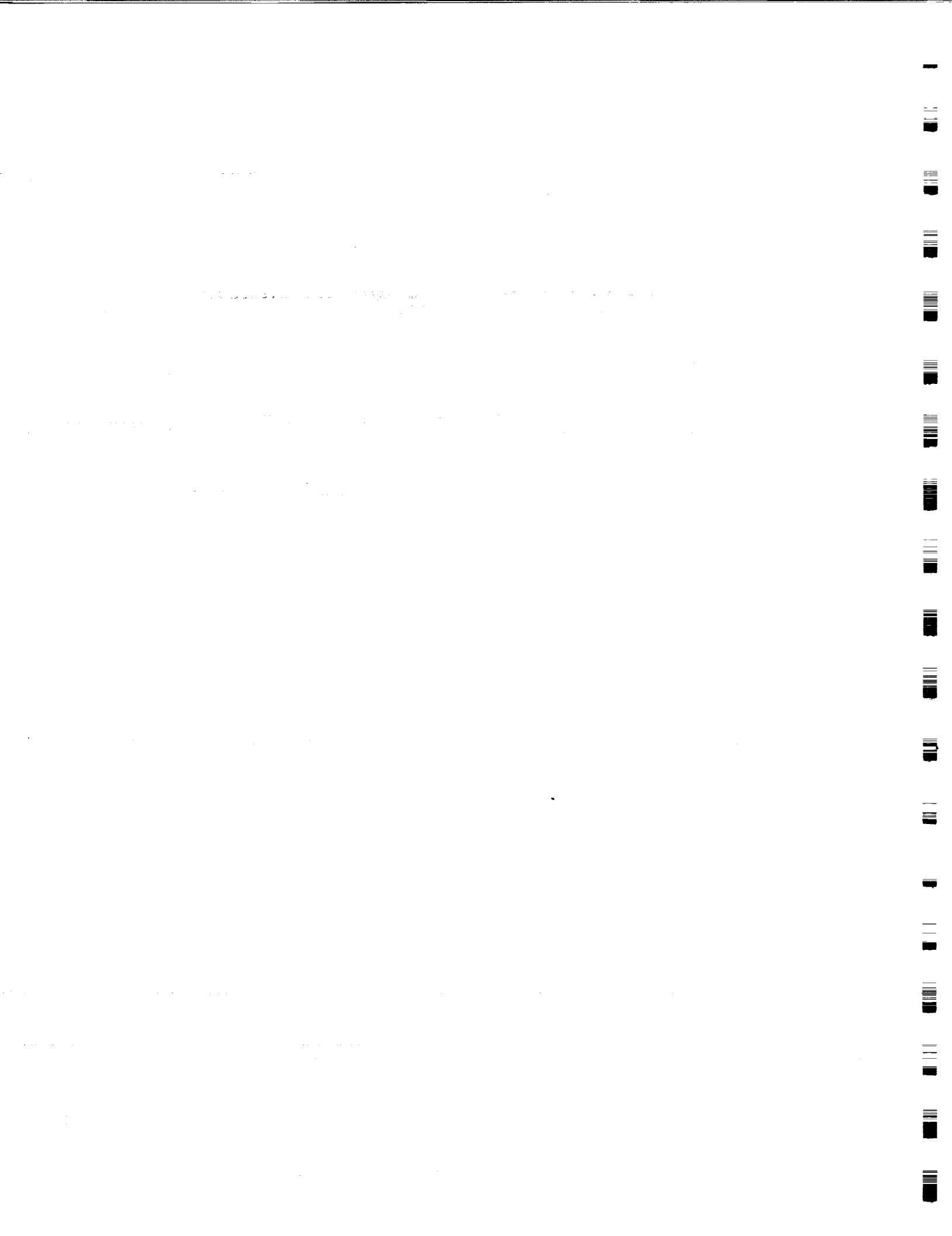


**Three Corner Sat Communications
System**

by

Bobby Anderson and Stephen Horan

NMSU-ECE-00-009



Three Corner Sat Communications System

Bobby Anderson and Stephen Horan

*Manuel Lujan Space Tele-Engineering Program
New Mexico State University
Las Cruces, NM*

Prepared for

NASA Goddard Space Flight Center
Greenbelt, MD

United States Air Force
Air Force Office of Sponsored Research

under Grant NAG5-7520

Grant F49620-99-1-0194

Universities Space Research Association
Grant F29601-98-D-0210

June 8, 2000



**Klipsch School of Electrical and Computer Engineering
New Mexico State University
Box 30001, MSC 3-O
Las Cruces, NM 88003-8001**



THREE CORNER SAT COMMUNICATIONS SYSTEM

BY

BOBBY ANDERSON, B.S.E.E.

A Thesis submitted to the Graduate School

In partial fulfillment of the requirements

for the degree

Master of Science in

Electrical Engineering

New Mexico State University

Las Cruces, New Mexico

July 2000

“Three Corner Sat Communications System,” a thesis prepared by Bobby Anderson in partial fulfillment of the requirements for the degree, Master of Science, has been approved and accepted by the following:

Timothy J. Pettibone
Dean of the Graduate School

Stephen Horan
Chair of the Examining Committee

Date

Committee in charge:

Dr. Stephen Horan, Chair

Dr. Russell P. Jedlicka

Dr. Timothy J. Pettibone

VITA

- ██████████ Born at ██████████
- 1993 Graduated from Kirtland Central High School, Kirtland, New Mexico
- 1998 B.S. from New Mexico State University, Las Cruces, New Mexico
- 1998-2000 Research Assistant, Klipsch Department of Electrical and Computer Engineering, New Mexico State University, Las Cruces, New Mexico

PUBLICATIONS

Anderson, B. and Horan, S., "Three Corner Sat Constellation – New Mexico State University: Communications, LEO Telecommunications Services, Intersatellite Communications, and Ground Stations and Network," SSC99-VI-7, 13th Annual AIAA/USU Conference on Small Satellites, August 1999.

ABSTRACT

THREE CORNER SAT COMMUNICATIONS SYSTEM

BY

BOBBY ANDERSON, B.S.E.E.

Master of Science in

Electrical Engineering

New Mexico State University

Las Cruces, New Mexico, 2000

Dr. Stephen Horan, Chair

Three Corner Satellite is a constellation of three nanosatellites designed and built by students. New Mexico State University has taken on the design of the communications system for this constellation. The system includes the forward link, return link, and the crosslink. Due to size, mass, power, and financial constraints, we must design a small, light, power efficient, and inexpensive communications system. This thesis presents the design of a radio system to accomplish the data transmission requirements in light of the system constraints. In addition to the hardware design,

the operational commands needed by the satellite's on-board computer to control and communicate with the communications hardware will be presented.

In order for the hardware to communicate with the ground stations, we will examine the link budgets derived from the radiated power of the transmitters, link distance, data modulation, and data rate for each link. The antenna design for the constellation is analyzed using software and testing the physical antennas on a model satellite. After the analysis and testing, a combination of different systems will meet and exceed the requirements and constraints of the Three Corner Satellite constellation.

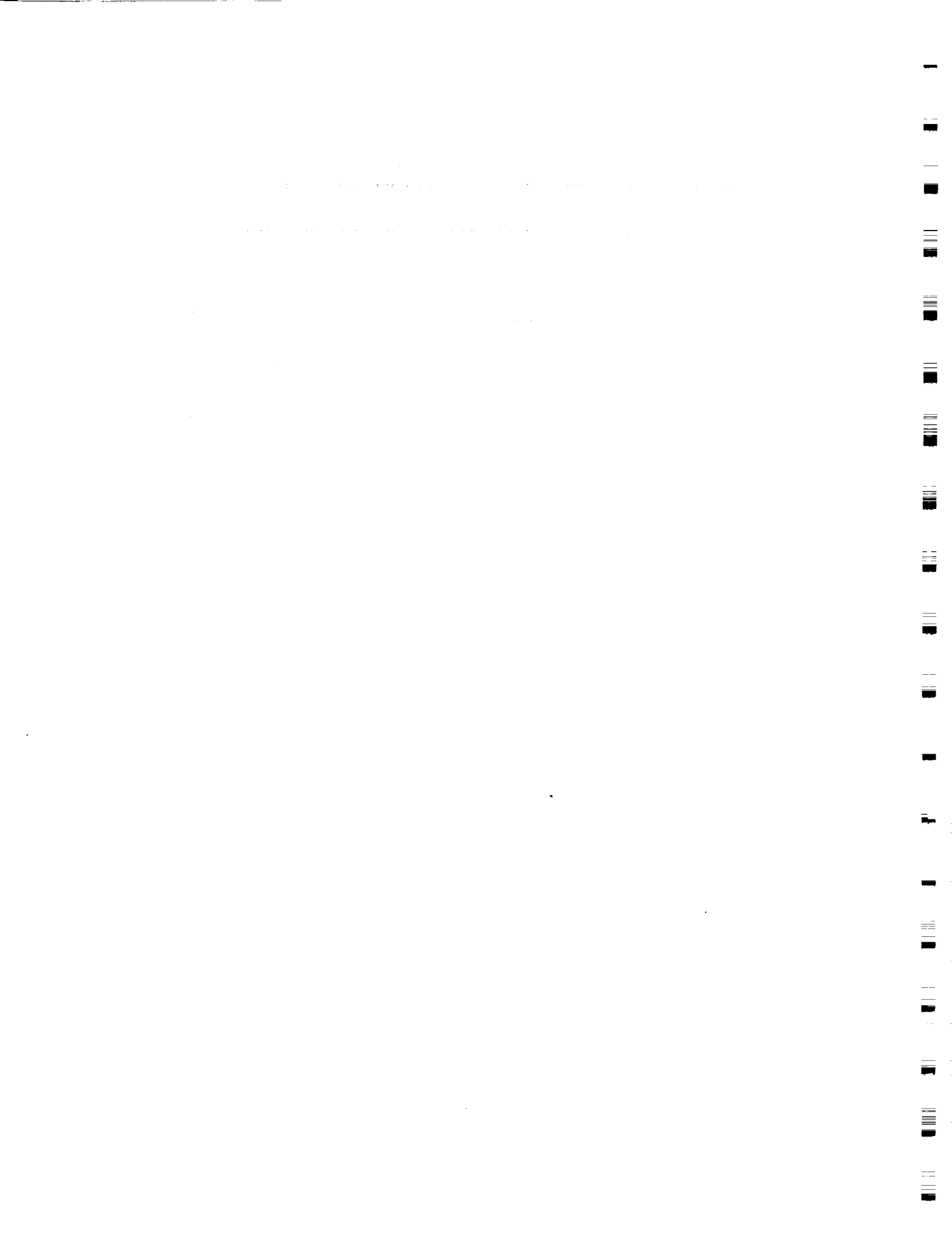


TABLE OF CONTENTS

LIST OF TABLES	x
LIST OF FIGURES	xi
LIST OF ACRONYMS	xiii
1 INTRODUCTION	1
1.1 Overview	1
1.2 Three Corner Sat Genesis	1
1.3 Science Objectives	3
1.4 Technology Objectives	3
1.4.1 Formation Flying	3
1.4.2 End-to-End Data System (EEDS)	4
1.4.3 Micropropulsion System	6
1.5 Thesis Outline	6
2 OPTIONS FOR VHF/UHF COMMUNICATION HARDWARE	8
2.1 Overview	8
2.2 Design Requirements	8
2.2.1 Power Requirements	8
2.2.2 Data Rate	10
2.2.3 Frequency Selection	10
2.2.4 Modulation Selection	11
2.2.5 Antenna Design	11
2.2.6 Size and Mass	12

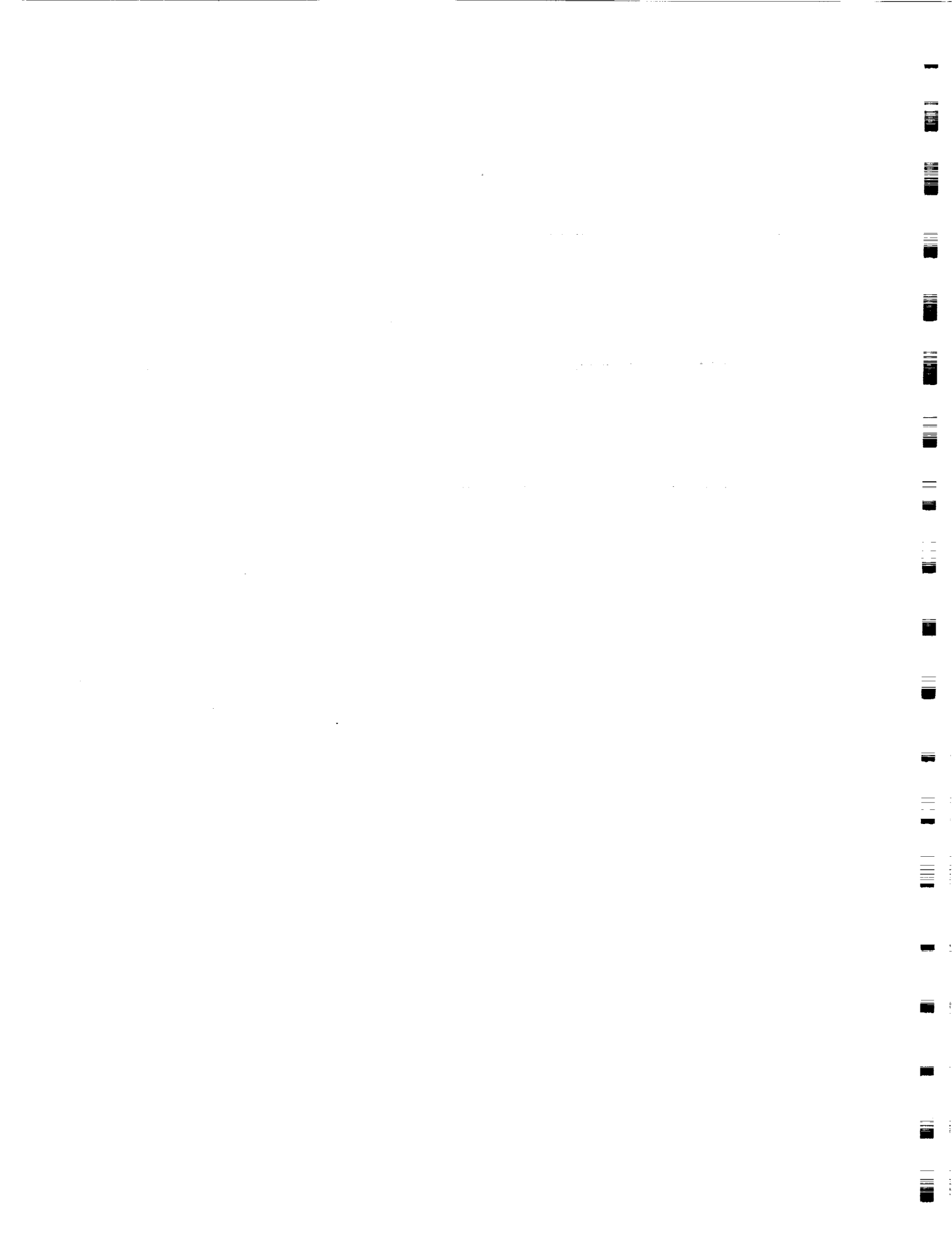
	2.2.7	Financial Budget	12
	2.2.8	Complexity Issues	12
	2.2.9	Versatility	13
	2.3	Transceiver Selection	13
	2.4	System Operation and Basic System Design	15
	2.5	Link Budget Analysis	15
	2.6	Summary	19
3		TESTING OF THE TH-D7A	23
	3.1	Overview	23
	3.2	Initial Testing Using Software Provided by Kenwood	23
	3.3	Testing Using Hyper Terminal	25
	3.4	Testing of Handset Using LabVIEW	27
	3.5	Modify the Handset to Increase Data Rate	34
	3.6	Final LabVIEW Simulation	35
	3.7	Consumed Power in Different Modes	39
	3.8	Summary	42
4		ANTENNA DESIGN	43
	4.1	Overview	43
	4.2	Design Requirements	43
		4.2.1 Antenna Impedance Matching	43
		4.2.2 Length	43
		4.2.3 Gain	44
	4.3	Field Patterns	45

4.4	Input Impedance	52
4.5	Connecting the Antennas to the TH-D7A	59
4.5.1	Duplexer	59
4.5.2	Frequency Selective Tee	60
4.5.3	Modification to Handset	63
4.6	Summary	64
5	MODIFICATIONS TO KENWOOD TH-D7A	66
5.1	Overview	66
5.2	Modification for Dual Antenna Configuration	66
5.3	Streaming Data into the Handset	69
5.4	Operation of Handset Outside of Amateur Frequencies	70
5.5	Future Modifications	71
6	S-BAND COMMUNICATIONS SYSTEM	72
6.1	Overview	72
6.2	Design Requirements	72
6.3	Link Budget Analysis	73
6.4	Modem Selection	76
6.5	S-band Antenna	76
6.6	Summary	81
7	CONCLUSION	82
7.1	Summary	82
7.2	Recommended Design	82

APPENDICES	85
A. LABVIEW VIRTUAL INSTRUMENTS	86
B. DERIVATION OF FIELD EQUATIONS	95
C. VHF/UHF ANTENNA DESIGN AND ANALYSIS	98
D. S-BAND ANTENNA DESIGN AND ANALYSIS.	110
REFERENCES	123

LIST OF TABLES

1	Components of an Individual Nanosatellite	2
2	Forward Link Budget	20
3	Return Link Budget	21
4	Crosslink Link Budget	22
5	Commands for Handset	29
6	Example of Overwriting the Buffer on the Handset	32
7	Power Consumption Calculations of the Handset	40
8	Real Part of the Input Impedance for the VHF Antenna	53
9	Impedance and VSWR Measurements of the VHF antenna	57
10	Impedance and VSWR Measurements of the UHF antenna	58
11	Simulated Results of the Frequency Selective Tee for Best Isolation	62
12	Simulated Results of the Frequency Selective Tee for Best VSWR	62
13	S-band Return Link Budget	75



LIST OF FIGURES

1	Physical Appearance of Individual Satellite and the Stack of Satellites	2
2	Overview of the Constellation	5
3	Basic Forward/Return Link with One Ground Station and One Satellite	16
4	Basic Crosslink Communications Between Satellites	16
5	Basic Kenwood TH-D7A Software	24
6	LabVIEW Control Panel for Handset	28
7	Handset and Packaging Delays	33
8	LabVIEW Control Panel	35
9	Antenna Interference with the Camera's Field of View	44
10	Linear Field Patterns for the VHF and UHF Antennas	49
11	Power Patterns (10 dB/division) for the VHF and UHF Antennas	49
12	Field and Power Patterns (10 dB/division) of the VHF Antenna Operating at 144.39 MHz	51
13	Nanosatellite Model with Tuned Antennas	55
14	Feed to the Antenna	57
15	Duplexer	59
16	Frequency Selective Tee	61
17	Modification to Handset in order to Connect Two Antennas	65
18	Modification to Handset in order to Connect Two Antennas	67
19	Kenwood TH-D7A After Antenna Modification	68
20	Bypass of the TNC and RSSI Modifications	70

21	Dimensions of Patch Antenna	77
22	Amplitude and Phase Split of the Patch as a Function of Frequency	78
23	VSWR of Antenna Connecting to a 50-ohm Line	79
24	Component Power Patterns (10 dB/division) in the $\Phi=\pi/2$ Plane	80
25	Recommended Communications System	84
A1	LabVIEW Control Panel	86
A2	Control Panel VI	86
A3	Operation VI Calling Transmit VI	87
A4	Operation VI Calling Stdby_Rx VI	87
A5	Stdby_Rx VI Prompting User to Select the Receive File	88
A6	Stdby_Rx VI Turns ON the TNC on the Handset	88
A7	Stdby_Rx VI Allowing TNC to Turn ON	89
A8	Stdby_Rx VI Prompting User to Enter TNC File	89
A9	Stdby_Rx VI Prompts User to Enter the Standby File	90
A10	Tx VI Prompting User to Enter Return File	90
A11	Tx VI Turns ON the TNC in the Handset	91
A12	Tx VI Allows the TNC to Turn On	91
A13	Tx VI Prompts User to Enter TNC File	92
A14	Tx VI Places the Handset in Converse Mode	92
A15	Tx VI Calls the ModeSelect3 VI	93
A16	ModeSelect3 VI Sends a Full Packet and Creates a Delay	93
A17	ModeSelect3 VI Sends the Remaining Portion of the File	94
A18	ModeSelect3 VI Turns OFF the TNC.	94

LIST OF ACRONYMS

A	amperes
AFOSR	Air Force Office of Scientific Research
AMSAT	Amateur Satellite
APRS	Automatic Position Reporting System
ASU	Arizona State University
BER	bit-error rate
BFSK	Binary Frequency Shift Keying
bps	bits per second
BT	Bandwidth Data Period Product
COTS	Commercial Off the Shelf
CP	Circularly Polarized
CU	Colorado University
DARPA	Defense Advanced Research Projects Agency
dB	decibels
EEDS	End-to-End Data System
EIRP	Effective Isotropically Radiated Power
EPS	Electrical Power System
FM	Frequency Modulation
GMSK	Gaussian Minimum Shift Keying
GPS	Global Positioning System
HPF	High Pass Filter

HT	Handi Talkie
LEO	Low Earth Orbit
LPF	Low Pass Filter
m	meters
MEMS	Micro-Electro-Mechanical Systems
MHz	Mega Hertz
mW	milliwatts
NASA	National Aeronautics and Space Administration
NMSU	New Mexico State University
PCB	Printed Circuit Board
PTT	Push-To-Talk
RF	Radio Frequency
RSSI	Receive Signal Strength Indicator
SMS	Short Message Service
SNR	Signal to Noise Ratio
3CS	Three Corner Sat
TNC	Terminal Node Controller
UHF	Ultra High Frequency
V	volts
VHF	Very High Frequency
VI	Virtual Instrument
VSWR	Voltage Wave Standing Ratio
W	watts

1 INTRODUCTION

1.1 Overview

In this chapter, we will discuss the origin of the Three Corner Sat constellation and the science objectives. After understanding the goals of Three Corner Sat, we will give a brief description of the major subsystems under the technology objectives section. We will then outline the remaining topics of the thesis, which include the communications hardware selection, the antenna design, and an overall recommended system design.

1.2 Three Corner Sat Genesis

In 1998, Arizona State University (ASU), University of Colorado at Boulder (CU), and New Mexico State University (NMSU) proposed to the Air Force Office of Scientific Research/Defense Advanced Research Projects Agency (AFOSR/DARPA) University Nanosatellite Program. The proposal was for the three schools to build a constellation of three identical satellites, which is named Three Corner Sat (3CS). The goal of 3CS will be to demonstrate stereo imaging, formation flying, and innovative command and data handling [1]. Although the details have changed as we actually designed the satellite and learned more about how the constellation would be launched, the basic configuration has remained the same. The components of an individual 3CS nanosatellite are shown in Table 1. The physical appearance of an individual satellite and the stack of the satellites are shown in Figure 1.

Table 1. Components of an Individual Nanosatellite

Primary exterior components:	Primary interior components:
1. VHF/UHF and Patch Antennas	1. Attitude Control System
2. Star Mapper	2. EEDS Electronics
3. Micropropulsion System	3. Power Control Board
4. Light-band Separation System	4. Communications System
5. GPS Patch Antenna	5. GPS Receiver
6. GaAs Body Mounted Solar Array	6. Paraffin Actuated Pin-Pullers
7. Hard Mounting Points	7. Structural Supports, Tubes and Panels
8. Passive and Active Pointing Cameras	8. Camera Boards and Micro Controllers

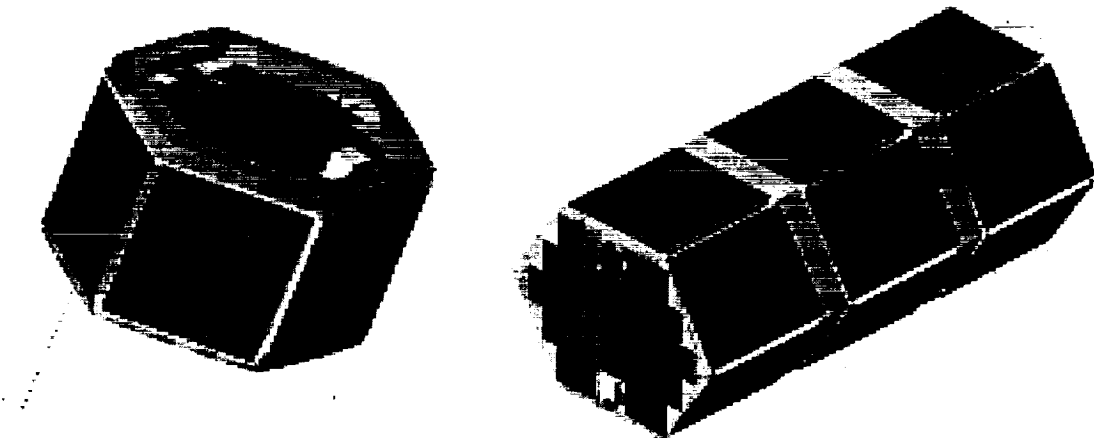


Figure 1. Physical Appearance of Individual Satellite and the Stack of Satellites

1.3 Science Objectives

The primary science objective of 3CS is to deliver highly dynamic (< 1 minute), small (< 250 meter), stereo image scenes. These scenes include deep convective towers, atmospheric waves, and sand/dust storms. The stereo images allow for the computation of range data to within 250 meters yielding accurate data regarding the height, shape, and thickness of the observed phenomena. The advantages of stereo imaging from space over conventional imaging is the ability to derive range data. The range data is significantly more accurate and can cover a much greater area. Three-dimensional images and depth maps can be created by the triangulation of the range data [2].

1.4 Technology Objectives

1.4.1 Formation Flying

In order for the science objective to be accomplished, virtual formation flying must be implemented. A virtual formation is the cooperative effort between satellites operating as a network allowing for targeting and data acquisition. The results are transmitted to the ground segment from the satellites via communications links without the need for strict physical proximity of the satellites. These links carry the command and control data necessary to accomplish the science mission regardless of the physical location of the satellites. The locations of the satellites need to be known to the ground controllers for each in order to support its portion of the mission.

For each nanosatellite's location to be known, each spacecraft will need an on-board GPS.

For stereo imaging to be accomplished, the required nominal spacing between the satellites is 20-150 kilometers. The originally proposed method of completing this link was to utilize a commercial communications satellite network in Low Earth Orbit (LEO). This would allow the 3CS satellites to communicate with one another and the ground stations regardless of their positions relative to the ground station. This ability is very desirable, but due to bankruptcy of available LEO commercial communications networks, it may not be an option for 3CS. If 3CS can find a LEO commercial network able to provide the needed cellular communications link, the system would be configured as illustrated in Figure 2 [1]. In this thesis, we will develop an alternative technique using radio communications.

1.4.2 End-to-End Data System (EEDS)

The End-to-End Data System (EEDS) is a fairly complex system allowing for simple user operations to be accomplished. This system supports the constellation of satellites and the three ground operations centers. It includes hardware, firmware, operating systems, software, applications, databases, algorithms, procedures, and user interfaces. EEDS not only aids in the mission operations, it also supports integration and test operations. The flight hardware on each satellite has three major components: the on-board computer (a 386 microprocessor with RAM and ROM), a critical decoder for command processing, and additional memory for storing data.

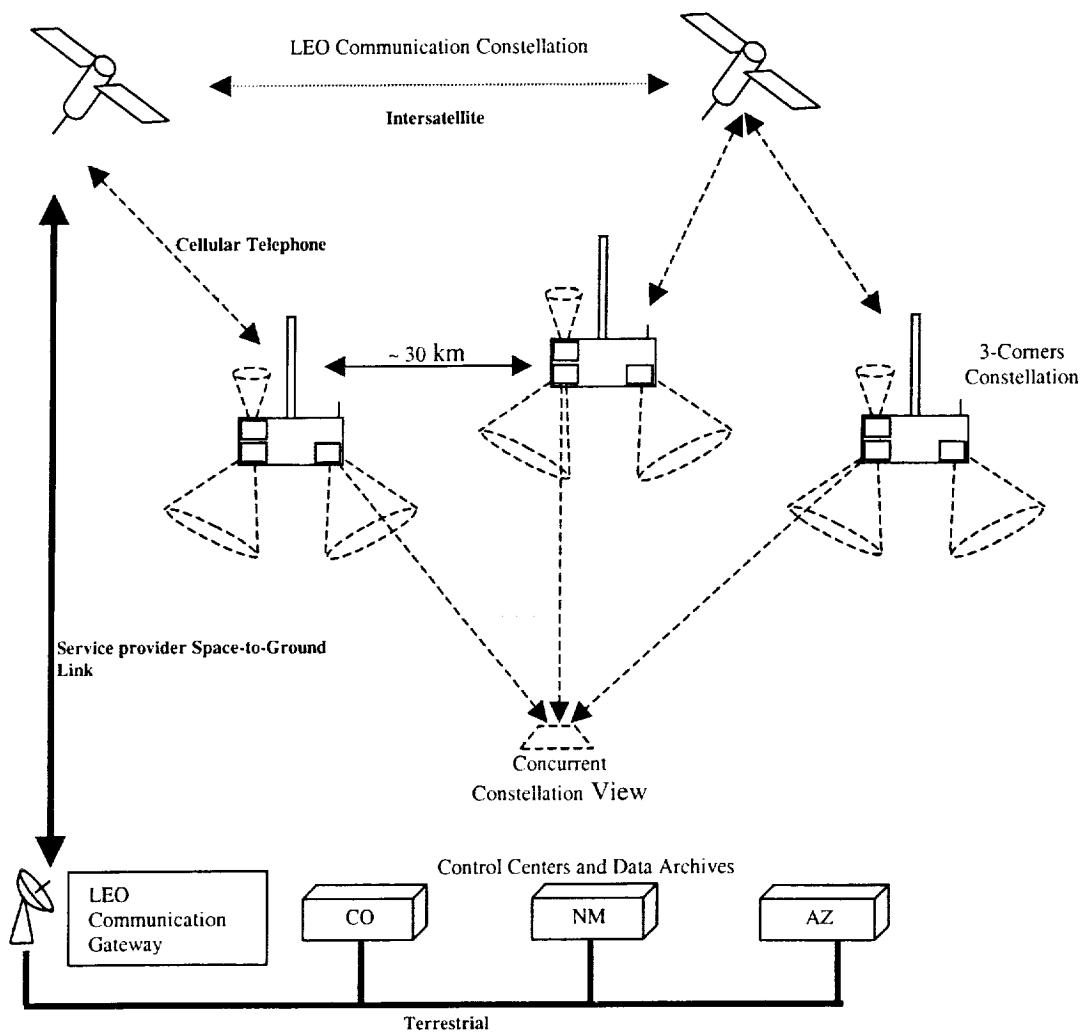


Figure 2. Overview of the Constellation

The constellation can be managed and controlled by a processor on any of the three satellites. The selected processor will be responsible for supervising the operation of the constellation, managing their resources, and initializing and distributing the commands that monitor each satellite and create the science data [2].

1.4.3 Micropropulsion System

The micropropulsion system designed by ASU offers a variety of mission options. These options may allow 3CS to maintain attitude control, orbital drag make-up, altitude raising, and de-orbit of the constellation. This system is designed to be very safe. Most propulsion systems use a gas to create thrust. The storage of the gas must be contained in a pressure vessel, which may be considered a hazard to the organization performing the launch of the satellite. 3CS's micropropulsion system utilizes the gas generated by the sublimation of ice resulting in a low-pressure system. The gas is then heated by a MEMS heater, which allows for additional thrust [3].

1.5 Thesis Outline

In this thesis, we will investigate design options and provide supporting analysis for the development of a radio communications system for the 3CS. This system will provide the command and telemetry links that were to have been accomplished using cellular telephone links. This system will also need to support inter-satellite communications through a crosslink.

Chapter 2 will cover the options for the VHF/UHF communication hardware. We will examine system constraints based on power requirements, data rate, size, mass, versatility, cost, and complexity. After analyzing the design requirements, we will select a transceiver and then verify its suitability based on its operational parameters. In Chapter 3, we will discuss the testing of the transceiver using

software. This will allow us to simulate the on-board CPU operations of each 3CS satellite. We will also discuss operational limitations discovered with the transceiver and how they will be overcome.

Chapter 4 will analyze the design for the VHF/UHF antenna system. This chapter will include the different antenna configurations considered in the design. We will also discuss the antenna design based upon a physical mock-up of the satellite. Chapter 5 discusses the modifications to the transceiver to meet our requirements. This includes the transceiver modifications that allow it to operate outside the amateur bands and provide transmitter/receiver isolation.

Chapter 6 discusses the initial design for the S-band system. This system will allow 3CS to operate at a higher data rate. Chapter 7 concludes the thesis with a summary of the previous chapters and a final recommended system configuration.

1. The first part of the document is a list of names.

2. The second part of the document is a list of names.

3. The third part of the document is a list of names.

4. The fourth part of the document is a list of names.



2 OPTIONS FOR VHF/UHF COMMUNICATION HARDWARE

2.1 Overview

This chapter discusses the major design requirements of the VHF/UHF communications system. The major constraints are power limitations, data rate, complexity, versatility, size, mass, and cost. After identifying the design requirements, we will select a transceiver. We will then analyze the transceiver and the requirements formulating the basic system design.

2.2 Design Requirements

2.2.1 Power Requirements

There are many design requirements that the overall communications hardware must abide by and fulfill. The most limiting constraint of the communications system is the maximum power consumption permitted. The Electrical Power System (EPS) of each satellite will be able to provide approximately 9 watts of continuous power. The overall EPS power budget allots 5 watts of continuous power to the communications system during a communications cycle. Since other subsystems require power at different times, the communications system design must be able to minimize the amount of stand-by power consumed. This implies that three operational modes are required in the communications system:

1. A low-power, stand-by mode where the minimal power consumption occurs and the receiver is ready to receive data.

2. A receive data mode where the receiver is active but the power draw is not much greater than the stand-by mode.
3. Transmit mode where data transmission occurs while the overall power constraint is not violated.

Another design constraint is the operational voltage of the communications system. Initially, a regulated 5 V bus is supplied by the EPS; therefore, the communications system must be fully operational with a 5 V input and consume no more than 5 W. There are many companies able to provide communications equipment capable of operating on a 12 to 15 volt bus. If the equipment requires this voltage, then a DC-DC conversion is required. Since a DC-DC converter is approximately 80-90 percent efficient at best, this may not be a viable option in this power-limited setting. The DC-DC conversion circuitry may be affected by temperature extremes resulting in poor efficiency. For example, if the DC-DC conversion is 80% efficient, then the power available to the communications system after the conversion will be 4 watts. The loss of 1 W would virtually guarantee we would not be able to close the communications link. Based upon these considerations, the 3CS team will try to find a Commercial Off The Shelf (COTS) communications system that is fully operational on a 5 V bus and consume no more than 5 W.

2.2.2 Data Rate

Another design requirement is finding a COTS communications system able to send and receive data at a rate that can support command and telemetry communications. To minimize the hardware on the spacecraft, 3CS will attempt to use a single transceiver for the forward link, return link, and crosslink. The minimum data rates for the crosslink, forward link, and return link communications are specified to be 1200, 1200 and 9600 bits per second (bps) respectively. In order to use the same transceiver for all the links, the data rate must be selectable or we may decide that a higher data rate is acceptable for the crosslink. The higher data rate for the crosslink is not necessary considering the amount of data that will actually be sent using this link. However, it is acceptable considering the minimal amount of hardware is used for all links. For mission success, eight megabytes of data per day must be sent from the 3CS satellites. This amount of data will require a high rate communication system on each of the 3CS satellites. In addition to the VHF/UHF system based on preliminary analysis, an S-band system will be needed for this task.

2.2.3 Frequency Selection

3CS needs the transceiver to operate in three different modes. These modes are the forward link, return link, and the crosslink. The forward link will need to operate at 450 MHz. This band is authorized for transmitting commands to satellites. The return link will need to operate in the 137-138 MHz band. This authorization is to relay meteorological data from satellites [4]. These particular frequencies for the

forward and return links were requested because each university already has ground station equipment capable of operating at these frequencies. There are several options for the crosslink frequency. The first option is the nominal Automatic Position Reporting System (APRS) frequency at 144.39 MHz. This would allow 3CS to conduct an experiment using this amateur radio protocol that allows the satellites to send their position and small amounts of data to one another. We may need to operate the crosslink at a higher frequency due to congestion at 144.39 MHz. This frequency is currently being coordinated through the Amateur Satellite (AMSAT) Corporation frequency coordinator.

2.2.4 Modulation Selection

In order to use the existing university ground station modem equipment, the 3CS team would like to use Binary Frequency Shift Keying (BFSK). In order to communicate with the ground stations, the transceivers on the satellites must be able to use BFSK modems and transmit the data using FM.

2.2.5 Antenna Design

Another reason for choosing 137-138 MHz for the return link and 450 MHz for the forward link is that the antennas are reasonably sized. These antennas will not obstruct the field of view of the camera. The most likely candidates are quarter-wavelength antennas.

2.2.6 Size and Mass

The physical dimensions and mass of the transceiver are design constraints. Since the internal volume of each satellite is limited, 3CS must take physical dimensions into consideration. To meet the size constraints, we must find a transceiver that requires a minimal volume. The constellation has total mass limitations based upon agreements with National Aeronautics and Space Administration for shuttle launch. Therefore the communications subsystem must be as light as possible to fit within the overall mass budget for the constellation. At the moment, we do not have specific mass limitations for the communications system.

2.2.7 Financial Budget

Cost is always an issue when designing any system. The communications system must cost less than \$10,000 for each satellite. This budget includes the hardware for the VHF/UHF transceiver, S-band transceiver, modem(s), cellular phones (if used), and antennas. Since 3CS has contracted a vendor to build the S-band transceiver, which will cost approximately \$5000-\$7000, the VHF/UHF transceiver, modem(s), and antennas will have to be designed or bought at cost of less than \$3000.

2.2.8 Complexity Issues

Simplicity of the VHF/UHF transceiver is always a benefit. 3CS operators would like to be able to control the amount of radiated power, data rate, and operation

mode of the transceiver. Since we will not be able to move switches or push buttons physically, we require a transceiver that is controllable via software. We would like the transceiver interface to be a RS232 interface to allow standard protocols and drivers to be implemented in the on-board computer system.

The communications hardware must be rugged in order to survive the shuttle launch and extreme space environment. The communications subsystem will be integrated into the each satellite and then undergo fairly rigorous testing, including shock and vibration tests.

2.2.9 Versatility

3CS would like the VHF/UHF transceiver to be used for crosslink communications. Crosslink communications will transfer very small amounts of data, about 45 characters. This information contains GPS data and some health/status data. Since small amounts of data are being sent, 3CS can lower the data rate and would like to pursue a unique method of sending this data. The cellular phones have the capability to send short messages to other cellular phones using a Short Message Service (SMS). Due to the lack of commercial service providers to accomplish this task, 3CS is looking for a transceiver with similar capabilities.

2.3 Transceiver Selection

Based upon the design requirements stated in Section 2.1, the 3CS team chose the Kenwood TH-D7A transceiver. This transceiver has many attractive features that

exactly fit the needs of the constellation. At the time of selection, it was the only commercially available unit having VHF and UHF capabilities, computer interfacing via RS232, standard GPS interfacing, a built-in modem, and built-in APRS messaging capabilities. Additionally, it met the power system goals. The 3CS team applied for frequency allocation in the following bands: 137-138 MHz for the return link, 450 MHz for the forward link, 144.39 MHz or slightly higher for the crosslink, 2200-2290 MHz for the S-band return link, and 2025-2110 MHz for the S-band forward link. The TH-D7A can be modified to operate in the 137-138 and 450 MHz bands and already operates at 144.39 MHz.

The main advantage of the TH-D7A is the built-in support to send data. This particular transceiver has a built-in TNC (terminal node controller) enabling data communications using the AX.25 protocol. This particular protocol, when used with a computer, allows for packet operation. The packets will contain headers as well as the data being sent.

Another useful feature of the TH-D7A is its ability to transmit data at different power levels and data rates. There are three different output power settings: extremely low (EL), low (L), and high (H). The L power setting for the crosslink and EL power setting for the return link will be used for their respective link budgets. Available options for the data rate are 1200 or 9600 baud (bps or bits per second). The baseline design will be to use 1200 baud for the crosslink and 9600 baud for the forward and return link communications. The crosslink communications will be configured around the APRS protocol built into the TH-D7A. The APRS protocol

will allow the satellites to communicate their position and health/status data to one another. The TH-D7A must have an onboard GPS receiver connected to the transceiver in order to use the APRS feature.

2.4 System Operation and Basic System Design

Due to limited power, both the TH-D7 and the S-band system will not be able to operate simultaneously. Each satellite's on-board computer will choose which transceiver to use based on the position of the constellation in space. If 3CS is above the universities, the computer will choose to use either the TH-D7 handset or the S-band transceiver depending upon operational state. If the constellation is above an S-band ground station, the computer will use the S-band transceiver. For public outreach purposes, 3CS may choose to send APRS messages throughout an orbit in order for other amateur users to track our constellation. The forward and return link communications system design is shown in Figure 3. The basic crosslink communications system used to transmit individual satellite position and health/status information to the other satellites is shown in Figure 4.

2.5 Link Budget Analysis

In order to determine if a satellite can communicate with a ground station or another satellite, we must perform a link budget analysis. A link budget takes into account all the gains and losses in the system. It also shows how the data rate and

data modulation affect the link. To ease the calculations in the link budget, we will convert all power measurements, gains, and losses to decibels (dB).

The link budget begins with the transmitter and all of the connecting components to the antenna. The budget starts with the power generated by the transmitter and subtract the line losses between the antenna and the transmitter. The

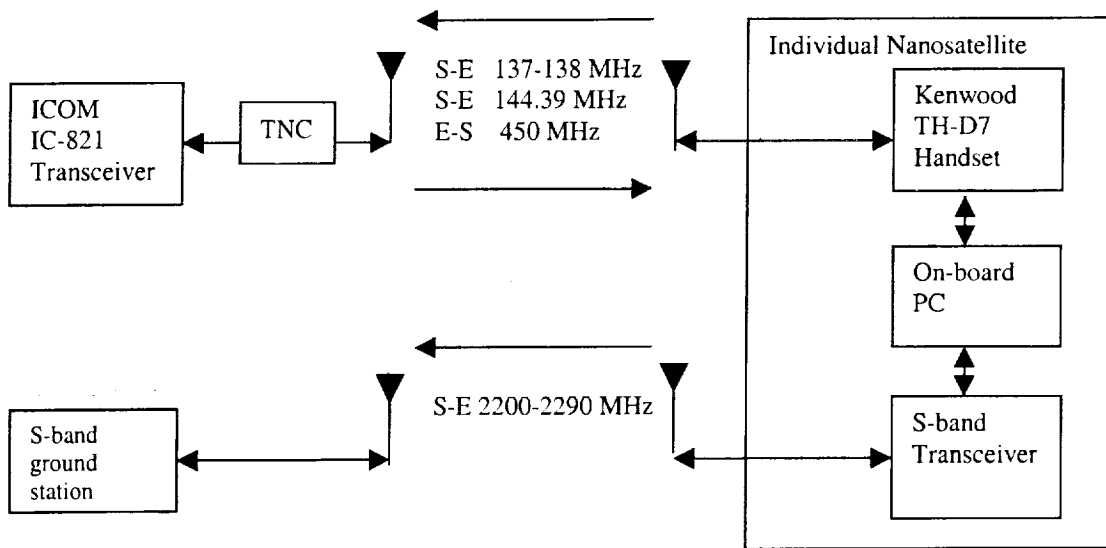


Figure 3. Basic Forward/Return Link with One Ground Station and One Satellite

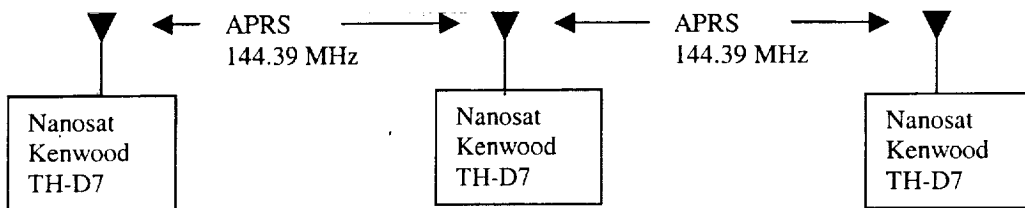


Figure 4. Basic Crosslink Communications Between Satellites

gain of the antenna minus the pointing loss and the radome loss are added to the previous result. This calculation yields the Effective Isotropically Radiated Power (EIRP) in dBm.

The next calculation is the propagation loss. This loss includes the free space loss and losses due to atmospheric absorption, and precipitation absorption. The free space loss is dependent on the wavelength of the signal and the distance between the transmit and receive antennas. The atmospheric and precipitation losses are frequency dependent.

Next, we analyze the receiver portion of the link budget. After the signal has arrived at its destination, it is gathered by the receiving antenna with an associated gain. The received signal may have a polarization mismatch causing a loss in the system. The line, radome, and pointing losses must also be taken into account. To be conservative, we will allow 1 dB of implementation loss. Adding the results of the transmitter budget, propagation losses, and receiver budget, we obtain the effective carrier power.

In any system, noise is created by internal components and background sources. The noise is parameterized by the thermal noise density, which is the noise generated by the molecular vibrations of the atmosphere and the receiver hardware. The receiver noise bandwidth is directly proportional to the data rate in bits per second. The noise figure of the receiver is calculated from the sensitivity and noise floor of the receiver. To compute the effective noise power in dBm, we add the

receive noise bandwidth in dBHz to the noise figure in dB and the thermal noise density in dBm/Hz.

Once these calculations and measurements have been made, we can summarize the results and determine the net signal margin. To calculate the available Signal-to-Noise Ratio (SNR), we subtract the effective noise power from the effective carrier power. In order to properly receive the data, we must achieve a minimal SNR depending on the modulation format. The net signal margin is the available SNR minus the required SNR and any additional implementation losses [5]. The required SNR can be estimated by analyzing standard tables or equations relating the Bit Error Probability and E_b/N_0 for FSK.

The net signal margin must be positive in order to receive the transmitted data at the desired Bit-Error Rate (BER). A common net signal margin for the link budget is at least 10 dB in the initial design stage slightly improving the BER. This allows for additional losses that were not taken into account because they were not fully known during the initial design. Also, a 10 dB net signal margin will ensure that the signal is received correctly above the required SNR. We will now analyze the different links in the nanosatellite program.

The first link budget we will analyze is the UHF forward link. This is the case when the ground station is transmitting data to the satellites. Using Table 2, we observe that the net link margin is 23.9 dB. Since this value is much greater than 10 dB, we can conclude that we will not have any problems transmitting data to the

satellites correctly. This link budget is based upon a 9600 bps data rate with a 10^{-6} BER. A reduction to 1200 bps data rate will increase the net link margin.

The next link budget is the return VHF link shown by Table 3. The return link is the transfer of data from the satellites to the ground station. This analysis shows that the net link margin is 10 dB. This margin is sufficient for the satellites to communicate with the ground station at 9600 bps with a 10^{-5} BER. Even with the link budget being slightly conservative, we must test all components of the system to ensure reliable communications.

In order for the satellites to communicate with one another, we must develop the crosslink link budget given in Table 4. The net crosslink margin is 23.4 dB at 9600 bps with a 10^{-6} BER. Again, with this margin, the satellites will have reliable communications. The link budget analysis with a 23.4 dB margin at 9600 bps, used a maximum distance of 50 kilometers. The satellites should be able to communicate with one another well beyond this distance.

2.6 Summary

We selected the Kenwood TH-D7A as the candidate VHF/UHF transceiver because it had the necessary data services and the power constraints. The link budget analysis shows that it would be possible to use it in this configuration and provide data services with the necessary quality and rates. Next we will examine the unit for ability to be controlled by the on-board computer and provide data services.

Table 2. Forward Link Budget

Forward 450 MHz Link	Value	Units
Transmitter (Tx)		
Tx Power, Pt	44.8	dBm
Tx Component Line Losses, Ltl	3.0	dB
Tx Antenna Gain (Peak), Gt	17.3	dBi
Tx Pointing Loss, Ltp	1.0	dB
Tx Radome Loss, Ltr	0.0	dB
EIRP	58.1	dBm
Propagation		
Transmission Frequency, f	450.0	MHz
Link Range, R	760.0	km
Propagation Factor, n	1.0	
Free Space Loss, Ls	143.1	dB
Atmospheric Absorption, Lpa	0.0	dB
Precipitation Absorption, Lpp	0.0	dB
Total Propagation Loss	143.1	dB
Receiver (Rx)		
Rx Antenna Gain (Peak), Gr	0.0	dBi
Rx Polarization Loss, Lrpol	1.0	dB
Rx Pointing Loss, Lrp	0.0	dB
Rx Radome Loss, Lrr	0.0	dB
Rx Component Line Losses, Lrl	1.0	dB
Rx Implementation Losses, Lri	1.0	dB
Received effective carrier power	-88.0	dBm
Noise		
Standard Thermal Noise, kT	-174.0	dBm/Hz
Rx Noise Bandwidth, W	43.0	dBHz
Rx Noise Figure, NF	5.0	dB
Effective Noise Power	-126.0	dBm
Result		
Available CNR	37.9	dB
Data Rate	39.8	dBHz
Available Eb/No	41.1	dB
Implementation Losses	3.0	dB
Required Eb/No	14.2	dB
Margin	23.9	dB

Table 3. Return Link Budget

Return 137 MHz Link	Value	Units
Transmitter (Tx)		
Tx Power, Pt	27.0	dBm
Tx Component Line Losses, Ltl	1.0	dB
Tx Antenna Gain (Peak), Gt	0.0	dB
Tx Pointing Loss, Ltp	1.0	dB
Tx Radome Loss, Ltr	0.0	dB
EIRP	25.0	dBm
Propagation		
Transmission Frequency, f	137.0	MHz
Link Range, R	770.0	km
Propagation Factor, n	1.0	
Free Space Loss, Ls	132.9	dB
Atmospheric Absorption, Lpa	0.0	dB
Precipitation Absorption, Lpp	0.0	dB
Total Propagation Loss	132.9	dB
Receiver (Rx)		
Rx Antenna Gain (Peak), Gr	15.1	dB
Rx Polarization Loss, Lrpol	3.0	dB
Rx Pointing Loss, Lrp	1.0	dB
Rx Radome Loss, Lrr	0.0	dB
Rx Component Line Losses, Lrl	3.0	dB
Rx Implementation Losses, Lri	3.0	dB
Received effective carrier power	-102.8	dBm
Noise		
Standard Thermal Noise, kT	-174.0	dBm/Hz
Rx Noise Bandwidth, W	43.0	dBHz
Rx Noise Figure, NF	5.0	dB
Effective Noise Power	-126.0	dBm
Result		
Available CNR	23.2	dB
Data Rate	39.8	dBHz
Available Eb/No	26.4	dB
Implementation Losses	3.0	dB
Required Eb/No	13.4	dB
Margin	10.0	dB

Table 4. Crosslink Link Budget

Cross Link	Value	Units
Transmitter (Tx)		
Tx Power, Pt	27.0	dBm
Tx Component Line Losses, Ltl	1.0	dB
Tx Antenna Gain (Peak), Gt	0.0	dBi
Tx Pointing Loss, Ltp	1.0	dB
Tx Radome Loss, Ltr	0.0	dB
EIRP	25.0	dBm
Propagation		
Transmission Frequency, f	144.0	MHz
Link Range, R	50.0	km
Propagation Factor, n	1.0	
Free Space Loss, Ls	109.6	dB
Atmospheric Absorption, Lpa	0.0	dB
Precipitation Absorption, Lpp	0.0	dB
Total Propagation Loss	109.6	dB
Receiver (Rx)		
Rx Antenna Gain (Peak), Gr	0.0	dBi
Rx Polarization Loss, Lrpol	0.0	dB
Rx Pointing Loss, Lrp	1.0	dB
Rx Radome Loss, Lrr	0.0	dB
Rx Component Line Losses, Lrl	1.0	dB
Rx Implementation Losses, Lri	1.0	dB
Received effective carrier power	-87.6	dBm
Noise		
Standard Thermal Noise, kT	-174.0	dBm/Hz
Rx Noise Bandwidth, W	43.0	dBHz
Rx Noise Figure, NF	5.0	dB
Effective Noise Power	-126.0	dBm
Result		
Available CNR	38.4	dB
Data Rate	39.8	dBHz
Available Eb/No	41.5	dB
Implementation Losses	3.0	dB
Required Eb/No	14.2	dB
Margin	24.3	dB



3 TESTING OF THE TH-D7A

3.1 Overview

This chapter discusses testing the Kenwood TH-D7A handset for operational utility. First, we will test the unit using software provided by Kenwood and then using our own techniques. In doing this, we will be attempting to simulate the commands and procedures that will be performed by the 3CS satellites. We will evaluate the performance of the unit and discuss our solution to overcoming the limitations encountered during testing.

3.2 Initial Testing Using Software Provided by Kenwood

The initial testing was intended to learn the operation modes of the TH-D7A so that the necessary commands and procedures for use in the satellite could be determined. The first check was to send data from a PC to the handset. The special Kenwood interface cable along with software was used to connect the handset to the PC and run basic tests [6]. To test the handset with a computer, we must have the proper equipment and software. The user manual for the handset states that a PG-4W cable must be used to connect the handset to the computer. The PG-4W cable is basically a simple null modem cable with a special plug for the handset. The cable connects to the handset via a PC plug inserted into the side of the handset. The opposite end of the cable connects to a 9-pin serial port on the PC. These tests verified the PC control of the handset. The basic setup of the software is shown in Figure 5.

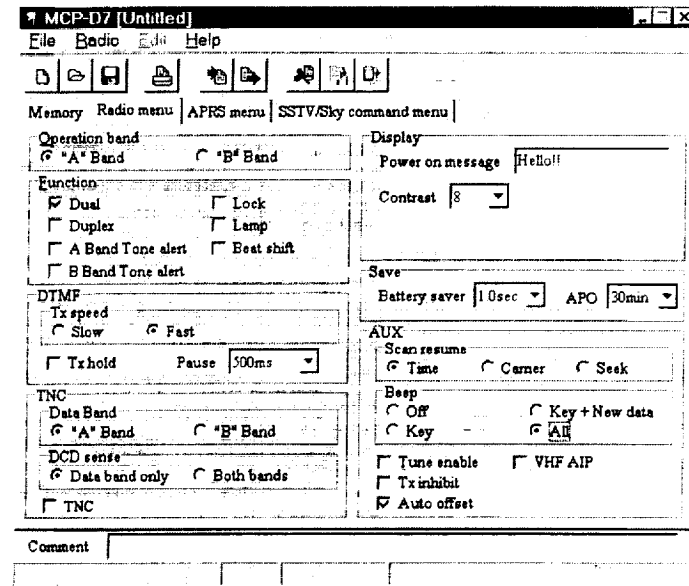


Figure 5. Basic Kenwood TH-D7A Software

Using this software, we can switch from one operation band to another. This allows the user to perform operations on “A” Band or “B” Band. We can turn the TNC ON or OFF and also select the data band when the TNC is turned ON. The main purpose of this demonstration is to show that the PC and handset are communicating with one another and the commands executed by the software are visible on the handset’s user display. With the initial functional verification completed, we begin developing the experience to configure the handsets for satellite use.

3.3 Testing Using Hyper Terminal

The next development step is to configure and control the handset using direct operator commands. To do this, we use the Hyper Terminal Program [7] to act as a simple user interface along with the cables used in the previous tests. To establish a Hyper Terminal session properly, the following parameters must be initialized on the PC for 9600 baud operation:

- Transfer Rate (TNC <-> Computer): 9600 bps
- Data Length: 8 bits
- Stop Bit: 1 bit
- Parity Bit: none
- Flow Control: Xon/Xoff

Since the channel between the PC and the handset is a cable, we are assuming that no errors will occur; therefore, we will disable the parity bit. After this has been established, we execute some basic commands [8].

The first goal is to choose which of the two bands on the handset we wish to use. For convenience, we will select Band A for VHF communications and Band B for UHF communications. The command utilized to accomplish this task is the Band selection Command, BC. To select Band A, one types "BC 0" in Hyper Terminal. After pressing the carriage return, we can verify that the handset is set to operate in A Band.

Next we would like to select the output power on the handset. The lowest power setting is Extremely Low (EL). This sets the output power to approximately 50 milliwatts (mW). This power setting is sufficient for the initial testing. The

command to control the output power is Power Control, PC. To execute this command properly, we must select the band and output power setting. For example, to set the A Band to the Extremely Low power setting, one types "PC 0, 3" into Hyper Terminal followed by a carriage return. Now we are ready to select the testing frequency.

To set the frequency of the handset, the frequency (FQ) command must be executed. For example, to set the frequency to 137 MHz, one enters "FQ 00137000000, 0" in Hyper Terminal followed by a carriage return.

In order to transmit and receive data, we must specify the data band. To set the data band to operate on Band A, we must enter the Data Transmission Band (DTB) Command followed by the band selection. The proper format of this command is "DTB 0" followed by a carriage return. Also, to avoid missing the first packet of transmission, we must turn the Battery Saver (SV) option off. The "SV 0" command followed by a carriage return is the correct format for turning this option off.

Now that the computer and handset are configured properly, the TNC inside the handset can be enabled to allow data flow. In order to turn the TNC on, we must enter the TC command, "TC 0", followed by a carriage return. For the initial testing, we allow the TNC to use its default values. These values will be changed as we learn more about the handset. Before transmitting any data, a valid call sign must be entered into the handset. To accomplish this task, we must enter "MY call sign" followed by a carriage return. The final step before transmitting data is to place the

handset in Converse mode. This is accomplished by entering “K” followed by a carriage return.

In order to view the data being transmitted, we set up another handset at the same frequency connected to another PC. After setting the receiver to the same mode, we can start typing data and watching the data arrive at the other terminal. The handset TNC does not send a data packet until the message buffer on the handset is full or a carriage return is entered. The result of the initial testing was a success. After successfully transmitting data correctly by direct operator commands, the next step is to simulate how the on-board PC of the satellite will actually send the data. The software used to simulate this process will be LabVIEW.

3.4 Testing of Handset Using LabVIEW

LabVIEW [9] is a useful tool for designing the command simulator. To emulate how the End-to-End Data System would need to be configured to support communications through the handset, we created a Virtual Instrument (VI) shown in Figure 6.

The VI has many functions, the first of which is the initialization of the handset. In order to communicate with the handset, we must specify the serial communications port and the baud for data communications between the handset and host computer. The second stage of initialization includes setting the proper output power levels, frequencies for each band, turning the battery saver option off, selecting dual band operation, and selecting the data band. The third stage of initialization sets

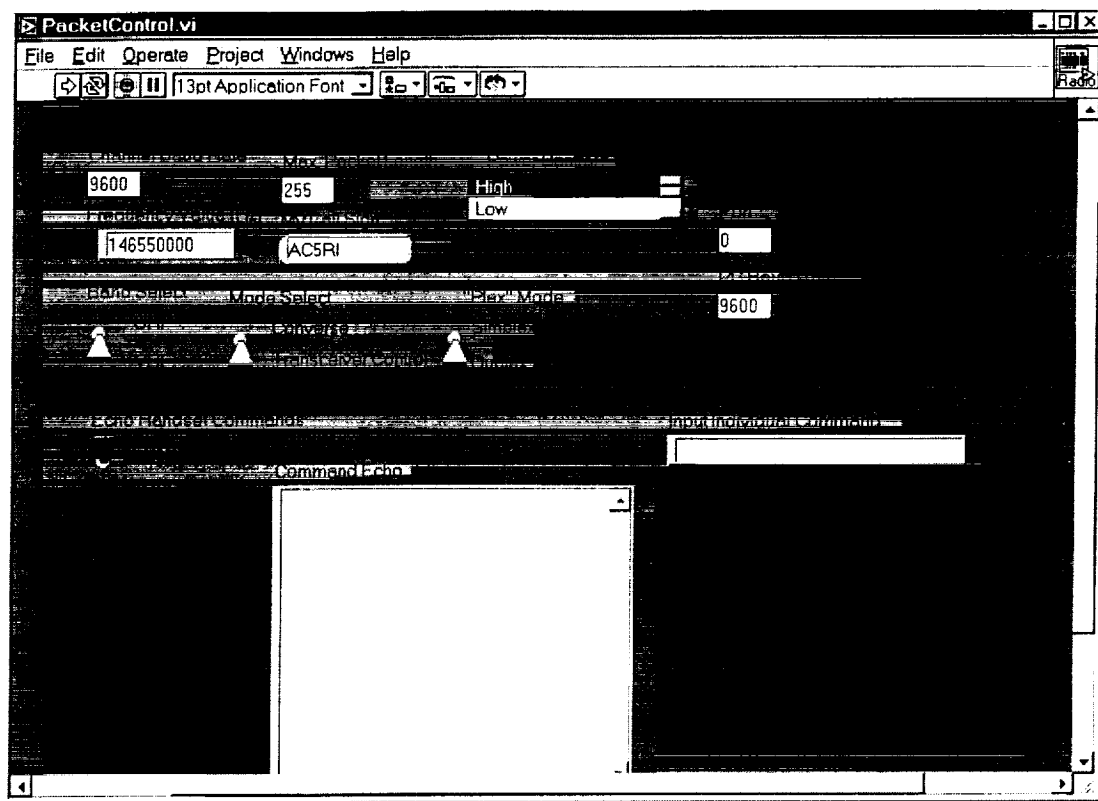


Figure 6. LabVIEW Control Panel for Handset

the RF data rate, packet length, maximum number of frames per packet, carriage returns after a packet, echo of executed or non-executed commands, passing all packets received, and call sign. Table 5 shows the commands and initialization sequence for the handset.

Table 5. Commands for Handset

Process	Command	Comment (all commands must be followed by a carriage return [ASCII symbol for a CR is a hex 0D])
Initialize Handset		
Set to Transceiver Control Mode	TC 1	Turns TNC Off
Turn Battery Saver Off	SV 0	Battery Saver is Off
Set frequency for Band A	BC 0	Select Band A
Set frequency for Band B	FQ 00137000000,0 BC 1 FQ 00450000000,0	Set frequency for Band A Select Band B Set frequency for Band B
Turn On Dual Band	DL 1	
Select Data Band	DTB 0 DTB 1	Band A Band B
Set Call Sign	MYC call sign	Call sign will differ for each Sat
Set Power Control	PC 0,2 PC 1,3	Output power on band A is set to low Output power on band B is set to extremely low, this may change if band B amplifier is stripped
Initialize TNC		
Set to TNC Mode	TC 0	Turns TNC On
Set number of data bits	AW 8	Handset must use 8 bits
Set Echo of desired	E ON E OFF	Set echo on Set echo off
Set Flow Control	X ON	Specifies Software Flow Control (must be used)
Select Parity	PAR 0	Selects non parity (must be used)
Set Transmission Data Rate	HB 9600	Set to 9600 bps
Send CR after end of packet	CR ON	Sends CR at the end of a packet
Set Packet Length	P 255	Set to max length
Receive all packets	PASSALL ON	Allows all packets to be received
Set max frames/packet	MAX 7	Set max frames/packet to 7

Table 5. Continued.

Process	Command	Comment (all commands must be followed by a carriage return [ASCII symbol for a CR is a hex 0D])
Receive (forward link)		
Set to Transceiver Control Mode	TC 1	Turns TNC Off
Select Band B	BC 1	Select Band B
Select Data Band	DTB 1	Band B
Set to TNC Mode	TC 0	Turns TNC On
Transmit (return link)		
Set to Transceiver Control Mode	TC 1	Turns TNC Off
Select Band A	BC 0	Select Band A
Set Power Control	PC 0, 2	Output power on band A is set to low
Select Data Band	DTB 0	Band A
Set to TNC Mode	TC 0	Turns TNC On
Enter Converse Mode	K	Converse Mode
Transmit (cross link)		
Set to Transceiver Control Mode	TC 1	Turns TNC Off
Select Band A	BC 0	Select Band A
Set Power Control	PC 0, 3	Output power on band A is set to extremely low
Select Data Band	DTB 0	Band A
Set to TNC Mode	TC 0	Turns TNC On
Enter Converse Mode	K	Converse Mode

When the handset is in transmit mode, after the Converse command is executed, data is received at the serial port, is packaged by the TNC, and then transmitted over the selected frequency. After data is finished transferring from the host computer to the handset, we turn off the TNC. This places the handset in a lower

power mode requiring minimal power consumption while the handset is in stand-by mode. To turn the TNC off while in the Converse mode, the VI transmits a carriage return to ensure all the data in the transmit buffer is sent. Then the VI writes "TC 1" followed by a carriage return to turn the TNC off.

After testing the VI with the handset and verifying correct operation, we started operations testing. The first test was to send small text files that would not overflow the handset's transmit buffer. We started with files that were 100 characters or fewer. The receiving unit for the test was another handset connected to another host computer using the Hyper Terminal software. The test was successful so the next test level was to increase the number of characters in the file.

The next test level was to set the maximum packet length on the handset to 255 bytes and create a file that was 255 characters long. After sending this file and receiving it properly on the Hyper Terminal station, we concluded that this test was successful. Then we increased the file size to 1000 characters and left the packet length at 255 bytes. This test was unsuccessful thereby indicating that the flow control was not working properly and the transmit buffer was being overwritten.

This was due to two major problems. The first problem is that the handset was transmitting data at 9600 bps and the serial port on the PC was streaming data at 9600 bps. This becomes a problem because the AX.25 protocol has overhead data in addition to the user's data. In this protocol, the user data throughput is less than 9600 bps. The user's manual states that software flow control must be used in order to communicate properly with the handset. We soon realized that the flow control was

Table 6. Example of Overwriting the Buffer on the Handset

Data Transmitted from CPU	Data Received
0123456789 Abcdefghijklmnopqrstuvwxyz Three Corner Sat New Mexico State University Arizona State University Colorado University	0123456789 AbcdefghijklmnopqThree Corner Sat New Mexico State University Arizona State UniveColorado University

not working properly and it was allowing the data streaming into the handset to overwrite the buffer before it was transmitted. A simple example of the results is shown in Table 6.

The second problem is the handset pauses after a packet is sent. There are three main instances when the handset sends a packet. A packet is sent when a carriage return occurs, when the maximum number of frames per packet is reached, or when the transmit buffer is full. This problem is illustrated in Figure 7. If the file being sent must be transmitted using many packets, there will be many delays. To solve this problem, we decided to parse the data into 255-byte segments. After 255 bytes are sent from the host computer to the handset, we will allow a small time to pass before sending the next 255 bytes. This is realized by using a timer in LabVIEW. After trial and error it was determined that the timer must be set to 1.5 seconds for best results. The setting of the timer does not increase the time between

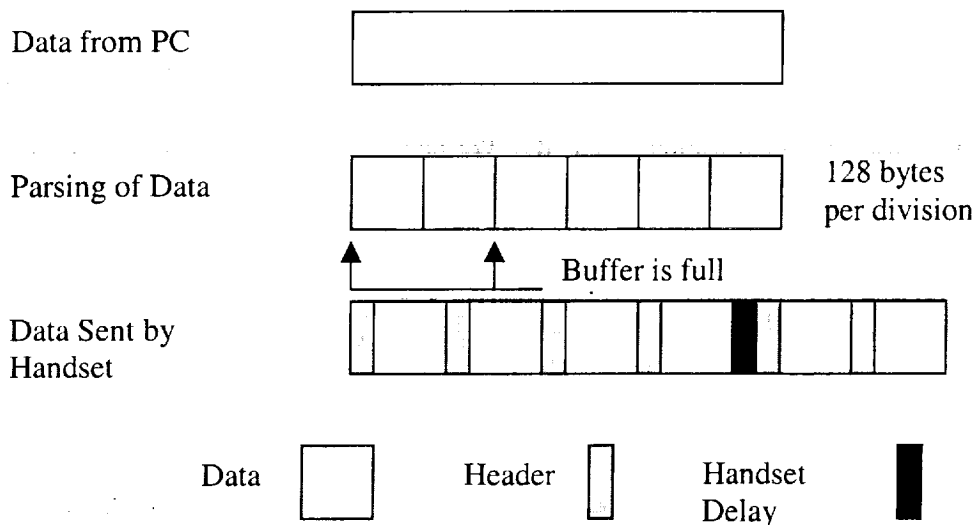


Figure 7. Handset and Packaging Delays

the packets. It simply keeps the transmit buffer on the handset from being overwritten. The audible sound generated from the speaker on the handset sounds exactly the same as if data was being streamed without any control. This was taken as an indication of proper operation. This particular setting allowed all of the data to be received correctly independent of the file size.

This solution has a major problem in that the throughput of the system is very poor. From the testing, we determined that the net throughput is approximately 700 bps. This result is poor compared with 9600 bps links having 10-20 percent overhead. Typical 9600 bps links will have a net data throughput of approximately 7500-8700 bps. We can see that the actual throughput is less than 10 percent of a normal 9600 bps link. Because of this result, we need to investigate a method to increase the throughput. A solution will be proposed in Section 3.5.

Another small problem with the handset is that changing from the transmit mode to the receive mode, resets TNC. Therefore, when switching from one mode to another, we must re-initialize the TNC. We need to incorporate the re-initialization into the operational procedures

3.5 Modify the Handset to Increase Data Rate

The native mode of the handset has poor throughput yielding two basic options. We can accept the handset operationally or modify the handset's hardware and/or control software. The first would require the End-to-End Data System to perform data compression and/or rely on the S-band system for bulk telemetry (image) transmission. Relying on the S-band system is the most sensible option; therefore, the handset will only be used for quick look data or as a backup telemetry system.

To increase the throughput of the handset, we must perform the modifications described in Section 5.3. By viewing the data from the TNC using an oscilloscope, we determined it is TTL format; therefore, the TNC can be bypassed. The End-to-End Data System must package the data using the AX.25 protocol to utilize existing university ground stations. The voltage amplitude of the TTL signal provided by the End-to-End Data System must be adjusted to replicate the 2 volt peak-to-peak TTL signal of the TNC inside the handset. Then the data can be directly injected into the modification while enabling the Push-To-Talk (PTT).

3.6 Final LabVIEW Simulation

Based on the previous results, the LabVIEW VI was simplified in order to simulate the on-board computer. The satellite will most likely store the commands in a file. To configure an operational mode, the on-board computer will send a script file to the handset. Using the same approach as described in the previous program, we created a second VI, whose control panel is shown in Figure 8.

The VI programming diagram shown in Figure A2 allows continuous operation of the handset. We can switch from one mode of operation to another without restarting the program by placing all the operations in an infinite While Loop. To exit the program, the user clicks the stop button in the tool bar.

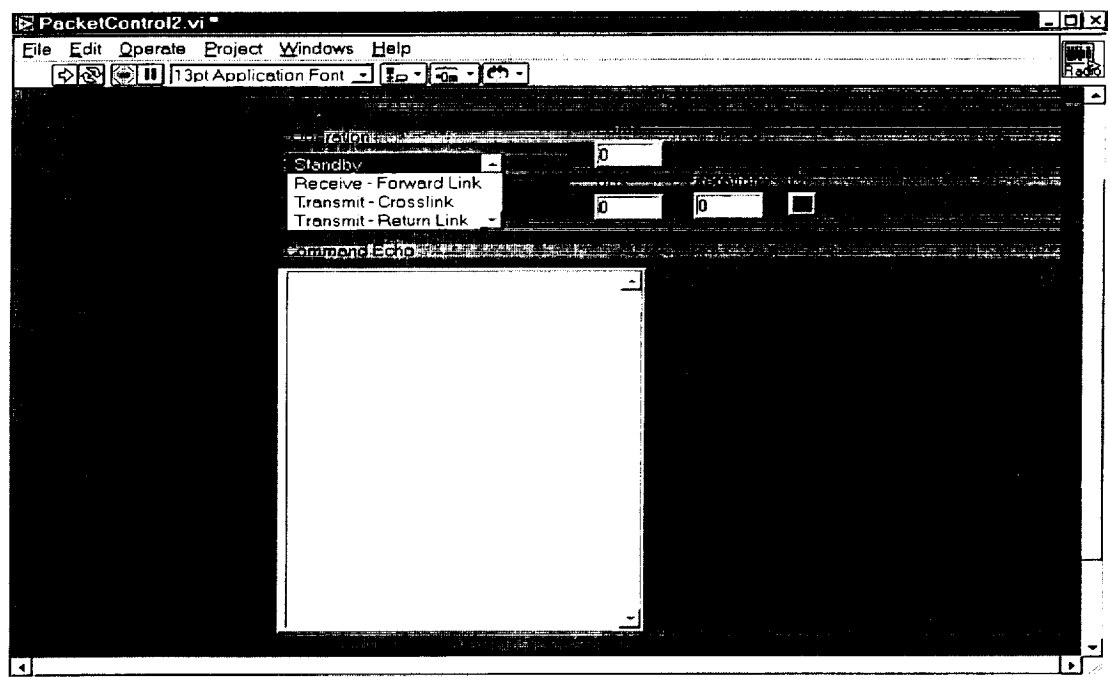


Figure 8. LabVIEW Control Panel

The Operation VI shown in Figures A3 and A4 decides which operation is to be performed. If the crosslink or return link option is selected, the Operation VI calls the Transmit VI. If the return link or standby mode is selected, the Operation VI spawns the Stdby_Rx VI. When the return link or standby mode has been chosen, the Stdby_Rx VI chooses which operation to perform. It then allows the user to select the file to be executed. Depending on the mode selected, the user should enter the correct file to be sent to the handset in order to control it.

The first mode of operation is the standby mode shown by Figure A9. This mode places the handset in the lowest power consumption setting. The TNC is turned off and the handset is operating on a single band set at the receive frequency. We will chose the standby mode to function on band B. The list of commands sent to the handset for standby mode is shown below.

- TC 1
- DL 0
- BC 1
- FQ 00450000000,0

When the receive mode has been selected, the Stdby_Rx VI prompts the user to enter the receive file and then turns on the TNC. The Receive VI is shown in Figures A5-A8. The commands to be executed in the Receive file are:

- TC 1
- BC 1
- DTB 1
- FQ 00450000000,0

The Receive VI waits for three seconds after turning on the TNC. This delay allows the TNC to initialize and become fully operational. After the delay, the user enters the TNC file, which configures the TNC properly. The commands that configure the TNC properly are shown below.

- AW 8
- E ON
- X ON
- PAR 0
- HB 9600
- CR ON
- PP ON
- PE 63
- P 255
- CP ON
- PACT A 2
- MAX 7
- PASSALL ON
- MY AC5RI
- F OFF
- K

These parameters may be changed in order to improve the performance of the handset when the satellites have deployed. We may be able to optimize the parameters with more testing. The last command of the TNC file places the handset into Converse mode allowing the on-board computer to receive the data.

There are two different modes when transmitting data: return link mode and crosslink mode. This program is designed to ensure that the data is transmitted.

Although the data throughput is very low, all the data in the file to be transferred is

transmitted by the handset. The first transmit mode to be explained is the return link. The program can be viewed in Figures A10-A15.

When the return link operation has been selected, the user is prompted to enter the return file. The return file executes these five commands:

- TC 1
- BC 0
- DTB 0
- FQ 00146550000,0
- PC 0,2

These commands turn off the TNC, then selects the proper band, data band, transmit frequency, and radiated power mode. After this file has been executed, the TNC is turned on. After a brief delay allowing the TNC to reinitialize itself, the user is prompted to enter the TNC file to be executed. Then the program places the handset into Converse mode allowing it to transfer data. Once in Converse mode, the program spawns the Mode Select VI shown in Figures A16-A18.

The Mode Select VI prompts the user to enter the file to be transmitted. The program reads the file and converts the data into an array of individual bytes. After the data is placed in the array, the While Loop begins to run. If the array is greater than 255 bytes, the program parses the first 255 bytes from the array and transmits the data. It allows 1.5 seconds for the handset to transmit the data. This process repeats itself until there are 255 bytes or fewer in the array. When the array size is less than or equal to 255 bytes, the program writes the data to the handset and waits another 1.5 seconds before turning off the TNC.

For the crosslink mode, the same steps are used as in the return link mode with minor changes. The first user prompt scene allows the user to enter the crosslink file. This file uses different power settings and a different frequency. The program then follows the same steps as the return link mode. A separate TNC file may be sent to the handset in order to operate at 1200 bps. The file may be the same except the HB command must be modified.

3.7 Consumed Power in Different Modes

In order to verify the handset meets the power requirements, we must calculate the power consumed for the various modes of operation. The bus voltages that will be provided to the communications system are either a regulated 5-volt supply or an unregulated 12-volt supply. In order to calculate the power, we must be able to measure the input voltage and the current being drawn by the handset. The power is calculated by multiplying the input voltage by the current. In order to estimate the power being consumed when using an unregulated bus, measurements will be made at 11, 12.5, and 14 volts when performing these measurements. All measurements are made at room temperature. When measuring the current drawn, the audio volume was turned to its minimum setting the internal speaker will not be used.

When operating on a regulated 5-volt bus, we can observe that the power consumption varies from 0.245 watts to 3.775 watts. This observation shows that the

Table 7. Power Consumption Calculations of the Handset

Bus Voltage (V)	5	11	12.5	14
	Power Consumed (W)			
No Signal Present				
Rx SB TNC 0	0.245	0.539	0.6125	0.686
Rx DB TNC 0	0.41	0.902	1.025	1.148
Rx SB TNC 1	0.335	0.77	0.8875	1.008
Rx DB TNC 1	0.4975	1.1385	1.30625	1.47
Signal Present				
Rx SB TNC 0	0.3425	0.825	0.9375	1.05
Rx DB TNC 0	0.51	1.188	1.35625	1.519
Rx SB TNC 1	0.4325	1.056	1.2125	1.372
Rx DB TNC 1	0.595	1.419	1.625	1.834
Power Set (EL)				
Tx SB TNC 1	1.065	2.959	3.4875	4.046
Tx SB TNC 0	0.985	2.739	3.2125	3.724
Tx DB TNC 1	1.075	3.003	3.525	4.074
Tx DB TNC 0	0.985	2.739	3.225	3.738
Power Set (L)				
Tx SB TNC 0	2.16	5.599	6.4875	7.406
Tx SB TNC 1	2.26	5.852	6.7875	7.756
Tx DB TNC 0	2.175	5.643	6.5375	7.462
Tx DB TNC 1	2.26	5.863	6.8	7.77

handset meets the power requirements. The modes that will most likely be used are shown in bold print in Table 7. The abbreviations for Table 7 are listed below:

- Receive Single Band (TNC OFF) – Rx SB TNC 0
- Receive Dual Band (TNC OFF) – Rx DB TNC 0
- Receive Single Band (TNC ON) – Rx SB TNC 1
- Receive Dual Band (TNC ON) – Rx DB TNC 1
- Transmit Single Band (TNC ON) – Tx SB TNC 1
- Transmit Single Band (TNC OFF) – Tx SB TNC 0
- Transmit Dual Band (TNC ON) – Tx DB TNC 1
- Transmit Dual Band (TNC OFF) – Tx DB TNC 0

When the satellites are operating in the receive mode, the TNC on the handset must be ON. This allows data to be received, unpackaged, and sent to the on-board computer of the satellite. As shown in Table 7, when the TNC is ON and a signal is not present, the power consumed is approximately 0.335 W on the 5-volt bus. The power consumption increases during the unregulated 12-volt bus. When the satellite is receiving a signal, the power consumed is 0.4325 W when connected to the 5-volt bus. The power consumption more than doubles if the handset is connected to the unregulated 12-volt bus.

In the transmit mode, the satellite will use the extremely low (EL) power setting for crosslinks or the low (L) power setting for return links. When using the EL power setting on the 5-volt bus, the power consumed is 1.065 W. While connected to the 12 volt bus, the consumed power triples over that of the 5-volt bus. When transmitting data using the L power setting, the consumed power is 2.26 W. The same results hold true when using the 12-volt bus. With these results in mind, it

is recommended that the handset should be connected to the regulated 5-volt bus on the satellite. This allows the least amount of power to be consumed from the power subsystem.

3.8 Summary

Based upon these operational tests, the handset can be controlled via on-board computer for the End-to-End Data System and configured for operations. The unit will work properly with the 5-volt regulated bus from the Electrical Power Subsystem. Also, we have determined that the TNC operational mode restricts data flow. The VHF will not be recommended for primary telemetry return link. The S-band system will be recommended for the primary telemetry return link. The operational software will need to be configured for correct data flow for the VHF as we have shown.

4 ANTENNA DESIGN

4.1 Overview

In this chapter we will discuss the design of the VHF/UHF antennas. Since we are using the satellite as a ground plane, we must tune the antennas on the spacecraft in a free space environment. Also, we apply an approximate image theory form to the design of monopole antennas since the mounting surface is approximately one wavelength. Another decision in designing the antennas is considering which materials to use in order for the deployment of the antennas to be relatively simple and reliable.

4.2 Design Requirements

4.2.1 Antenna Impedance Matching

3CS will be connecting the antennas to the transceiver using 50-ohm coaxial cable. In order to minimize the losses, we must design an antenna with a 50-ohm input impedance. If we can accomplish this goal, the reflection coefficient will be zero and the Voltage Standing Wave Ratio (VSWR) will be unity. In practice, this goal is not obtainable; therefore we must specify an acceptable level. Here, a VSWR less than two is acceptable.

4.2.2 Length

The length of the antennas is usually a minor design requirement. Since the 3CS satellites are physically small and the antennas will be perpendicular to the same

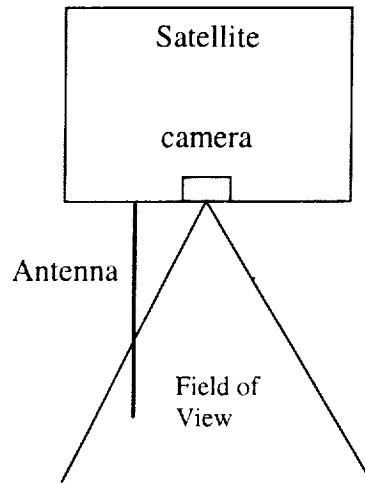


Figure 9. Antenna Interference with the Camera's Field of View

mounting surface as the camera, they must be designed so as to not interfere with the camera's field of view. An example of antenna obstruction with the camera's field of view is shown in Figure 9. By placing the antenna as close to the outside edge of the satellite as possible, antenna interference in the field of view of the camera may not be an issue. However, other internal components will be mounted to the sides of the satellite, which will cause the antennas to be mounted closer to the camera.

4.2.3 Gain

The gain of the antennas is relatively important. The quarter wave ($\lambda/4$) monopole antennas will not have a significant gain. Also considering the inclination angle of the satellites in space and the geographical location of the ground stations, designing the antennas with a positive gain will enable the link to have closure.

Assuming the antennas will be nadir pointing, each ground station will not be in the

peak gain of the antennas because the peak of the main lobe will be above the horizon.

4.3 Field Patterns

The first stage of designing monopole antennas is to make reasonable assumptions. The first assumption is that the antenna is thin relative to the wavelength of operation. This implies that the current is longitudinal and circumferential currents are zero. We will also make use of the far field approximations. The fields generated by the antenna then have properties of local plane waves and decay in magnitude as the distance (r) increases.

The result of the thin approximation reduces the three-dimensional integral into a one-dimensional integral. Also, we need to decide on a good approximation for the current distribution along the antenna. We use the solutions of Maxwell's equations applied to antennas and formulate Equations 4.1 and 4.2 [10].

$$I(z) = I_m \sin\left[\beta\left(\frac{\lambda}{4} - z\right)\right] \quad 0 \leq z \leq \frac{\lambda}{4} \quad (4.1)$$

$$\bar{A} = \hat{z}\mu \frac{e^{-j\beta r}}{4\pi r} \int I(z') e^{j\beta z' \cos(\theta)} dz' \quad (4.2)$$

Equation 4.1 and 4.2 assume a sinusoidal current distribution along a z-directed antenna. The field patterns are not computed using image theory. The difference is negligible if an image current is used and one allows radiation into all space. However, if image theory is used we are supposed to translate the pattern to half space, which is much different. The sinusoidal distribution has a maximum value, I_m , at the base of the antenna and is zero at the end of the antenna. The equation for the vector potential, \mathbf{A} , shows that we are integrating the z-directed line source. By using the vector potential, we can find the Electric field, or E-field, as a function of \mathbf{A} . This relationship is shown in Equation 4.3.

$$\vec{E} = -j\omega\vec{A} \quad (4.3)$$

To simplify the analysis, we will change from the Cartesian coordinate system to the spherical coordinate system using the following matrix multiplication:

$$\begin{bmatrix} A_r \\ A_\theta \\ A_\phi \end{bmatrix} = \begin{bmatrix} \sin(\theta)\cos(\phi) & \sin(\theta)\sin(\phi) & \cos(\theta) \\ \cos(\theta)\cos(\phi) & \cos(\theta)\sin(\phi) & -\sin(\phi) \\ -\sin(\phi) & \cos(\phi) & 0 \end{bmatrix} \begin{bmatrix} A_x \\ A_y \\ A_z \end{bmatrix} \quad (4.4)$$

Since there is not a current in the x- and y-directions, A_x and A_y are equal to zero.

After computing the coordinate conversion, the vector potential in spherical coordinates is:

$$\begin{bmatrix} A_r \\ A_\theta \\ A_\phi \end{bmatrix} = \begin{bmatrix} A_z \cos(\theta) \\ -A_z \sin(\theta) \\ 0 \end{bmatrix} \quad (4.5)$$

In the far-field, the radial component of the E-field is negligible leaving only one term, E_θ . The general form of the E-field for a z-directed current is shown by Equation 4.6.

$$E_\theta = j\omega \sin(\theta) A_z \quad (4.6)$$

Since all of the terms have been defined, we can solve for the vector potential in the z-direction. The formal integration of the vector potential can be viewed in Appendix B, which uses an arbitrary length antenna. Equation 4.1 assumes a $\lambda/4$ antenna. We will redefine Equation 4.1 with a length of $L/2$. Then the vector potential as a function of r and θ is shown below:

$$A_z = \frac{e^{-j\beta r}}{4\pi r} \frac{\mu I_m}{\beta \sin^2(\theta)} \left[e^{j\beta L \cos(\theta)} - (j \cos(\theta) \sin(\beta L) + \cos(\beta L)) \right] \quad (4.7)$$

As θ varies, the right hand side of the equation is periodic, but due to the short length, it only varies the magnitude slightly. This equation also shows that the main decay in

the equation is due to the r term. As r (distance) increases, the vector potential decays, which meets our general assumptions. This equation is then substituted into Equation 4.6. Combining terms, we may define the E-field equation.

$$E_{\theta} = j \frac{e^{-j\beta r}}{4\pi r} \frac{\eta I_m}{\sin(\theta)} \left[e^{j\beta L \cos(\theta)} - (j \cos(\theta) \sin(\beta L) + \cos(\beta L)) \right] \quad (4.8)$$

Now that we finally have the E-field, we can plot the electric field pattern. Using the Mathcad software [10], we can plot the normalized electric field pattern. The normalized field pattern is Equation 4.9 divided by the maximum value of this equation as θ varies from 0 to 2π .

$$f(\theta) = \frac{1}{\sin(\theta)} \left[e^{j\beta L \cos(\theta)} - (j \cos(\theta) \sin(\beta L) + \cos(\beta L)) \right] \quad (4.9)$$

Figure 10 displays the magnitude of the normalized electric field pattern for both the VHF and UHF antennas. The z-axis is the horizontal line passing from 0 degrees to 180 degrees. We can see that the field pattern is very similar to that of an ideal dipole. As predicted, the nulls of the field pattern occur along the z-axis. Figure 11 shows normalized the power pattern plots, in dB, for both antennas. Power patterns

are used to show where the majority of the power is concentrated in the field pattern.

Figure 11 shows the half power beamwidth of both antennas.

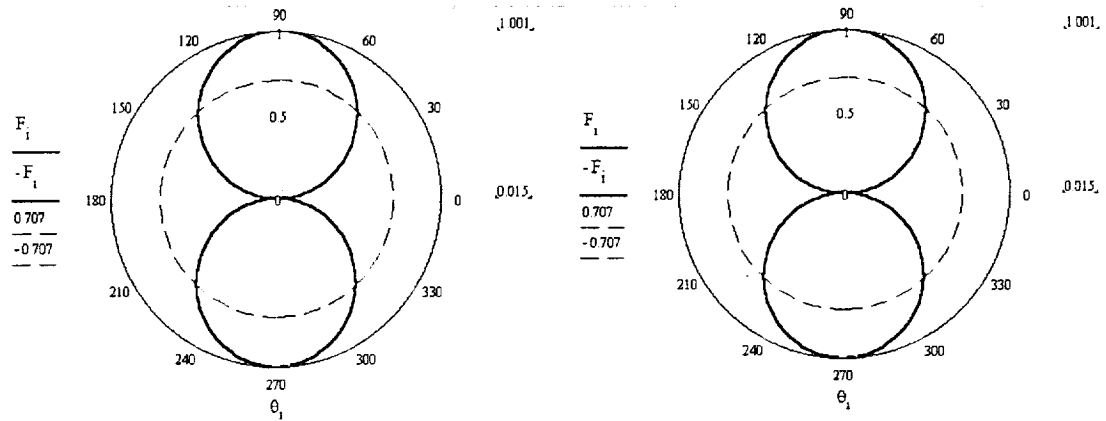


Figure 10. Linear Field Patterns for the VHF and UHF Antennas

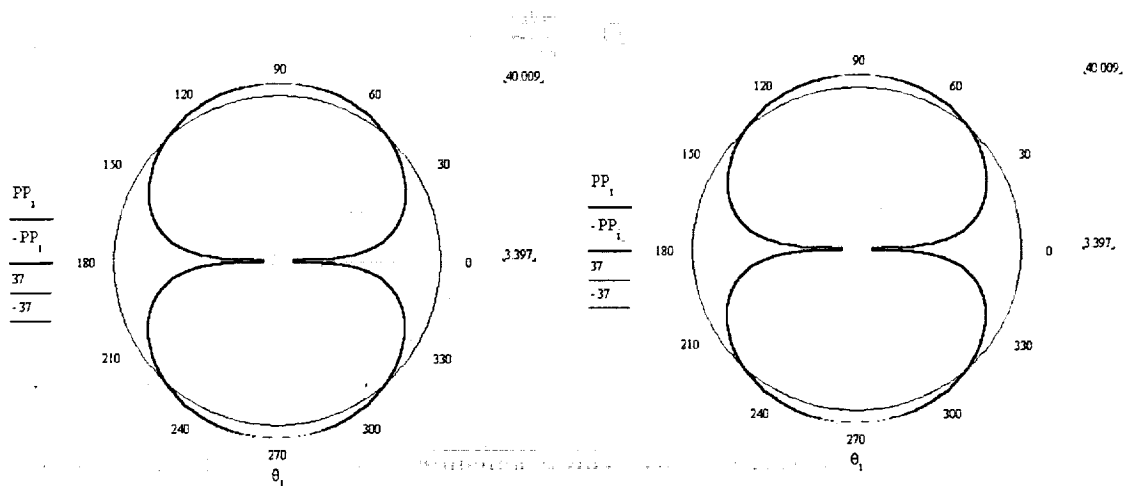


Figure 11. Power Patterns (10 dB/division) for the VHF and UHF Antennas

This plot has a line 3-dB down from the peak of the mainlobe. The half power beam width is determined by the angular distance between the -3 dB points on each side of the peak of the normalized mainlobe.

Using the normalized version of Equation 4.9, we can determine the theoretical gain of the antennas. In order to calculate the gain, we must compute the beam solid angle. This is represented by Equation 4.10.

$$\Omega_A = \iint |F(\theta, \phi)|^2 d\Omega \quad (4.10)$$

Equation 4.10 allows the directivity to be computed using Equation 4.11. The theoretical gain of the antenna is determined by multiplying the directivity of the antenna by the efficiency. The gain equation is shown in Equation 4.12.

$$D = \frac{4\pi}{\Omega_A} \quad (4.11)$$

$$G = e_r D \quad (4.12)$$

The efficiency of the antennas is computed in Appendix C. The gain of both the VHF and UHF antennas is 1.83 dB. This calculation is 10 times the log base 10 of the result of Equation 4.12. The gain is the same because each antenna is designed to be a quarter wavelength of their respective frequencies.

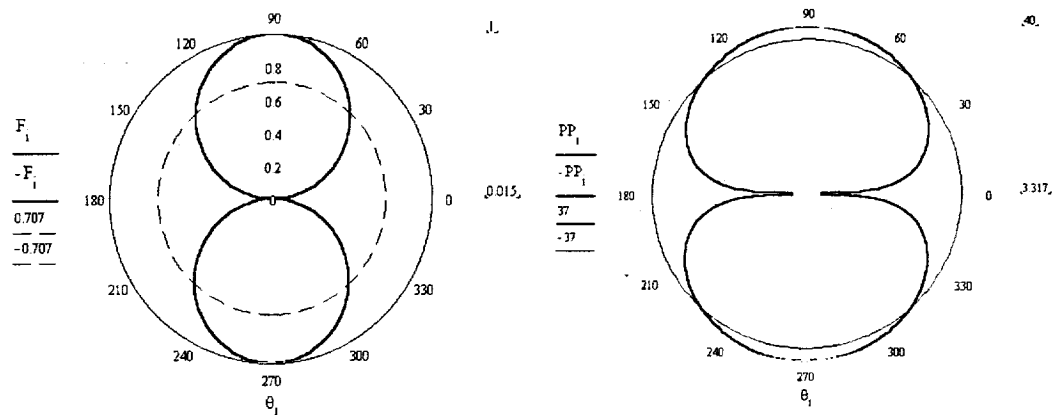


Figure 12. Field and Power Patterns (10 dB/division) of the VHF Antenna Operating at 144.39 MHz

The VHF antenna is a dual-purpose antenna. It must also function as the crosslink antenna. Therefore, we must analyze the VHF antenna at the crosslink frequency, 144.39 MHz. First, we will plot the field patterns as before and determine the half power beamwidth. Then, we will determine the gain of the antenna at the crosslink frequency. Figure 12 shows the normalized field pattern and the power pattern, in dB, of the VHF antenna operating at the crosslink frequency.

By analyzing the field pattern plot, we can observe that the beam is slightly more narrow than the antenna when operating at the return frequency. This observation is not as apparent in the power pattern. However, we can measure the

half power beamwidth much easier in the power pattern. The half power beamwidth for the VHF antenna operating at the crosslink frequency is approximately 85 degrees. As expected, this is slightly smaller than the half power beamwidth of the VHF antenna operating at its optimal frequency. Due to the slightly smaller half

power beamwidth, we can expect a higher gain. Using the same procedure, the gain of the VHF antenna operating at the crosslink frequency is approximately 1.85 dB.

4.4 Input Impedance

In order to minimize the losses in the communications system, we must match the input impedance of the antenna to the output impedance of the communications system. The output impedance of the communications system will be assumed to be 50-ohms since the transceivers are designed to be used with 50-ohm antennas. To simplify the impedance analysis, we will compute the input impedance of a dipole antenna. The length of the model dipole is the height of the satellite plus $\lambda/4$. The feed to the antenna will be offset from the center of the antenna by a distance, d . This analysis is needed because impedance of the satellite and the $\lambda/4$ antenna can be approximately modeled by a $3\lambda/8$ antenna. The satellite acts as the other part of the dipole with an offset.

The complex input impedance of a dipole antenna is composed of the radiation resistance, reactance, and the ohmic resistance of the antenna. The equations for the radiation resistance and the reactance can be viewed in Appendix C. These equations do vary with the material properties, length, and width of the antenna. The input impedance of a dipole antenna is shown Equation 4.13.

The ohmic resistance is a function of the conductivity of the conductor used for the antenna and the diameter of the antenna. The equation for the ohmic resistance with a sinusoidal current distribution is represented in Equation 4.14.

$$Z_A = R_\Omega + R_r + jX_r \quad (4.13)$$

$$R_\Omega = \frac{R_s L}{4\pi a} \left(1 - \frac{\sin(\beta L)}{\beta L} \right), \text{ where } R_s = \sqrt{\frac{\omega\mu}{2\sigma}} \quad (4.14)$$

R_s represents the surface resistance of the conductor. Since we will most likely use tape measures for the antennas, the material will be steel. The conductivity for steel is 2 MS/m. L and a represent the length and radius of the antenna respectively.

After computing the results from Equation 4.13, we account for the offset in the feed for the VHF antenna. The results for each antenna are shown in Table 8. These impedances match the 50-ohm network. We can compute the reflection coefficient, return loss, and VSWR. The VSWR is less than 1.5 for the frequencies of operation and assuming the can be minimized. These computed values as a function of frequency are shown in Appendix C. The UHF antenna is not easily modeled due to the local ground plane and the height of the satellite. The satellite with a $\lambda/4$

Table 8. Real Part of the Input Impedance for the VHF Antenna

Frequency	VHF Antenna (ohms)
Forward Link (137 MHz)	60.554
Cross Link (144.39 MHz)	71.501

antenna at 450 MHz is very difficult to model mathematically; therefore, we must build a model of a satellite and actually measure the input impedance and VSWR of the antenna. Figure 13 is the model satellite with the VHF and UHF antennas. This model allows the antennas to be tuned to the physical and electrical properties of the satellite.

In order to measure the input impedance and the VSWR of the antenna on the model satellite, we must calibrate a network analyzer. The network analyzer used to measure these values is the HP 8510B. The model satellite is placed in an anechoic chamber. The following steps are used to calibrate the network analyzer.

- Turn on the HP 8510B and allow it to come up to its PRESET configuration.
- Create a dual channel display.
- Set channel 1 to measure the S11 parameter using a Smith Chart.
- Set channel 2 to measure the VSWR.
- Set the source power to 10 dBm.
- Set the start and stop frequencies to 137 and 450 MHz respectively.
- Set the number of points to 801 x 1.
- Establish a reference plane by pressing CAL, then CAL2 and select S11.
- Place the SMA open on the end of the cable, then press OPEN.
- Place the SMA short on the end of the cable, then press SHORT.
- Place the SMA 50-ohm load on the end of the cable, then press LOAD and broadband.
- Save the calibration to Register 1.
- Adjust the electrical delay.
- Use a marker to measure specific values at specific frequencies.

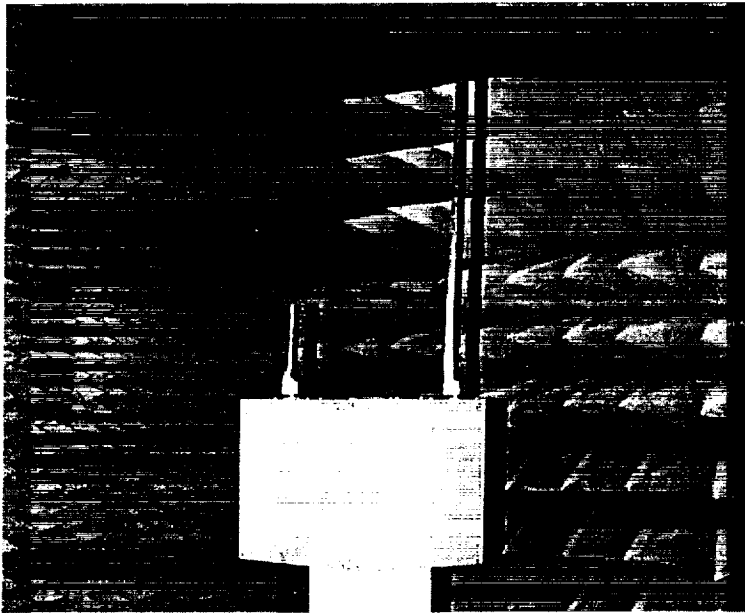


Figure 13. Nanosatellite Model with Tuned Antennas

Since we would like to tune the antenna to a 50-ohm network, the antennas should be longer than the theoretical length. This will allow the antenna to be trimmed in small increments. This type of procedure is optimal because it is much easier to trim the antenna than add length if it is too short. First, we will trim the VHF antenna. Table 9 shows the length of the antenna with the impedance and VSWR measurements. Table 10 analyzes the impedance and VSWR measurements of the UHF antenna as a function of length.

An acceptable VSWR for an RF system is a value less than two. After trimming the VHF antenna to 21.5 inches, we obtain an input impedance of $44.45 + j15.1$ ohms. This input impedance yields a VSWR of 1.40. We can see that the input impedance decreases as the length of the antenna is shortened. Although the VSWR

keeps decreasing, there will be a point when it starts to increase. This results because the input impedance becomes too small and becomes mismatched to the 50-ohm system. This length is very close to the quarter wavelength in the Mathcad simulations.

By trimming the UHF antenna to 6.625 inches, we obtained very favorable results. The input impedance at this length is $53.4 + j3.1$ ohms. The VSWR at 450 MHz measured to be 1.10. This result is excellent. The input impedance of the antennas on the satellite looks like the input impedance of dipole antennas. The antennas could have been trimmed slightly more, but these results meet the needs of 3CS.

When placing the antennas on the actual satellites, I recommend following the same procedures as above. The physical model and electrical connections of the actual satellite will be different than the lab and model satellite.

The feed to the antenna is illustrated by Figure 14. The length of the antennas in Tables 9 and 10 represent the overall length. The feed is connected 0.5" above the bottom edge of the antenna. The bottom edge of the antenna is approximately 3/8" above the mounting surface. There is a 0.25" gap between the antenna and the connector. The center conductor of the connector extends through the 0.25" gap and is soldered to the antenna.

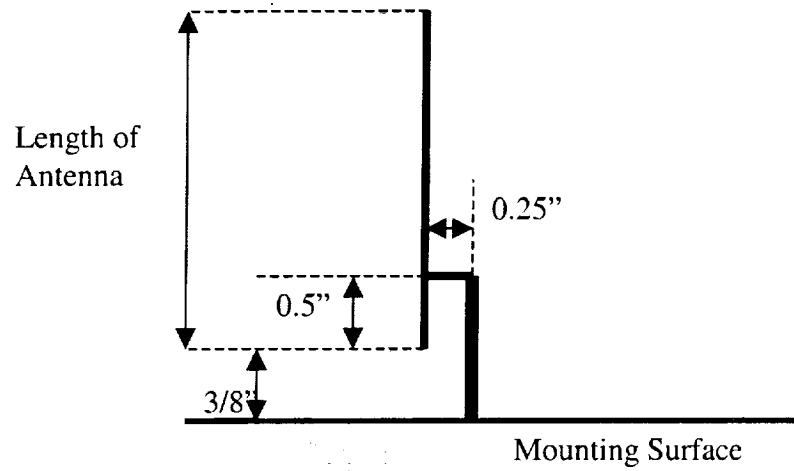


Figure 14. Feed to the Antenna

Table 9. Impedance and VSWR Measurements of the VHF Antenna

Antenna length (inches)	Impedance (ohms)	VSWR
23.25	85.8 + j52.1	2.54
23.00	77.3 + j44.9	2.27
22.75	70.5 + j40.1	2.10
22.50	65.2 + j35.9	1.95
22.25	59.9 + j30.3	1.78
22.00	52.9 + j24.4	1.61
21.75	48.8 + j20.1	1.50
21.50	44.4 + j15.1	1.40

Table 10. Impedance and VSWR Measurements of the UHF Antenna

Antenna length (inches)	Impedance (ohms)	VSWR
9.00	30.0 - j 56.4	4.03
8.75	36.0 - j57.0	3.66
8.50	41.4 - j56.7	3.31
8.25	47.0 - j55.7	2.99
8.00	54.2 - j52.5	2.63
7.75	62.1 - j44.7	2.28
7.50	67.5 - j35.8	1.96
7.25	69.7 - j23.3	1.67
7.00	66.2 - j10.1	1.39
6.75	58.9 - j1.5	1.18
6.625	53.4 + j3.1	1.10

4.5 Connecting the Antennas to the TH-D7A

Connecting the antennas to the handset may be a problem for optimal design. Since the handset has one RF connection, a parallel network of the antennas is the first obvious solution. If we connect the antennas in parallel, the input impedance of the antenna network will not be 50-ohms; therefore, some of the power radiated by the transmitter will be reflected back into the system. If we are receiving a signal, some of the power received will be radiated out of the other VHF antenna. Due to this problem, we must connect the antennas in a different manner. Here we will consider three possible solutions: an duplexer, a frequency selective tee, and modifications to the handset.

4.5.1 Duplexer

The first solution considered was the use of a duplexer. The switch will enable the transceiver to receive with one antenna and transmit with the other antenna. This configuration is represented in Figure 15.

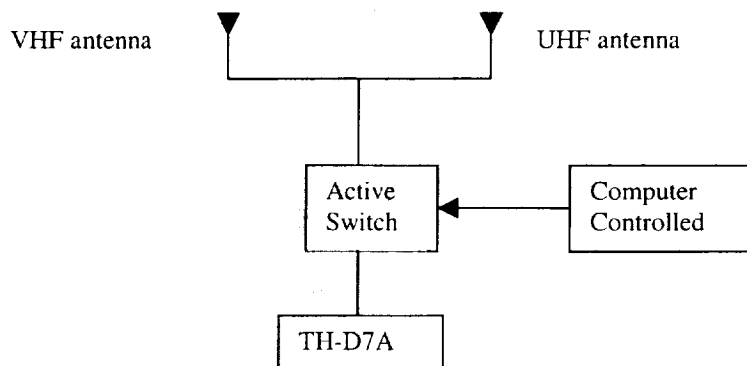


Figure 15. Duplexer

The advantage of using an active switch is that it allows the antennas to be matched at their respective frequencies. This allows the design to remain optimal. Also, when a signal is being received, it will not be reradiated out of the other antenna. When transmitting a signal, the transmitter will only use one antenna, which remains optimal and allows for good isolation between the antennas.

The disadvantage of using an active switch is that the switch may fail. If the switch failed, one antenna or possibly neither antenna will be connected to the transceiver. The possibility of failure causes the design to not be optimal. Also, the active switch must be controlled. The on-board computer on the satellite must select which antenna to use. This creates more complexity in the satellite's design. Due to the disadvantages, we will choose to hardwire the antennas to its respective transmitter or receiver.

4.5.2 Frequency Selective Tee

Design of a frequency selective tee is fairly difficult. Since the forward and return link frequencies are separate, we may be able to use the properties of quarter wave transformers to our advantage. The matching line labeled one in Figure 16 is a quarter wavelength long at 450 MHz and is terminated with an open circuit. The open circuit is transformed through the quarter wave transformer creating a short circuit at the tee. Appearing at the tee is a virtual short circuit and the impedance of the VHF antenna connected in parallel. Computing the parallel impedance of the two elements results in a short circuit. Then if we reflect the short circuit at the tee

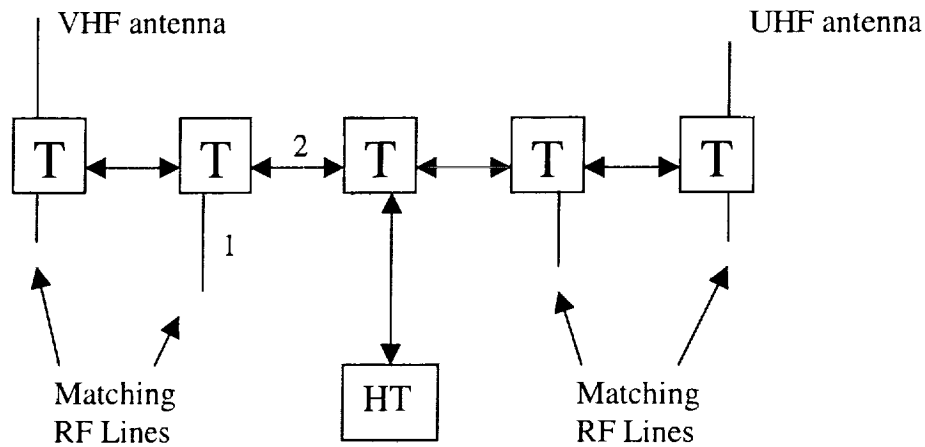


Figure 16. Frequency Selective Tee

through another 450 MHz quarter wave transformer labeled two, the impedance at the center tee looking into the left side of the system is an open circuit. Therefore, at 450 MHz, the left side of the system appears to be an open or not there. The same method is used for the UHF side when operating at the VHF frequency.

If we simulate this system, we find that the results are unfavorable. The isolation between the antennas is not acceptable. If we vary the lengths of the matching lines, we can obtain better isolation but the VSWR increases, which creates mismatch losses between the handset and the tee. The results of this system are tabulated in Table 11 and Table 12. Table 11 shows the results for the best isolation design and Table 12 tabulates the results for the best VSWR design.

Looking into the VHF side of the network, we lose 0.5 dB at the operational frequency. At 450 MHz, the left side creates a 62 dB loss, which is favorable since we would like for it to act as an open circuit. Looking into the UHF side of the

network, we lose 1.4 dB at its operational frequency and 14 dB at 137 MHz. This result is slightly unfavorable since the isolation isn't very high and we create additional losses at the operational frequency. When connecting to the handset, the VSWR is 1.65 and 3.15 at 137 MHz and 450 MHz respectively. The VSWR is acceptable at 137 MHz, but not at 450 MHz since the VSWR is above 2.

Table 11. Simulated Results of the Frequency Selective Tee for Best Isolation

Frequency (MHz)	VSWR	Isolation (dB)	
		VHF side	UHF side
137	1.65	-0.5	-14
450	3.15	-62	-1.4

Table 12. Simulated Results of the Frequency Selective Tee for Best VSWR

Frequency (MHz)	VSWR	Isolation (dB)	
		VHF side	UHF side
137	1.32	-0.4	-12
450	1.77	-4.2	-2.7

If we attempt to design a system with an acceptable VSWR at both frequencies, the isolation of each side decreases when operating at its respective frequency. When operating at 137 MHz, the VHF side creates a 0.4 dB loss and the UHF side allows for 12 dB of isolation. When receiving at 450 MHz, the UHF side has a 2.7 dB loss and the VHF side allows for 4.2 dB of isolation. The system does not perform well because the third resonance of the 137.5 MHz is near 450 MHz. These results are unacceptable since each antenna has an influence on the system regardless of the frequency of operation.

The advantages of the frequency selective tee is that the antennas are hard wired, there is not a possibility of switch failure, and the on-board computer of the satellite does not have to control a switch. Due to the poor isolation between the antennas and the possibility of a high VSWR, we may have to select a different solution in order to connect the antennas for optimal design.

4.5.3 Modification to Handset

The schematic of the handset shows a filter network at the single antenna connector [12]. The filter network consists of two low pass filters and a high pass filter. The filter network serves two purposes: filters out any frequencies about the UHF band, and isolate the VHF and UHF transceivers. The filter network acts like an RF tee allowing for the VHF and UHF frequencies to operate with there respective transceivers.

After this observation, we can physically isolate the VHF and UHF transceivers by modifying the filter network. This can be accomplished by cutting the connection between the VHF low pass filter, which connects in between the low pass filter connecting to the antenna and the high pass filter connecting to the UHF transceiver. We can connect a second antenna lead at this point. This can be seen in Figure 17.

The two main advantages of this method for connecting two antennas leading to optimal design are that the antennas are hard wired and there is not a possibility for switch failure. An additional advantage is that the system should be matched if the antennas are designed properly. The only true disadvantage of this method is internal modification. The filter components are very small and fragile. Soldering to the components is not trivial, especially when avoiding damage to the filter components. Based on the three methods for connecting the antennas to the handset, we will choose the modification of the handset. We will discuss the steps of the modification in Chapter 5 where all modifications of the handset are documented.

4.6 Summary

Through theoretical analysis and testing physical antennas on a model satellite, we determined a reasonable design for the VHF/UHF antennas. Also, we investigated a method to simply connect the antennas to the handset. This method has the advantage of not requiring computer control or insufficient isolation between the antennas. It has the disadvantage of requiring a handset modification.

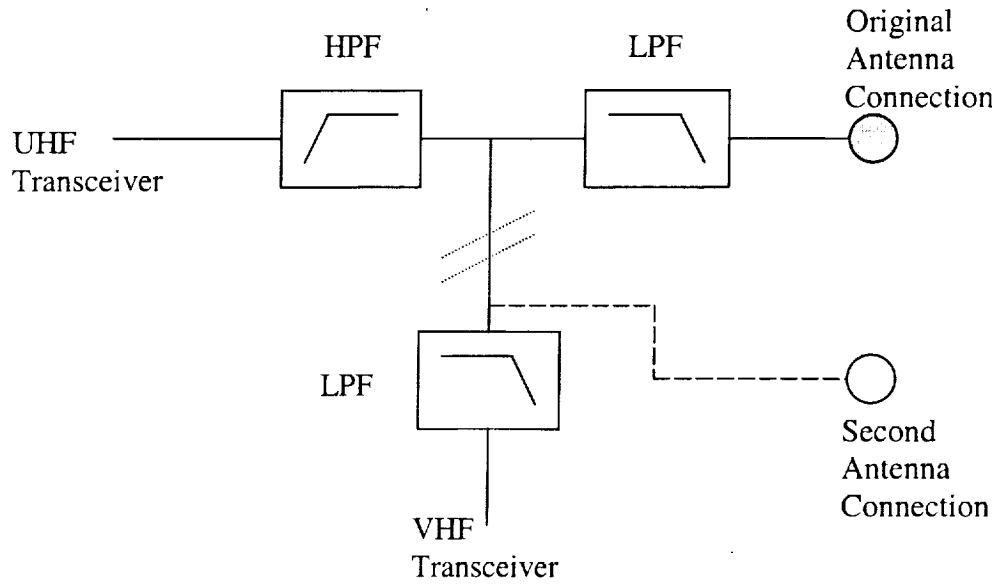


Figure 17. Modification to Handset in order to Connect Two Antennas



5 MODIFICATIONS TO KENWOOD TH-D7A

5.1 Overview

The Kenwood TH-D7A must be modified in order to connect different components to the handset. The first modification to be made is adding a second antenna connection. This is accomplished by disconnecting the filter network near the original antenna port.

5.2 Modification for Dual Antenna Configuration

In order to radiate all of the power generated by the transmitter for each band, the handset must be modified. As stated in Chapter 4, we chose to modify the filter network connected to the original antenna port. This involved disconnecting the low pass filter for the VHF transceiver. The point of disconnection is shown in Figure 17. Inside the handset, the low pass filter is a series and parallel network of inductors and capacitors. The first component that connects the low pass filter on the VHF transceiver side is the inductor labeled L in Figure 18.

We removed the inductor and covered the outside of the component with shrink-wrap. The shrink-wrap serves several purposes. The first is to avoid short circuits. When beginning this modification, we were unsure if any other metals would touch the inductor, since we were adding another connector. Then next reason for placing shrink-wrap around the inductor is for protection. The inductor is basically a coiled wire. The wire is coated protecting each turn of the coil from touching adjacent turns. If the coil were uncoated, it would act as a short without any

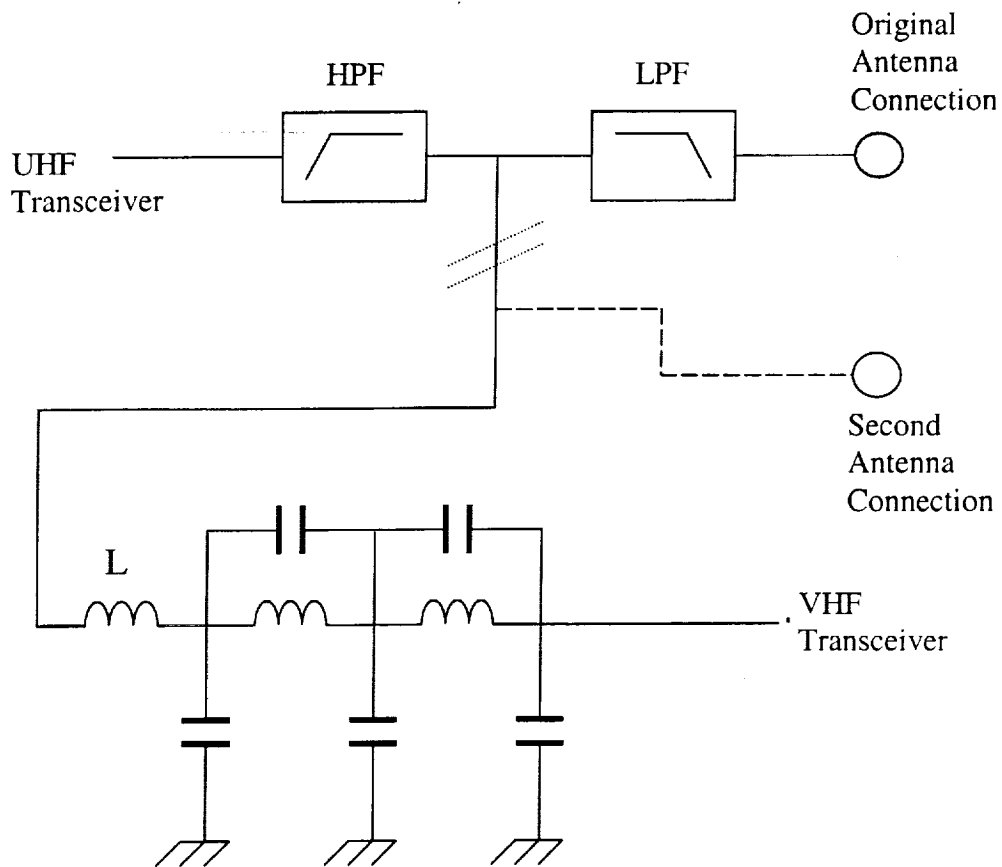


Figure 18. Modification to Handset in order to Connect Two Antennas

inductance. The last purpose of the shrink-wrap is to maintain the proper length of the coil. If the coil is pulled, the turns will separate causing the inductance to change. This change will affect the performance and cut-off frequency of the filter.

After removing the inductor and applying the shrink-wrap, we soldered one end back to the printed circuit board, PCB. We soldered the inductor to the point where it connects to the rest of the low pass filter on the VHF transceiver side. After completing this task, we soldered the opposite end of the inductor to the center

conductor of a coaxial cable. The outer conductor of the coaxial cable is connected to the ground of the handset. This configuration is the same for the original antenna port. At the opposite end of the coaxial cable is a female BNC connector. This allows the handset to connect to the antenna with a variety of options when testing. The final result of the modification is shown in Figure 19.

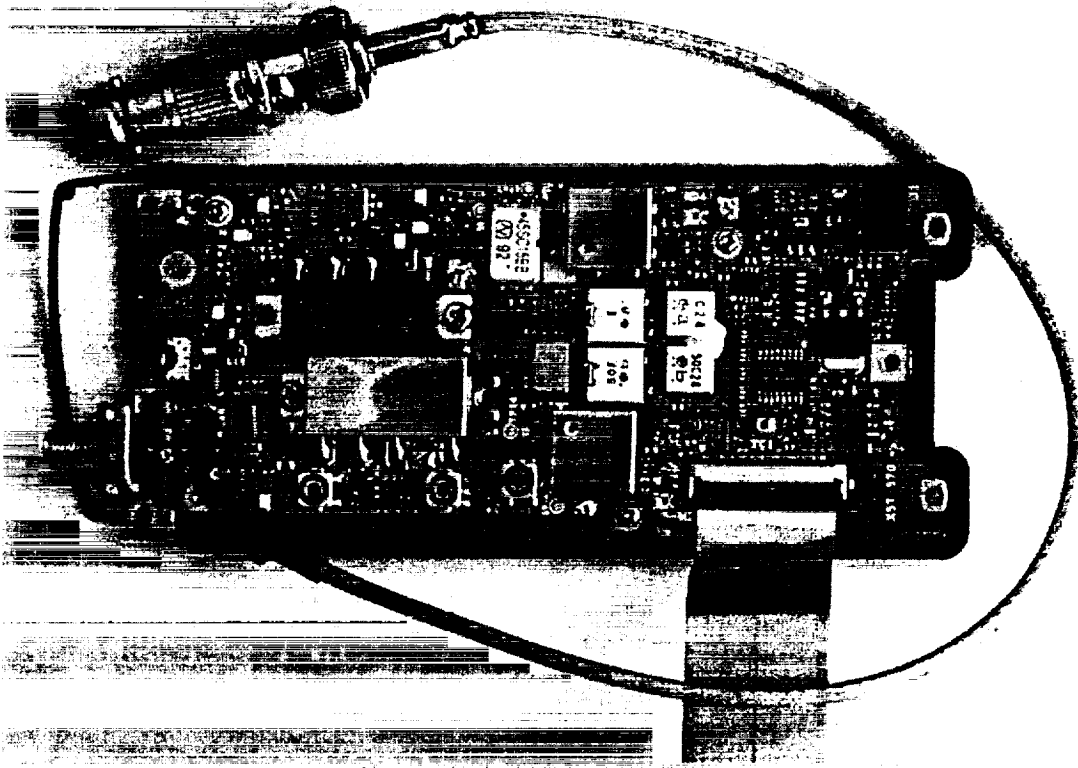


Figure 19. Kenwood TH-D7A After Antenna Modification

5.3 Streaming Data into the Handset

Due to the poor data throughput discovered earlier, we have analyzed the schematic of the handset in order to create a point in which we could inject a separate signal and operate the handset as a transmitter. During the analysis, we observed that the TNC has a separate pin that sends data at 9600 bps. This pin is labeled “T9600” on the MODEM-ASIC. This chip is labeled “IC510” in the schematic diagram. We soldered a wire to a near by resistor, which connects to the T9600 pin. The reason for soldering to the resistor instead of the pin is because the resistor displayed more contact surface area. This modification will not be needed if there is an S-band transmitter on the satellite. This modification is shown in Figure 20.

For operational monitoring reasons, the End-to-End Data System needs to monitor the UHF Received Signal Strength Indicator (RSSI). By analyzing the schematic of the handset, we observed that we could solder a wire near the ribbon cable connecting the two separate boards inside the handset. Again, we decided to solder to a resistor located near the ribbon cable connector. The output of the RSSI wire has not been analyzed; this is a follow-up task to characterize this signal for the End-to-End Data System. This modification can be viewed in Figure 20.

There are two wires appearing at each modification. A white wire was placed next to the original wire because the original wires are not apparent in a black and white photo. One white wire is placed next to the TNC bypass and the other white wire is placed next to the RSSI output.

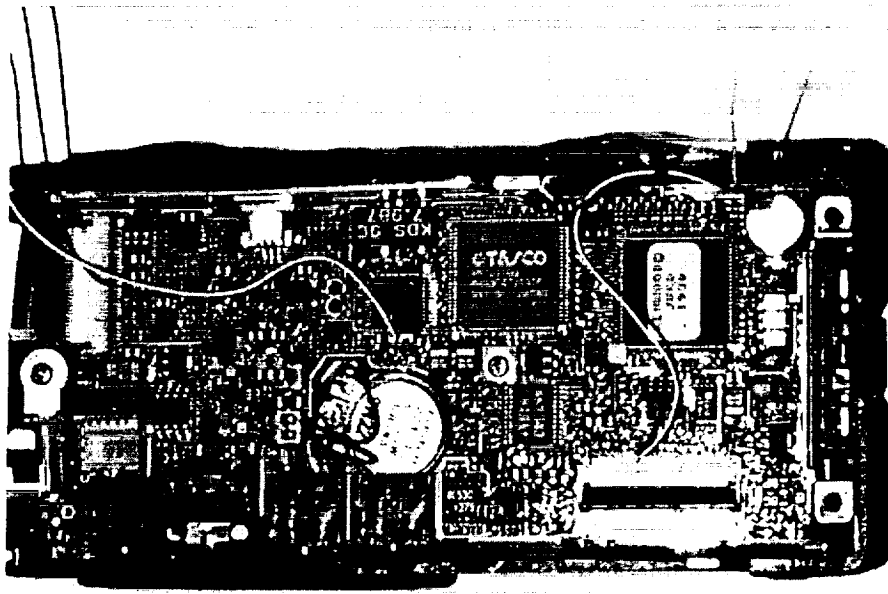


Figure 20. Bypass of the TNC and RSSI Modifications

5.4 Operation of Handset Outside of Amateur Frequencies

The Kenwood TH-D7A nominally operates in the amateur VHF/UHF bands. The normal frequencies of operation in the VHF band are 144-148 MHz. For the UHF band, the normal frequencies of operation are 438-450 MHz. In order to operate the handset outside of these bands, we removed two diodes. These modifications can be found by purchasing the service manual or via the Internet.

5.5 Future Modifications

In order for the handset to be space qualified, several modifications need to be made. The first modification is removing the two boards from the housing of the handset. These boards will be mounted inside an aluminum box, which will be mounted inside the satellite. The aluminum box supplies a radiation resistant housing in space. The box will also yield structural integrity to the unit.

Another modification is removing the Liquid Crystal Display (LCD) from the handset. The LCD is not needed for on-orbit operations. After removing the LCD, we must test the handset to ensure the functionality.

The speaker and microphone also need to be removed. This modification slightly reduces the weight of the unit and eliminates unused functions of the handset. The amplifier connecting to the speaker may also be removed since the speaker has been removed. Removing the amplifier connecting to the speaker may save power. Again, when removing one component at a time, the functionality must be re-verified.

Securing the leads and additional antenna connection is needed. Securing these connections avoids disconnecting the external components during the launch. The coaxial cable connecting the second antenna is of concern. The outer conductor of the cable needs to be connected to the ground as close as possible where the inner conductor of the cable connects to the inductor of the low pass filter. By connecting these conductors as close as possible, the coaxial cable holds a 50-ohm impedance.

6 S-BAND COMMUNICATIONS SYSTEM

6.1 Overview

This chapter describes the basic design of the S-band communications system. The S-band transmitter is being designed and built by a private company. Our responsibility is to deliver the specifications for the transmitter. In order to interface the transmitter with the End-to-End Data System on the satellite, we must design or buy a modem with certain specifications. The last component of the S-band communications system is the patch antenna. In this chapter, an approximation of the dimensions, gain, field patterns, and impedance analysis will be designed, analyzed, and documented.

6.2 Design Requirements

Many of the S-band system requirements are the same as the VHF/UHF design requirements. Since the S-band frequencies are much higher than the VHF/UHF frequencies, we can use more bandwidth in order to transmit the data. The increase in bandwidth allows the satellites to transfer data at a higher data rate. We are applying for allocation in the 2200-2290 MHz region. We will use this allocation for the return link.

The first requirement of the S-band communications system is to operate at a minimum data rate of 50 kbps. If we can supply enough power to the transmitter, we may be able to achieve a 100 kbps data rate. This will allow a satellite to transmit approximately 13 megabytes of data per day. The amount of data that could be

transmitted exceeds the requirement from CU of receiving approximately 8 megabytes of data per day.

Another design requirement of the communications system is to consume less than 5 watts of power. This requirement is the same for both the S-band and VHF/UHF communications systems. Weight and volume of the transmitter are also constraints. We would like the transmitter to consume the least amount of space and weight the least amount possible. The design must be able to meet the shock and vibration tests; therefore, the transmitter must be rigid.

6.3 Link Budget Analysis

This link budget analysis uses the same techniques as the VHF/UHF link budgets. There are a few parameters that differ from the previous link budgets. These differences are the gain of the transmit and receive antennas, free space losses, atmospheric losses, precipitation losses, and the power required to transmit at a higher data rate due to the increase in bandwidth. The S-band link budget is located in Table 13.

When considering various S-band ground stations, we created a design requirement that the transmitter must radiate 0.5 W. Assuming the antenna on the satellite has a gain of 5 dB and the total losses on the satellite are 3 dB with an additional 3 dB pointing loss, the EIRP is approximately 26 dBm. The next calculation in the link budget is the channel loss. With a maximum distance of 780 kilometers, the free space loss at the S-band frequencies is 157.1 dB. Since the

wavelength is fairly small, atmospheric and precipitation losses must be accounted for. We will allow a 1 dB loss from both the atmosphere and the precipitation. The total propagation loss is 158.1 dB.

The gains and losses of the receiver in the ground station must be calculated in the link budget. The current option for an S-band ground station has a 60-foot dish antenna. At 2200 MHz, the dish antenna has an approximate gain of 49 dB.

Assuming a 10 dB loss due to the pointing loss, line and component losses, implementation loss, and polarization mismatch, the received effective carrier power is -93.1 dBm.

The noise component of the link budget is calculated next. Using the standard thermal noise of -174 dB/Hz, a receive noise bandwidth of 48.8 dBHz assuming a 75 kHz bandwidth, and a noise figure of 3 dB, the effective noise power is -122.2 dBm. By subtracting the effective noise power from the received effective carrier power, we obtain the available carrier-to-noise ratio. This calculation yields a 29.1 dB available carrier-to-noise ratio. Assuming a 50 kbps data rate, we can calculate the available E_b/N_0 , which is 30.8 dB. After subtracting additional implementation losses and the required E_b/N_0 , the link margin is 15.4 dB. With this amount of margin, we should be able to close the link and receive the data correctly given a bit-error rate of 10^{-5} . Hopefully, the link budget is very conservative, which would allow the margin to increase.

Table 13. S-band Return Link Budget

Return S-Band Link	Value	Units
Transmitter (Tx)		
Tx Power, Pt	27.0	dBm
Tx Component Line Losses, Ltl	3.0	dB
Tx Antenna Gain (Peak), Gt	5.0	dB
Tx Pointing Loss, Ltp	3.0	dB
Tx Radome Loss, Ltr	0.0	dB
EIRP	26.0	dBm
Propagation		
Transmission Frequency, f	2200.0	MHz
Link Range, R	780.0	km
Propagation Factor, n	1.0	
Free Space Loss, Ls	157.1	dB
Atmospheric Absorption, Lpa	0.5	dB
Precipitation Absorption, Lpp	0.5	dB
Total Propagation Loss	158.1	dB
Receiver (Rx)		
Rx Antenna Gain (Peak), Gr	49.0	dB
Rx Polarization Loss, Lrpol	1.0	dB
Rx Pointing Loss, Lrp	3.0	dB
Rx Radome Loss, Lrr	0.0	dB
Rx Component Line Losses, Lrl	3.0	dB
Rx Implementation Losses, Lri	3.0	dB
Received effective carrier power	-93.1	dBm
Noise		
Standard Thermal Noise, kT	-174.0	dBm/Hz
Rx Noise Bandwidth, W	48.8	dBHz
Rx Noise Figure, NF	3.0	dB
Effective Noise Power	-122.2	dBm
Result		
Available CNR	29.1	dB
Data Rate	47.0	dBHz
Available Eb/No	30.8	dB
Implementation Losses	2.0	dB
Required Eb/No	13.4	dB
Margin	15.4	dB

6.4 Modem Selection

While searching for a modem for the VHF/UHF communications system, one was found that would meet the VHF/UHF and S-band modem requirements. The CMX589A High Speed GMSK Modem made by MX COM has a variable data rate [13]. The data rate can vary from 4 kbps to 200 kbps. The BT or bandwidth-data period factor can be set to 0.3 or 0.5. The BT is a ratio between the -3dB point of the filter and the data rate. By lowering the BT, fewer high frequency components are transmitted, thus producing a narrower bandwidth. The disadvantage of using a low BT is that intersymbol interference occurs.

The power consumption of the modem is extremely low. For a data rate of 50 kbps, the power consumed by the modem should be less than 20 mW. If we increase the data rate to 100 kbps, the consumed power will increase, but it is not unreasonable.

The modem offers several features, which will not be used for this project. We will only use the modem to transmit the data. With this in mind, all of the external components will not be variable. We should be able to configure the proper BT and data rate by using the correct resistors and capacitors. Testing the modem at 50 kbps or 100 kbps will need to be done will be done as a follow-up project.

6.5 S-band Antenna

A common antenna used for S-band communications is microstrip antenna. Microstrip antennas are often referred to as patch antennas. For 3CS, we will design

a circularly polarized (CP) square patch antenna. In order to tune a CP patch, we must trim the sides of the patch to obtain equal amplitude currents in phase quadrature.

We will modify the Mathcad program [14] to design and analyze our patch antenna. The program, plots, and analysis are located in Appendix E. First, we will observe the dimensions of the patch.

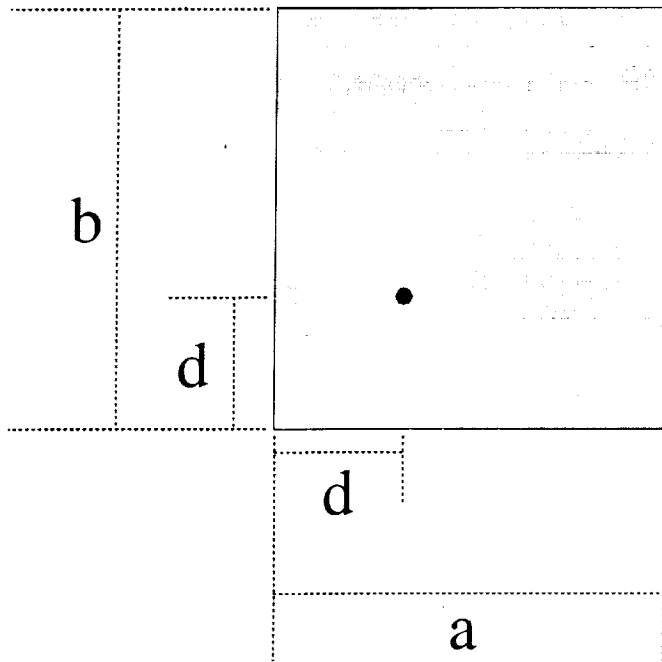


Figure 21. Dimensions of Patch Antenna

The length and height of the patch antenna are represented by a and b , respectively. The length of the antenna is 0.04202 meters and the height of the antenna is 0.04338 meters. The feed is connected at the distance, d , from the edges of the antenna. After determining the input impedance due to the different edges of the

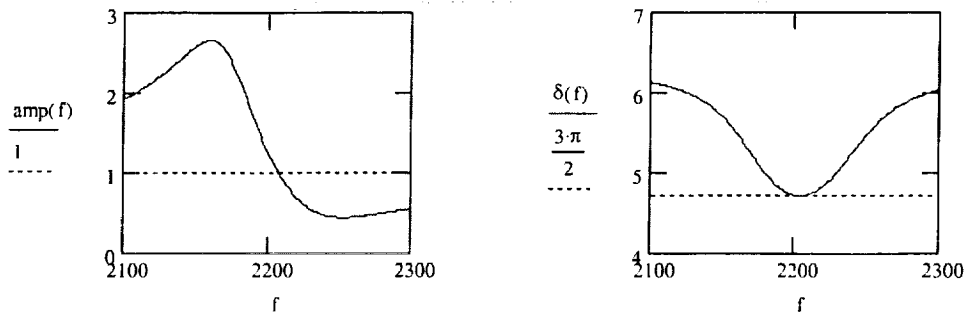


Figure 22. Amplitude and Phase Split of the Patch as a Function of Frequency

patch, we can plot the relative amplitude and phase of the current. Figure 22 illustrates that the antennas are right hand circularly polarized, or RCHP.

The amplitudes of the currents are equal at a frequency slightly higher than the design frequency. The currents are in phase quadrature at the same slightly higher frequency because one mode is inductive reactive while the orthogonal one is capacitive reactive. This condition is achieved when zero reactance occurs at the slightly higher frequency. The length and height should be the same before trimming. When determining the length and height of the patch, we used the dielectric constant of the substrate when we should have calculated the effective dielectric constant first and used its value. There is no point in determining the exact length and height of the patch until we know the exact frequency allocated to 3CS. The axial ratio of the patch is equal to one at a slightly higher frequency than 2200 MHz. At this particular frequency, circular polarization is obtained.

In order to connect the antenna to the S-band transmitter, we must calculate the VSWR on the line. If the VSWR is too high, the transmitter could be damaged. An acceptable value for the VSWR is less than two. After calculating the VSWR when connecting to a 50-ohm line, we see in Figure 23 that it is less than two. The bandwidth with an acceptable VSWR is approximately 85 MHz. By analyzing the 20 log base 10 of the axial ratio plot in Appendix D, the bandwidth under 6 dB is 44 MHz. Using the frequencies at the 6 dB points, the PML to RHCP is less than 0.5 dB. The full scale gain, or FSG, varies from 6.485 dB to 6.553 dB over the band.

The gain of the patch antenna can be calculated after we analyze the field patterns. In order to simplify the analysis, we will assume that the field along the

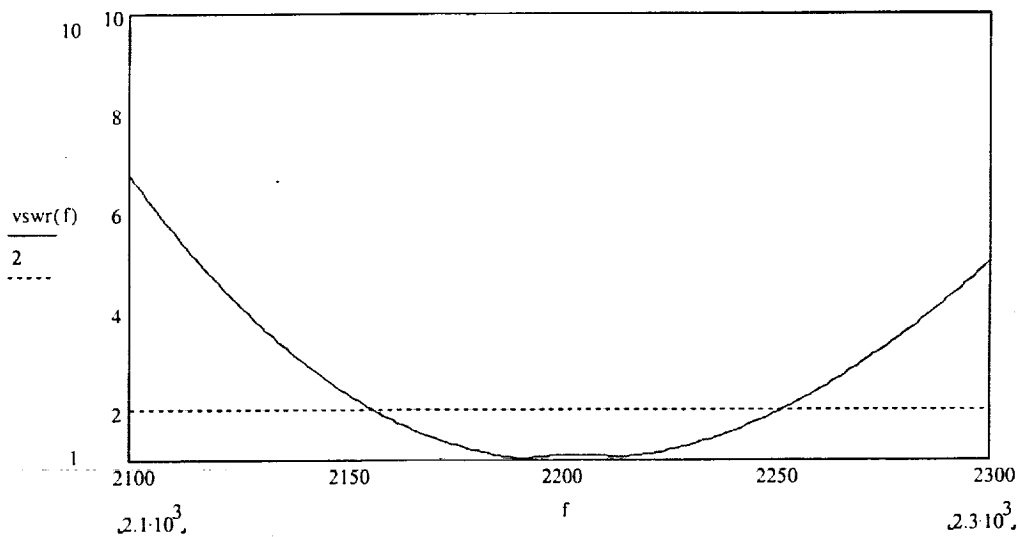


Figure 23. VSWR of Antenna Connecting to a 50-ohm Line

radiating edge is uniform. From this model, the fields at the edges are approximately one-half wavelength apart; therefore, we can assume the radiating edges act as an array. Using the program described in Appendix D₂ we can obtain the several power pattern plots. These plots can be viewed in the same program. The patch obtains CP on axis and as we deviate off axis, polarization mismatch losses occur. An example of the polarization mismatch is shown in Figure 24. When the two fields are of equal amplitude, CP is obtained; otherwise, slight polarization mismatch losses occur. Polarization mismatch occurs because the Φ component of the E-field is larger than the θ component off axis.

With the field patterns known, we can compute the gain of the patch antenna at the designed frequency. After computing the directivity of the patch, the gain is

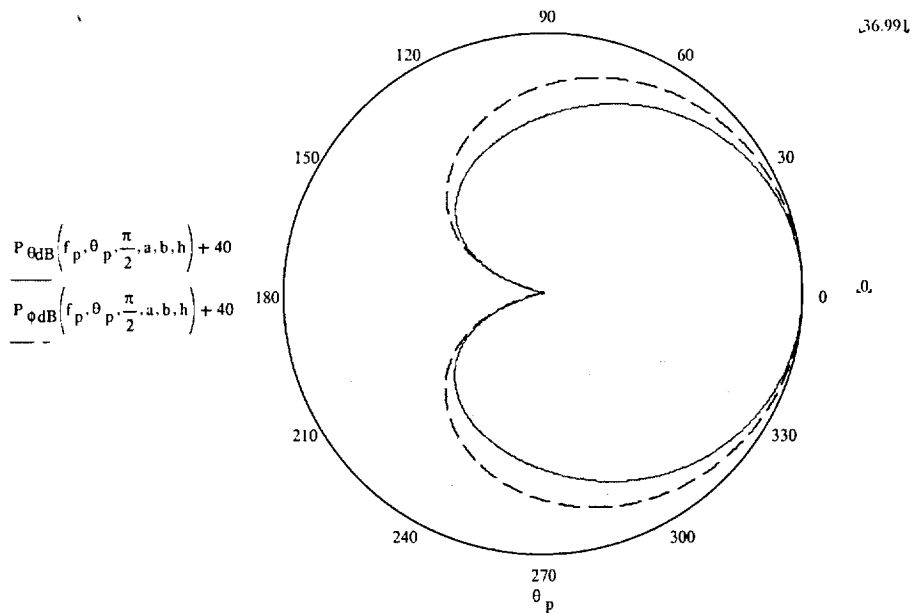


Figure 24. Component Power Patterns (10 dB/division) in the $\Phi=\pi/2$ Plane

simply the multiplication of the directivity and the efficiency of the antenna. The efficiency of a patch antenna is usually close to one hundred percent; therefore, the directivity of the patch is a very close estimate of the gain. By converting the directivity of the patch to decibels, the full-scale gain of the patch is approximately 6.5 dB at 2200 MHz.

6.6 Summary

We have verified that the S-band transmitter under consideration can close the link at the desired data rate and BER. The CMX589A High Speed GMSK Modem made by MX COM is the recommended modem for the S-band system. Also, we have designed a reasonable antenna system to meet the specifications.

7 CONCLUSION

7.1 Summary

The overall constraints and requirements for the communications system are providing a minimum data rate of 1200 bps for the crosslink and forward link, 9600 bps for the return link while operating on a regulated 5-volt bus and consuming fewer than 5 W. Based upon these constraints and requirements, we have selected the Kenwood TH-D7A handset. The handset offers the right services, can be modified for the frequency bands, and can interface to the End-to-End Data System. We determined that the handset has operational problems, which can be overcome if used as a secondary transmitter. The handset will support commands to each satellite and provide the crosslink services.

For the primary return link, we have decided to use an S-band communications system. We have provided a preliminary S-band system design to meet the requirements. This system consists an S-band transmitter built by a private vendor, a GMSK modem, and a patch antenna.

7.2 Recommended Design

The overall system consists of two radios that will provide the necessary services. The radios can be operationally controlled by the End-to-End Data System. Due to power limitations, simultaneous operation of the radios is prohibited. A second UHF receiver is suggested for a backup if the handset fails and if the mass

budget and internal volume allow. The overall system suggested would look like Figure 25.

In Figure 25, Nanosatellite #1 is composed of the entire communications system. All three nanosatellites will contain the same communications system as Nanosatellite #1. For simplicity, Nanosatellite #2 is only showing the crosslink options in this illustration. This diagram illustrates how one satellite can communicate with the ground stations and the other satellites in the constellation. The S-band transmitter is used as the primary return link for image data and the TH-D7A's UHF receiver is used for the primary forward link for commands. The TH-D7A will operate at 144.39 MHz or 430 MHz for the crosslink. The VHF transmitter on the TH-D7A will provide a secondary return link for small images and health/status data.

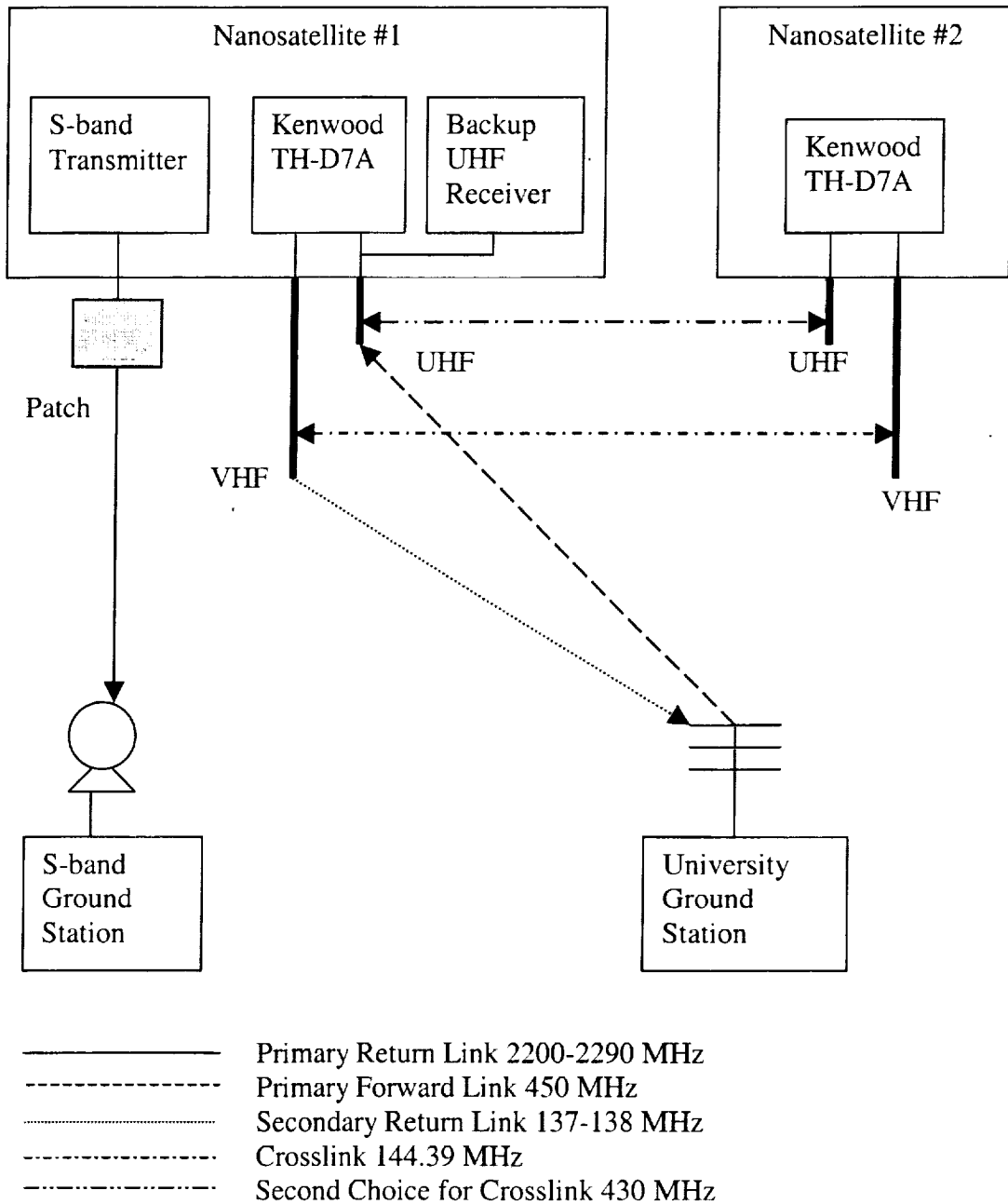


Figure 25. Recommended Communications System

APPENDICES

A. LABVIEW VIRTUAL INSTRUMENTS

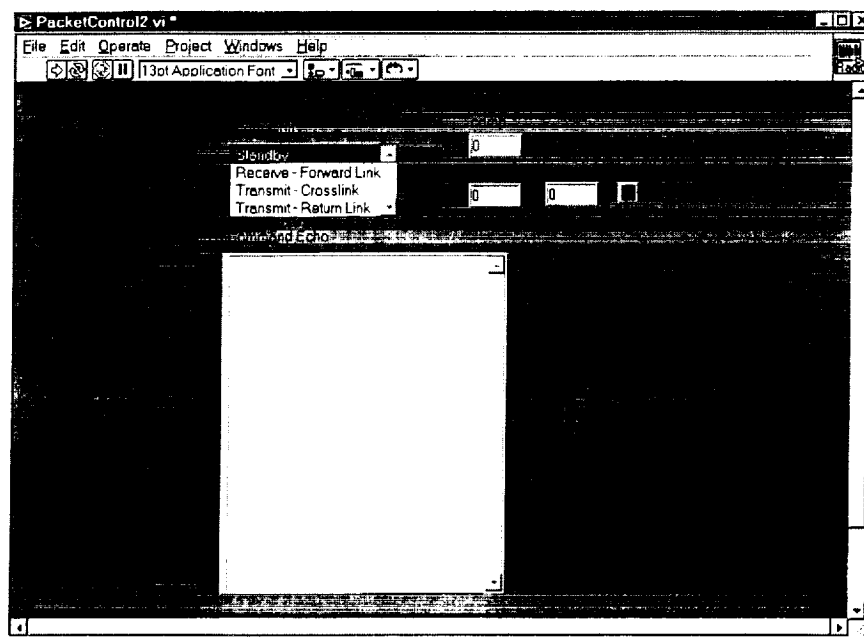


Figure A1. LabVIEW Control Panel

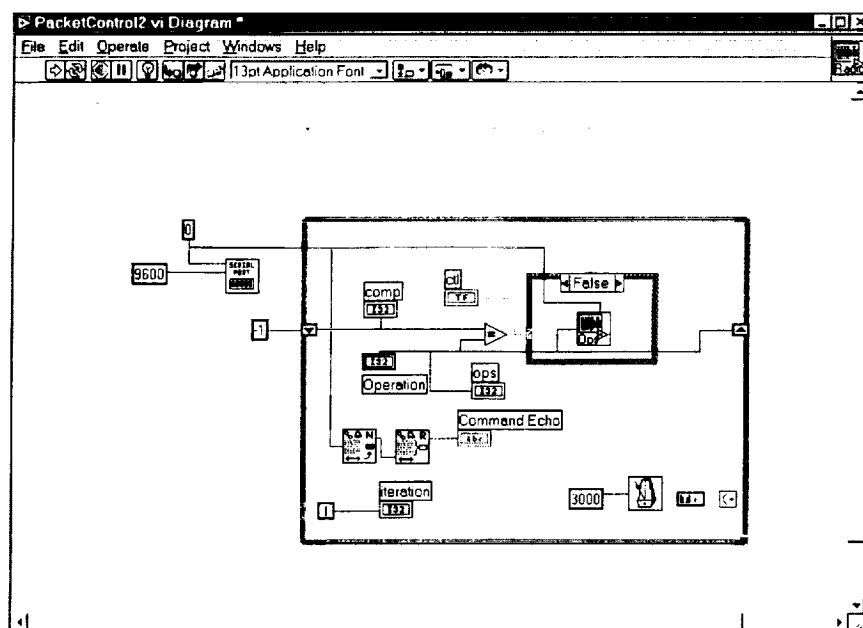


Figure A2. Control Panel VI

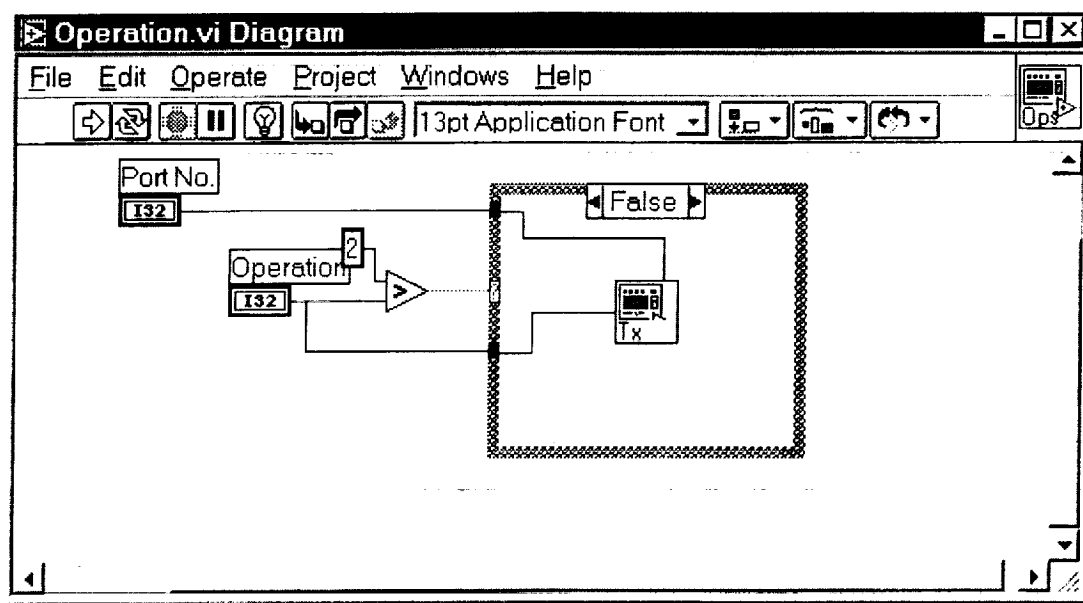


Figure A3. Operation VI Calling Transmit VI

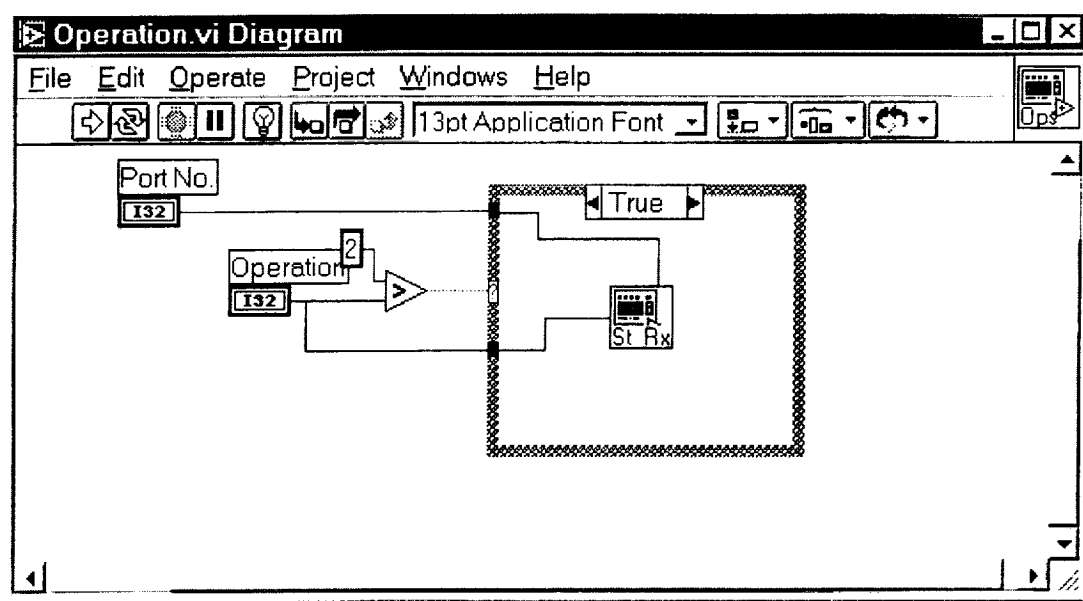


Figure A4. Operation VI Calling Stby_Rx VI

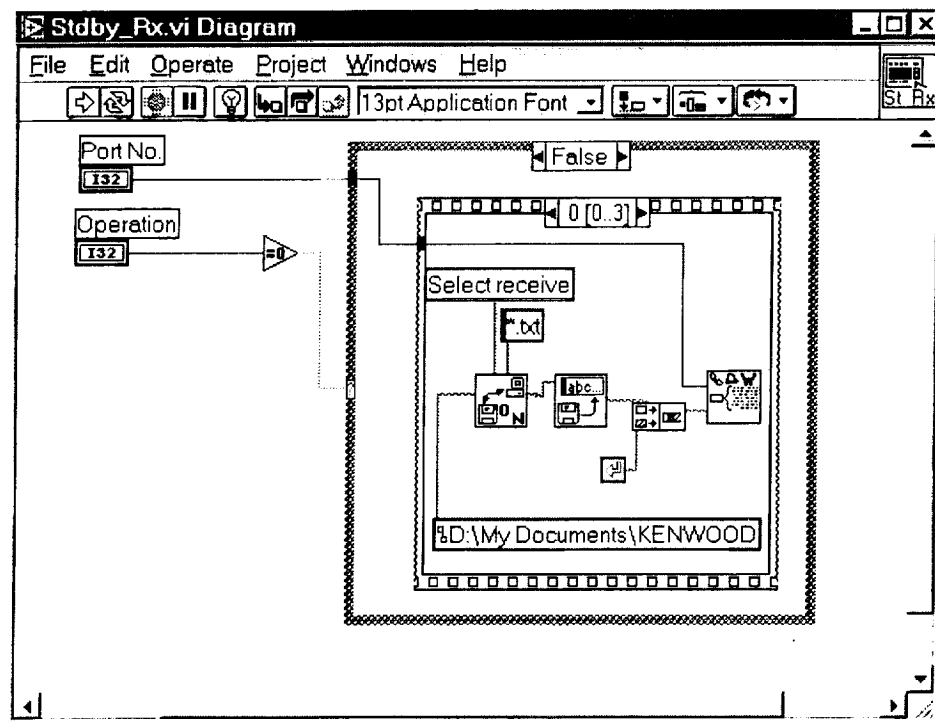


Figure A5. Stdbby_Rx VI Prompting User to Select the Receive File

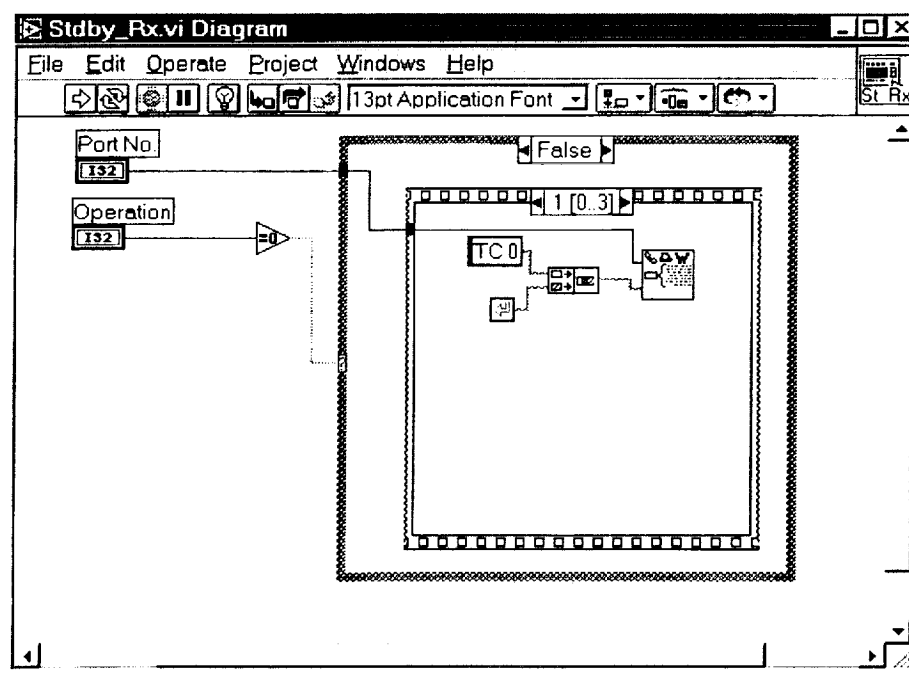


Figure A6. Stdbby_Rx VI Turns ON the TNC on the Handset

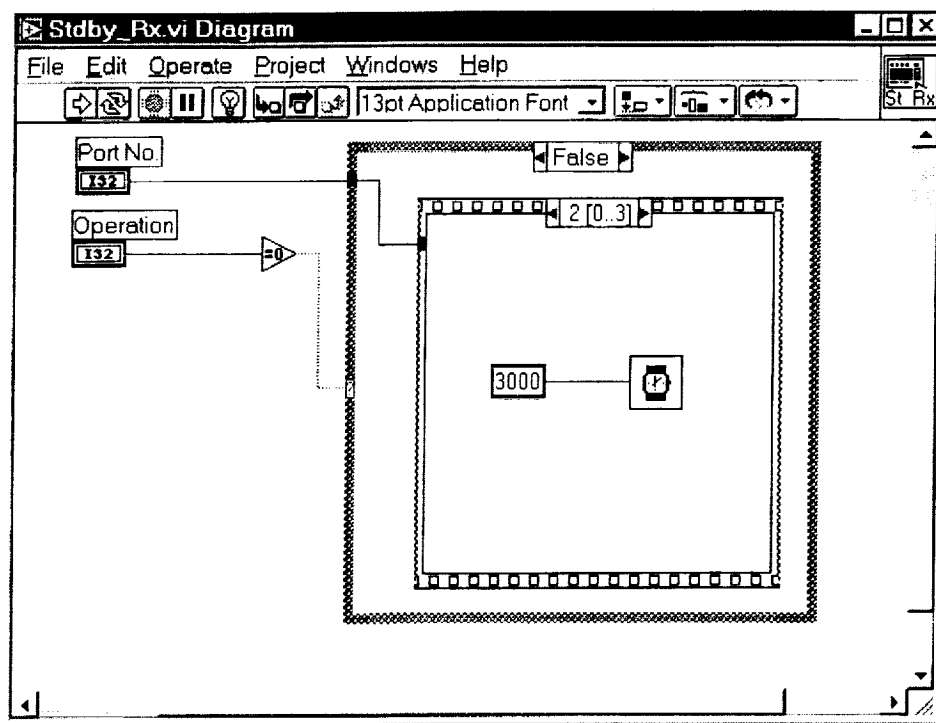


Figure A7. Stdbby_Rx VI Allowing TNC to Turn ON

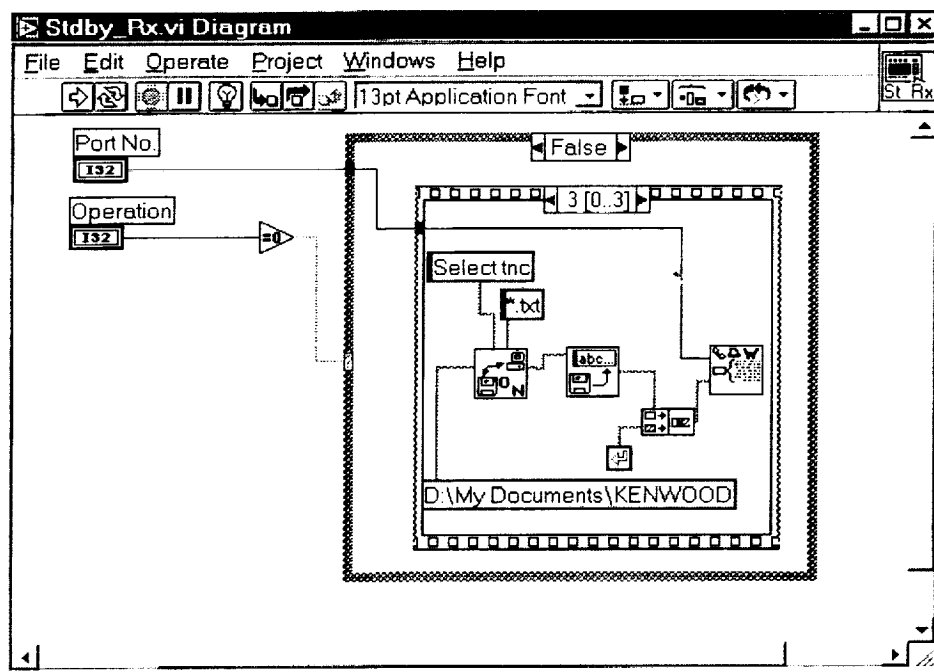


Figure A8. Stdbby_Rx VI Prompting User to Enter TNC File

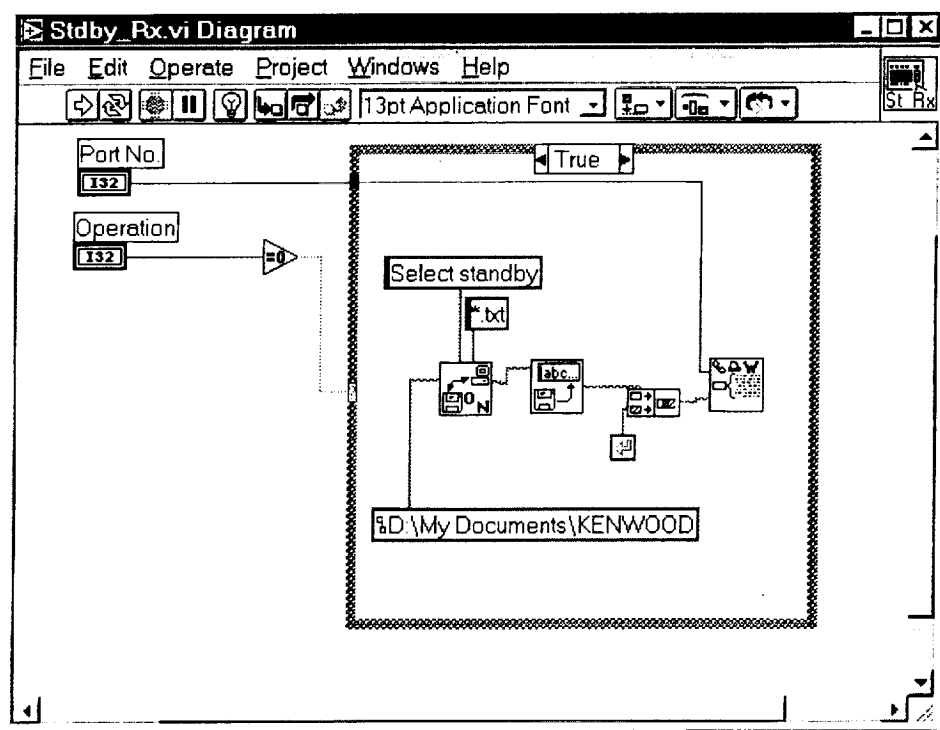


Figure A9. Stdbby VI Prompts User to Enter the Standby File

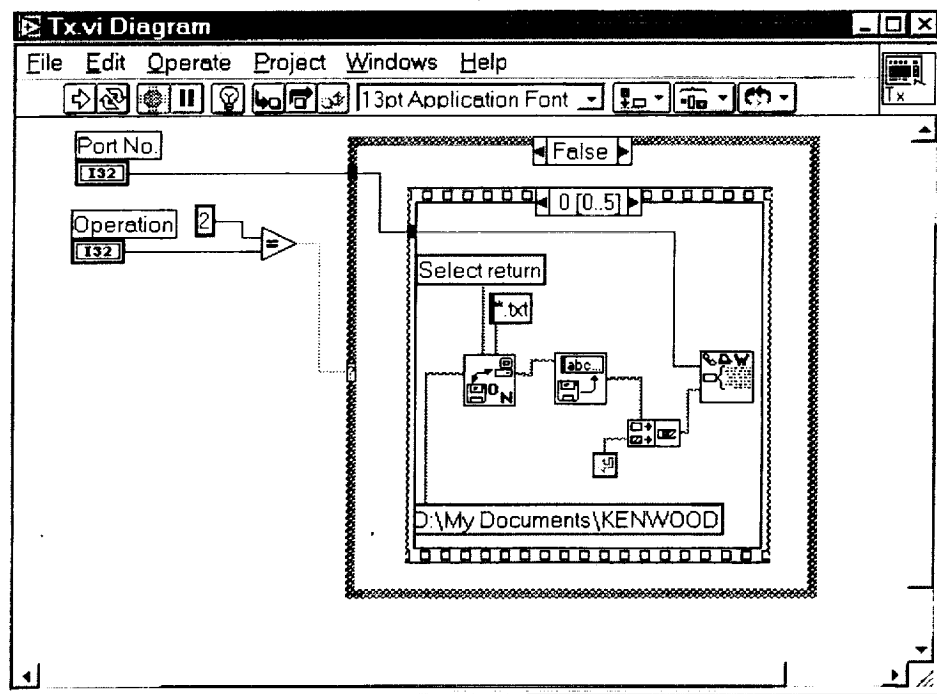


Figure A10. Tx VI Prompting User to Enter Return File

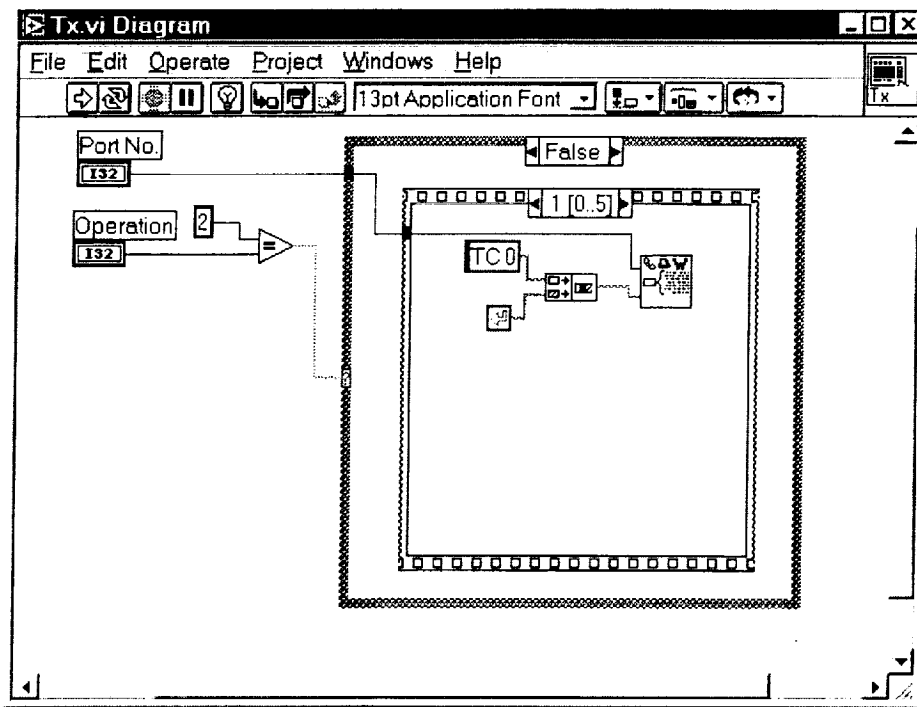


Figure A11. Tx VI Turns ON the TNC in the Handset

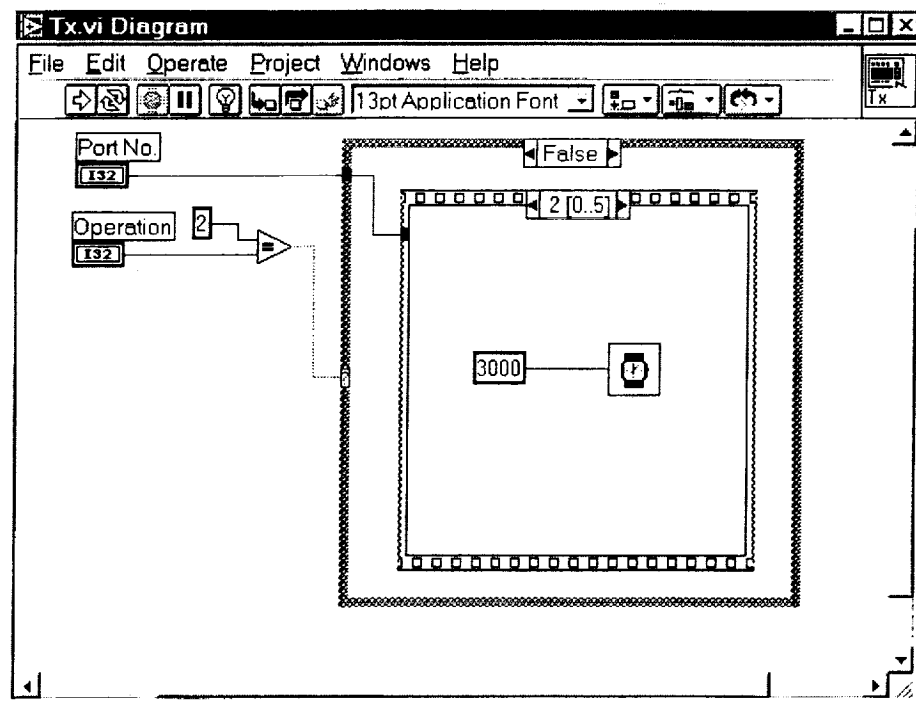


Figure A12. Tx VI Allows the TNC to Turn ON

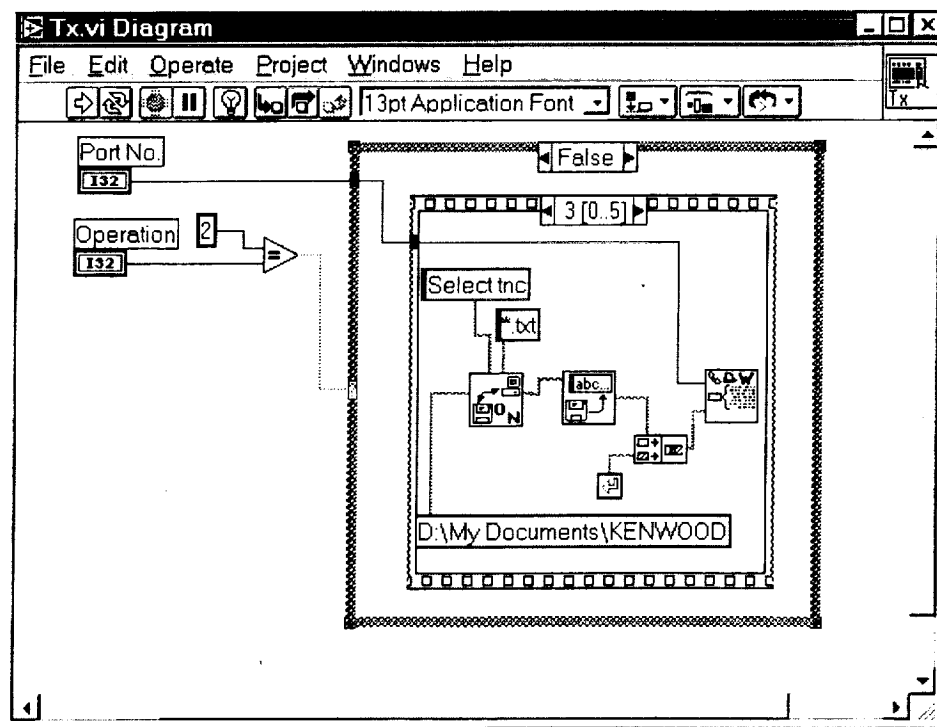


Figure A13. Tx VI Prompts User to Enter TNC File

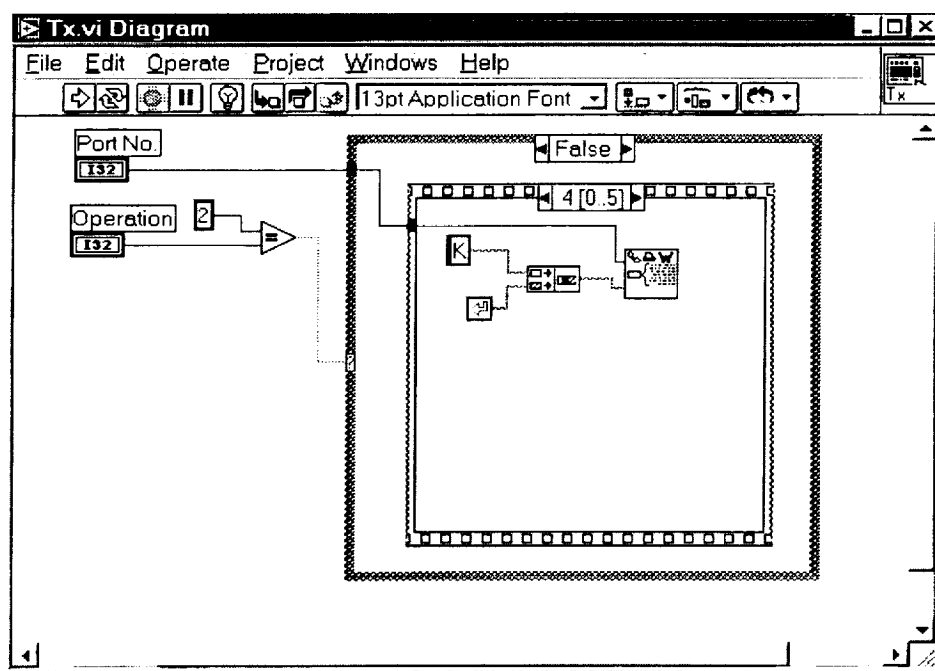


Figure A14. Tx VI Places the Handset in Converse Mode

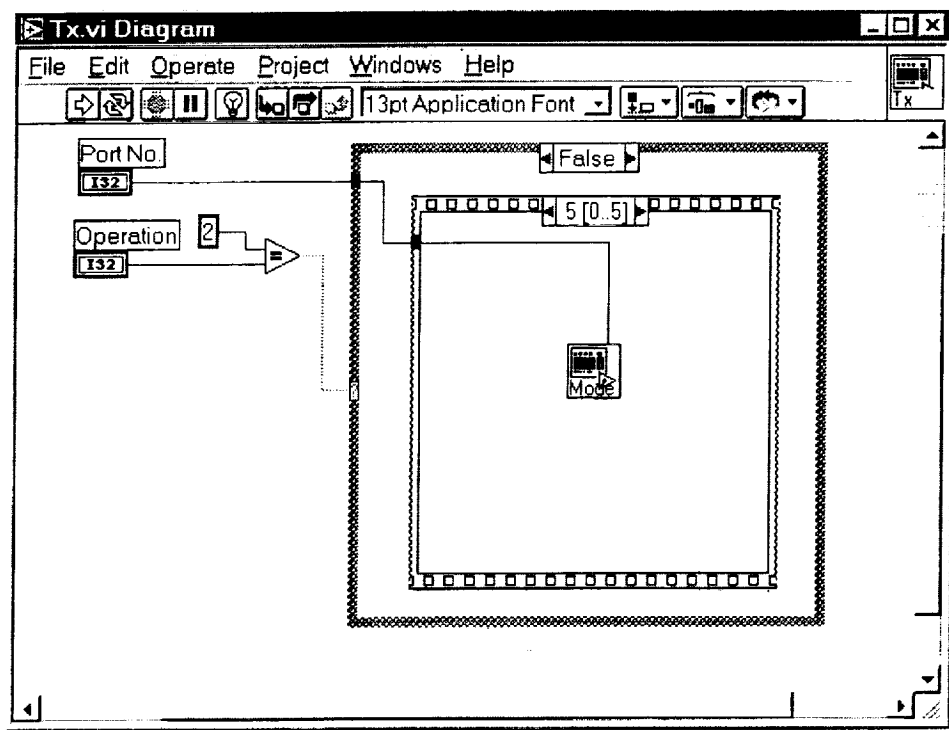


Figure A15. Tx VI Calls the ModeSelect3 VI

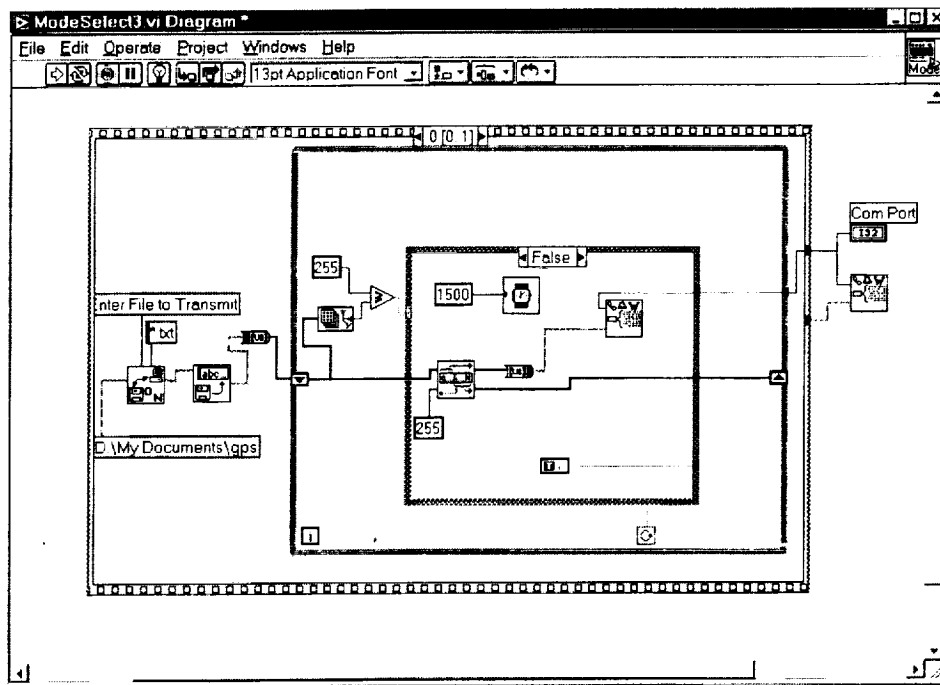


Figure A16. ModeSelect3 VI Sends a Full Packet and Creates a Delay

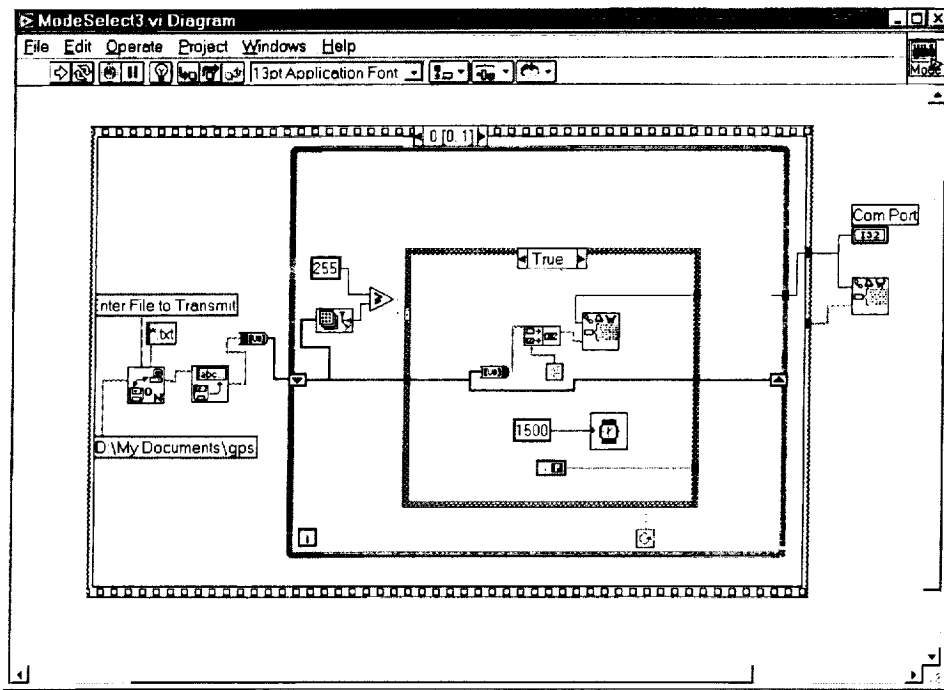


Figure A17. ModeSelect3 VI Sends the Remaining Portion of the File

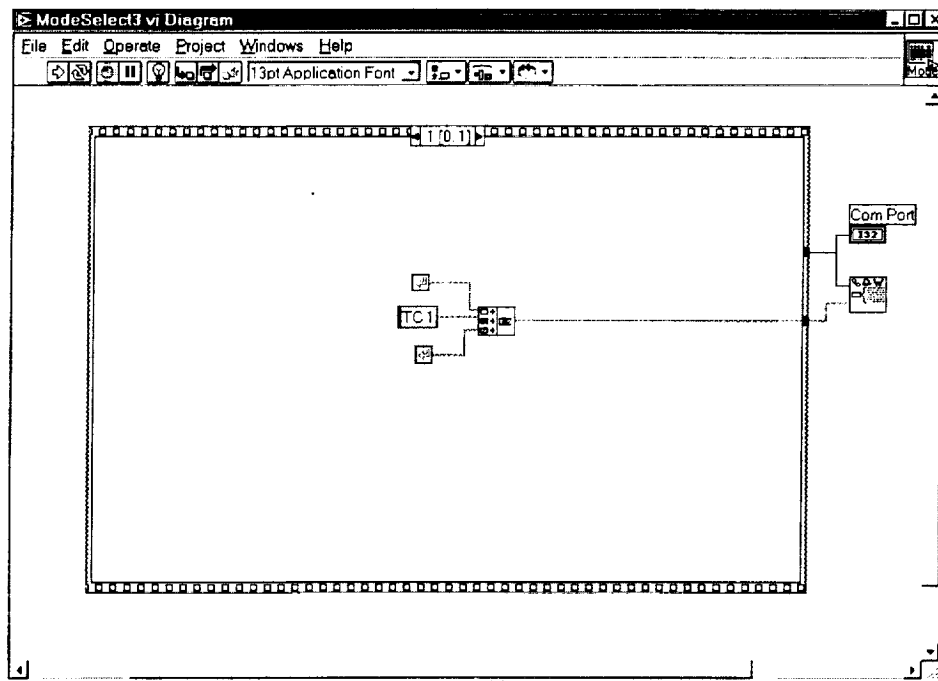
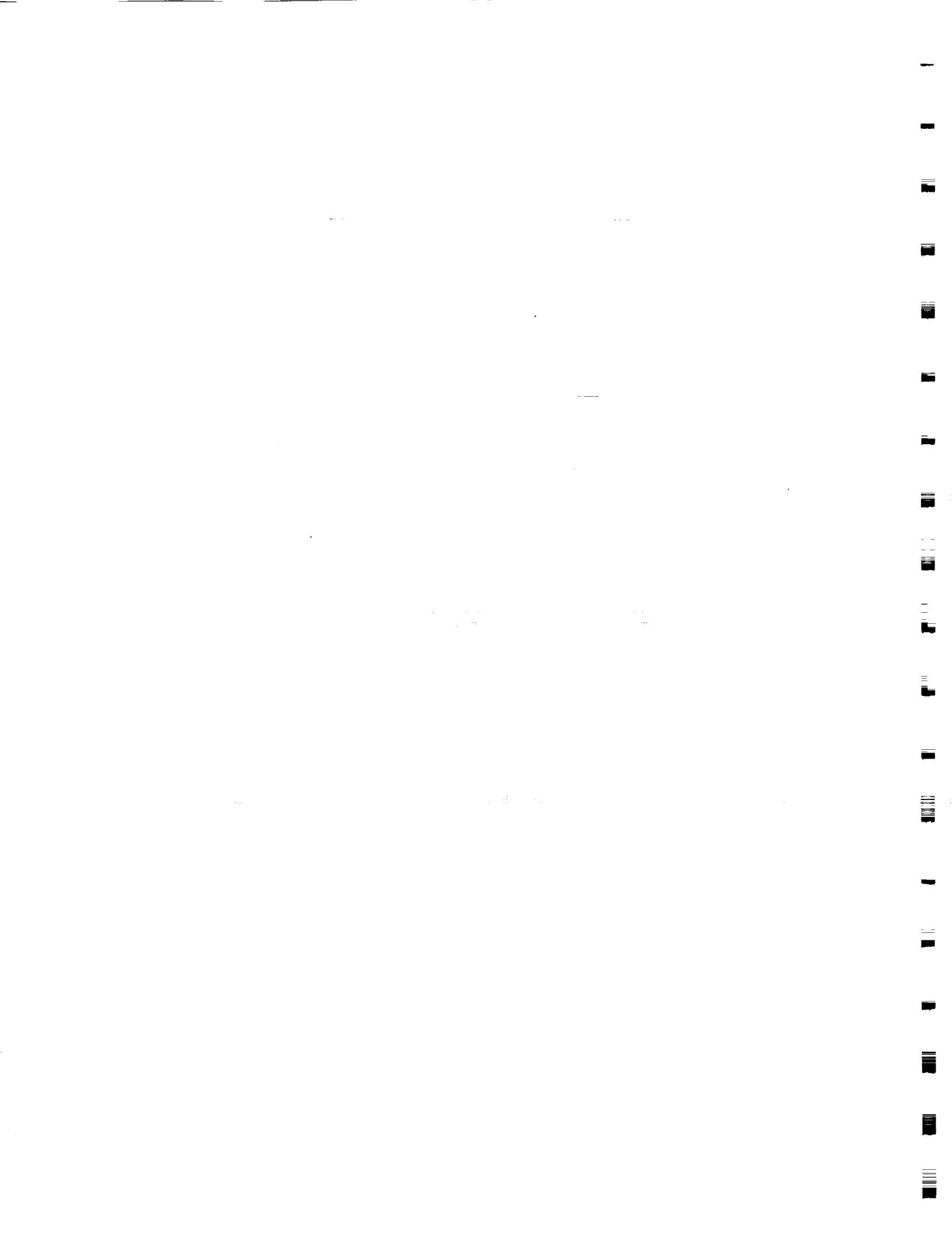


Figure A18. ModeSelect3 VI Turns OFF the TNC



B. DERIVATION OF FIELD EQUATIONS

Here, we derive the field equations for the VHF/UHF monopole antennas. After solving Maxwell's equations, we may take the following approach [9].

First, we will assume a z-directed sinusoidal current distribution. Assume that the current is zero outside the described boundary.

$$I(z') = I_0 \sin[\beta(L - z')] \quad \text{for } 0 \leq z' \leq L$$

Define the vector potential:

$$A_z = \frac{\mu_0 e^{-j\beta r}}{4\pi r} \int_0^L I(z') e^{j\beta(\hat{r} \cdot \bar{r}')} dz'$$

$$\hat{r} = \hat{x} \sin(\theta) \cos(\phi) + \hat{y} \sin(\theta) \sin(\phi) + \hat{z} \cos(\theta)$$

$$\bar{r} = \hat{z} z'$$

$$\therefore \hat{r} \cdot \bar{r} = z' \cos(\theta)$$

Next, we can substitute all values in the vector potential equation and solve.

$$A_z = \frac{\mu_0 e^{-j\beta r}}{4\pi r} \int_0^L I_0 \sin[\beta(L - z')] e^{j\beta z' \cos(\theta)} dz'$$

$$A_z = \frac{I_0 \mu_0 e^{-j\beta r}}{4\pi r} \int_0^L \sin[\beta(L - z')] e^{j\beta z' \cos(\theta)} dz'$$

Using the following integration and substitution:

$$\int \sin(a + bx) e^{cx} = \frac{e^{cx}}{b^2 + c^2} [c \sin(a + bx) - b \cos(a + bx)]$$

$$\text{and } c = j\beta \cos(\theta), \quad b = -\beta, \quad a = \beta L$$

We can obtain this equation.

$$A_z = \frac{I_o \mu_o e^{-j\beta r}}{4\pi r} \left[\frac{e^{j\beta \cos(\theta) z'}}{(-\beta)^2 + (j\beta \cos(\theta))^2} [j\beta \cos(\theta) \sin(\beta L - \beta z') + \beta \cos(\beta L - \beta z')] \right]_0^L$$

$$A_z = \frac{I_o \mu_o e^{-j\beta r}}{4\pi r} \left[\frac{e^{j\beta \cos(\theta) L}}{(-\beta)^2 + (j\beta \cos(\theta))^2} [j\beta \cos(\theta) \sin(\beta L - \beta L) + \beta \cos(\beta L - \beta L)] \right]$$

$$- \frac{I_o \mu_o e^{-j\beta r}}{4\pi r} \left[\frac{e^{j\beta \cos(\theta) 0}}{(-\beta)^2 + (j\beta \cos(\theta))^2} [j\beta \cos(\theta) \sin(\beta L - 0) + \beta \cos(\beta L - 0)] \right]$$

$$A_z = \frac{I_o \mu_o e^{-j\beta r}}{4\pi r} \left[\frac{e^{j\beta \cos(\theta) L}}{\beta^2 - \beta^2 \cos^2(\theta)} \beta - \frac{1}{\beta^2 - \beta^2 \cos^2(\theta)} [j\beta \cos(\theta) \sin(\beta L) + \beta \cos(\beta L)] \right]$$

After canceling the beta terms and substitution, we can reduce this equation to:

$$A_z = \frac{I_o \mu_o e^{-j\beta r}}{4\pi r} \frac{1}{\beta \sin^2(\theta)} [e^{j\beta \cos(\theta) L} - (j \cos(\theta) \sin(\beta L) + \cos(\beta L))]$$

Since, the vector potential is in terms of r and theta, we shall change coordinate systems. We will change to the spherical coordinate system. We will use the following matrix multiplication:

$$\begin{bmatrix} A_r \\ A_\theta \\ A_\phi \end{bmatrix} = \begin{bmatrix} \sin(\theta) \cos(\phi) & \sin(\theta) \sin(\phi) & \cos(\theta) \\ \cos(\theta) \cos(\phi) & \cos(\theta) \sin(\phi) & -\sin(\theta) \\ -\sin(\phi) & \cos(\phi) & 0 \end{bmatrix} \begin{bmatrix} A_x \\ A_y \\ A_z \end{bmatrix}$$

This leaves us with these terms:

$$\begin{bmatrix} A_r \\ A_\theta \\ A_\phi \end{bmatrix} = \begin{bmatrix} A_z \cos(\theta) \\ -A_z \sin(\theta) \\ 0 \end{bmatrix}$$

We usually only analyze the theta and phi components of a vector in this situation, which leaves us with only the theta component. After substitution, the vector potential is:

$$A_{\theta} = \frac{-I_o \mu_o e^{-j\beta r}}{4\pi r} \frac{1}{\beta \sin(\theta)} \left[e^{j\beta \cos(\theta)L} - (j \cos(\theta) \sin(\beta L) + \cos(\beta L)) \right]$$

Now, we are ready to compute the E-field using the transformation shown below.

$$E_{\theta} = -j\omega A_{\theta}$$

Last, after a few minor substitutions, the final E-field equation is:

$$E_{\theta} = \frac{I_o \eta e^{-j\beta r}}{4\pi r} \frac{1}{\sin(\theta)} \left[e^{j\beta \cos(\theta)L} - (j \cos(\theta) \sin(\beta L) + \cos(\beta L)) \right]$$

C. VHF/UHF ANTENNA DESIGN AND ANALYSIS

We will find the input impedance of the VHF antenna.

INPUT IMPEDANCE consists of the radiation resistance and reactance as well as the ohmic resistance. First define Sine and Cosine integrals. Note: Due to numerical difficulties, calculate Cin and then Ci from that result.

$$j := \sqrt{-1}$$

$$\text{Si}(x) := \int_0^x \frac{\sin(t)}{t} dt \quad \text{Cin}(x) := \int_0^x \frac{1 - \cos(t)}{t} dt \quad \text{Ci}(x) := 0.5772 + \ln(x) - \text{Cin}(x)$$

The radiation resistance of a monopole of length L is given by

$$\text{Rr}(\beta L) := 60 \cdot \left[\text{Cin}(\beta L) + \left(\frac{\sin(\beta L)}{2} \right) \cdot (\text{Si}(2 \cdot \beta L) - 2 \cdot \text{Si}(\beta L)) \dots \right. \\ \left. + \left(\frac{\cos(\beta L)}{2} \right) \cdot \left(0.5772 + \ln\left(\frac{\beta L}{2}\right) + \text{Ci}(2 \cdot \beta L) - 2 \cdot \text{Ci}(\beta L) \right) \right]$$

The radiation reactance of a monopole of length L and radius a is given by

$$\text{Xr}(\beta L, \beta, a) := 30 \cdot \left[2 \cdot \text{Si}(\beta L) + \cos(\beta L) \cdot (2 \cdot \text{Si}(\beta L) - \text{Si}(2 \cdot \beta L)) \dots \right. \\ \left. + (-1) \cdot \left[\sin(\beta L) \cdot (2 \cdot \text{Ci}(\beta L) - \text{Ci}(2 \cdot \beta L) - \text{Ci}\left(2 \cdot \frac{\beta \cdot a^2}{\beta L}\right)) \right] \right]$$

The medium is free space. $\epsilon_0 := 8.854 \cdot 10^{-12}$ $\mu_0 := 4 \cdot \pi \cdot 10^{-7}$

The ohmic resistance of a monopole of length L, with sinusoidal current, is given by

$$\text{R}_\Omega(\beta, L, a, \text{R}_{\text{sur}}) := \frac{\text{R}_{\text{sur}} \cdot L}{4 \cdot \pi \cdot a} \cdot \left(1 - \frac{\sin(\beta \cdot L)}{\beta \cdot L} \right)$$

Initialize variables and loops for calculations, set the start, end frequencies and the number of impedance calculation points.

$$\text{ORIGIN} := 1$$

$$\text{N}_f := 101 \quad i := 1..N_f \quad f_s := 135 \text{ MHz} \quad f_e := 145 \text{ MHz}$$

$$f_i := (i-1) \cdot \frac{f_e - f_s}{(\text{N}_f - 1)} + f_s \quad \beta_i := 2 \cdot \pi \cdot f_i \cdot 10^6 \cdot \sqrt{\mu_0 \cdot \epsilon_0} \quad \lambda_i := \frac{10^{-6}}{f_i \cdot \sqrt{\mu_0 \cdot \epsilon_0}}$$

Select an antenna length plus the height of the satellite, L, and diameter, d, in meters. Assume the wire is steel

$$L := \frac{21.5 + 10}{39.37} \quad \sigma := 2 \cdot 10^6 \quad \text{S/m}$$

$$L = 0.8 \quad \text{m} \quad d := \frac{1}{39.37} \quad \text{m} \quad a := \frac{d}{2} \quad R_s(f, \mu_0, \sigma) := \sqrt{\frac{\pi \cdot f \cdot 10^6 \cdot \mu_0}{\sigma}}$$

$$\frac{L}{\lambda_{Nf}} = 0.38698 \quad \frac{a}{\lambda_{Nf}} = 6.143 \cdot 10^{-3}$$

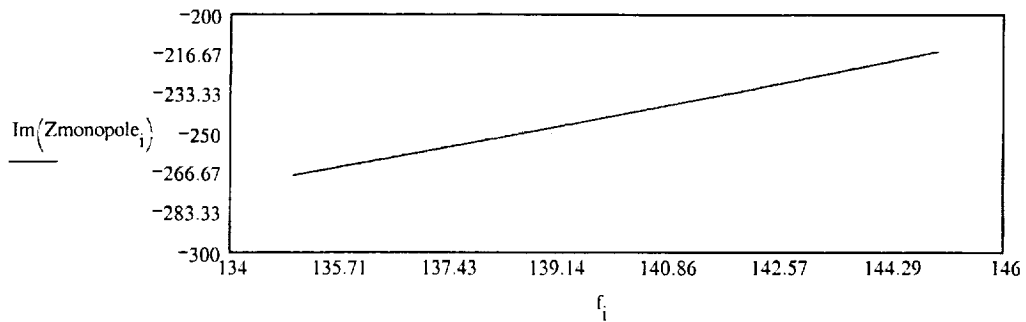
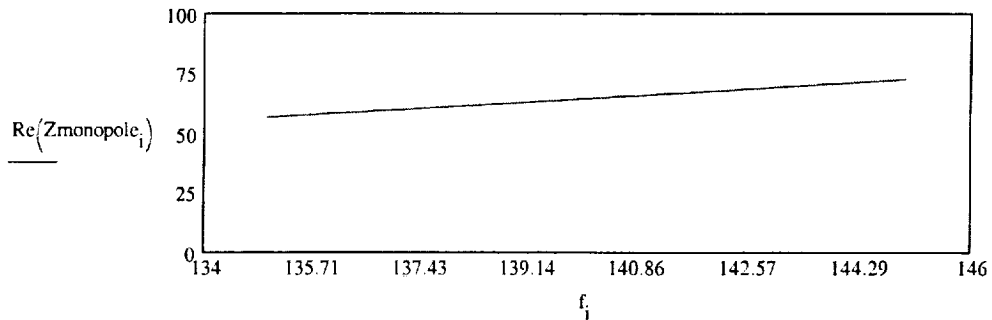
Intermediate variables in impedance calculation.

$$BL_1 := \beta_1 \cdot L \quad Ba_1 := \beta_1 \cdot a$$

Model the monopole as a dipole with an offset, d.

$$wl := \frac{3 \cdot 10^8}{137.5 \cdot 10^6}$$

$$d := \frac{L}{2} - \frac{10}{39.37} \quad Z_{\text{monopole}_1} := \frac{\left(\text{Rr}(BL_1) + R_{\Omega}(\beta_1, L, a, R_s(f_1, \mu_0, \sigma)) \right) + j \cdot \text{Xr}(BL_1, \beta_1, a)}{\left[\sin \left[\frac{2 \cdot \pi}{wl} \cdot \left(\frac{L}{2} - d \right) \right] \right]^2}$$

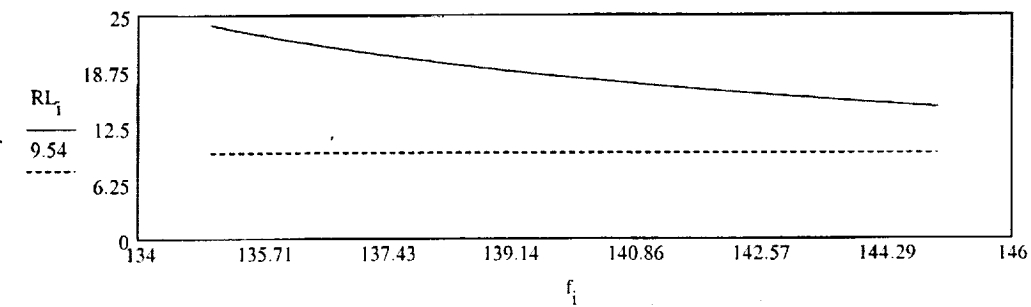
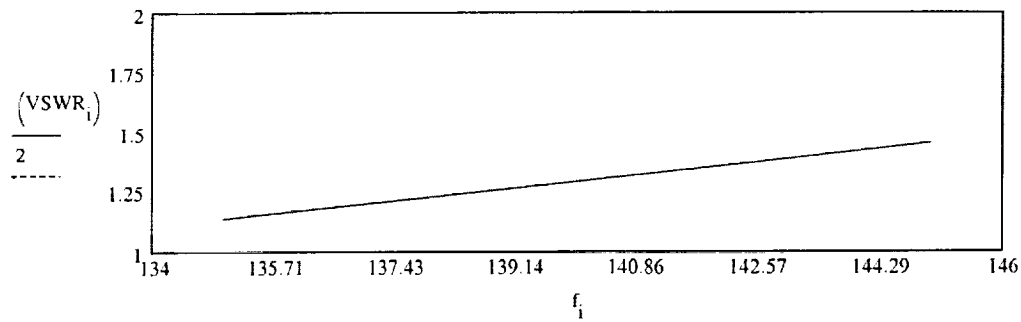
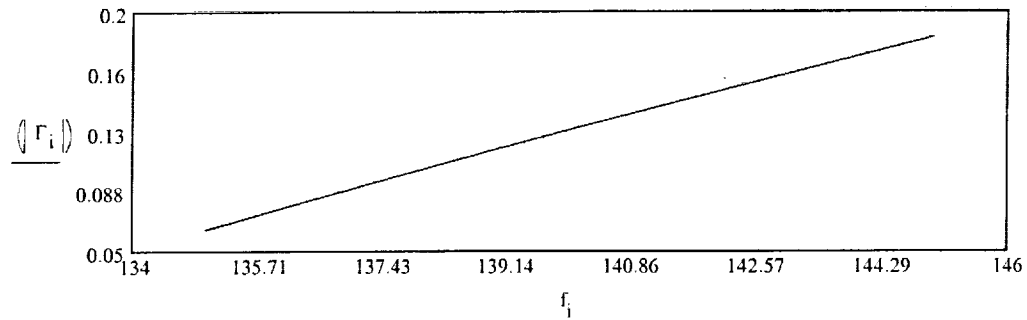


For a 50 ohm system with $Z_0 = 50$, we will determine the reflection coefficient, return loss, and VSWR.

If we can minimize the reactance of the antenna, we can reduce the VSWR.

$$Z_0 := 50 \quad \Gamma_i := \frac{\text{Re}(Z_{\text{monopole}})_i - Z_0}{\text{Re}(Z_{\text{monopole}})_i + Z_0}$$

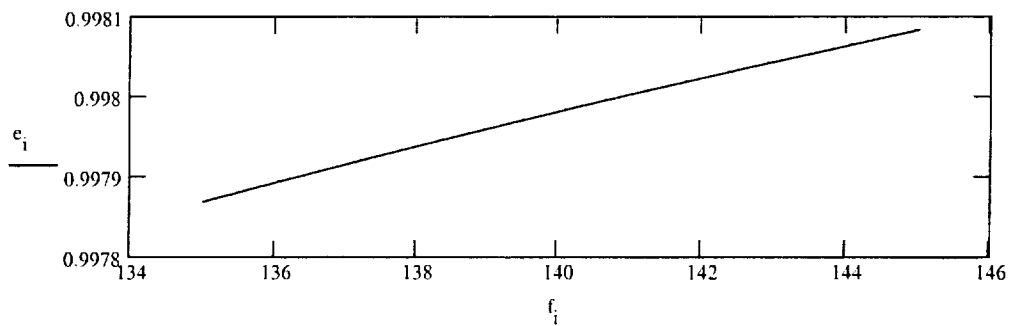
$$\text{RL}_i := -10 \cdot \log \left[\left(|\Gamma_i| \right)^2 \right] \quad \text{VSWR}_i := \frac{1 + |\Gamma_i|}{1 - |\Gamma_i|}$$



We can see that the magnitude of the reflection coefficient is close to one at 137 MHz. This result states that the antenna is not matched to the 50 ohm network. The VSWR and return loss calculations also support the result. These plots are based upon the magnitude of the reflection coefficient. Due to this result, the theoretical model may not be of use to us since we will have a small local ground plane which will change these results.

In order to determine the gain of the antenna, we must solve for the efficiency of the antenna as a function of frequency. The gain calculation will be shown in the program for the field pattern plots.

$$e_i := \frac{\text{Rr}(BL_i)}{\text{Rr}(BL_i) + R_{\Omega}(\beta_i, L, a, R_s(f_i, \mu_o, \sigma))}$$



Three Corner Sat UHF/VHF antennas. Design a VHF monopole antenna that can transmit at 137 and 144.39 MHz and receive at 144.39 MHz. Design a UHF monopole antenna to receive 450 MHz.

Through theoretical derivation, we can analyze the following Electric field. The E-field is in the θ direction. This is an approximation to the E-field.

First, we will start by initializing variables:

For vector and phase notation: $j := \sqrt{-1}$

Permittivity of free space: $\epsilon_0 := 8.854 \cdot 10^{-12}$

Permeability of free space: $\mu_0 := 4 \cdot \pi \cdot 10^{-7}$

Phase constant for a plane wave: $\beta(f) := 2 \cdot \pi \cdot f \cdot \sqrt{\epsilon_0 \cdot \mu_0}$

The derived E-field equation:

$$E(\beta, l, \theta) := \frac{1}{\sin(\theta)} \cdot \left(e^{j \cdot \beta \cdot l \cdot \cos(\theta)} - j \cdot \cos(\theta) \cdot \sin(\beta \cdot l) - \cos(\beta \cdot l) \right)$$

Next, we will define the numbers of points for the evaluation of all equations.

Then

we define the vector θ which has a range from $-\pi/2$ through $\pi/2$.

$N := 100$

$i := 1 .. N$

$$\theta_i := \left[\frac{-\pi}{2} + \pi \cdot \frac{(i - 1)}{(N - 1)} \right]$$

We will start with the design of the VHF antenna. We will define the frequency for the design. After the frequency has been set, we can determine the length of the antenna. We will use a quarter wave monopole.

Frequency : $f1 := 137 \cdot 10^6$

Length of the antenna: $L1 := 3 \cdot \frac{10^8}{f1 \cdot 4}$ $L1 = 0.547$ m

Conversion of meters to inches: $L_inches := L1 \cdot \frac{100}{2.54}$ $L_inches = 21.553$ in

In order to plot the normalized field pattern of the antenna, we must compute the magnitude of the E-field divided by the maximum value of the field.

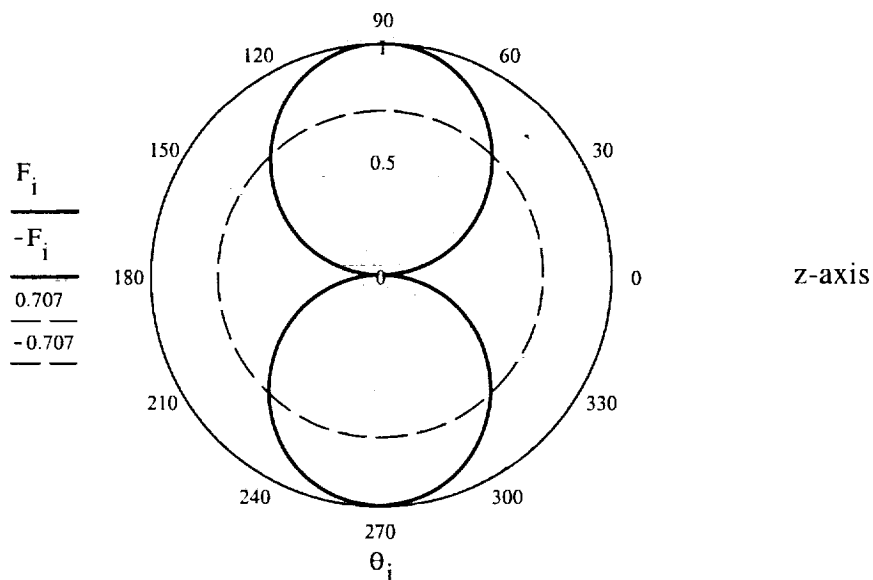
Phase constant: $\beta1 := \beta(f1)$

Magnitude of the E-field: $f\theta_i := |E(\beta1, L1, \theta_i)|$

Maximum value: $max_f := 1$

Normalized field pattern: $F_i := \left(\frac{f\theta_i}{max_f} \right)$

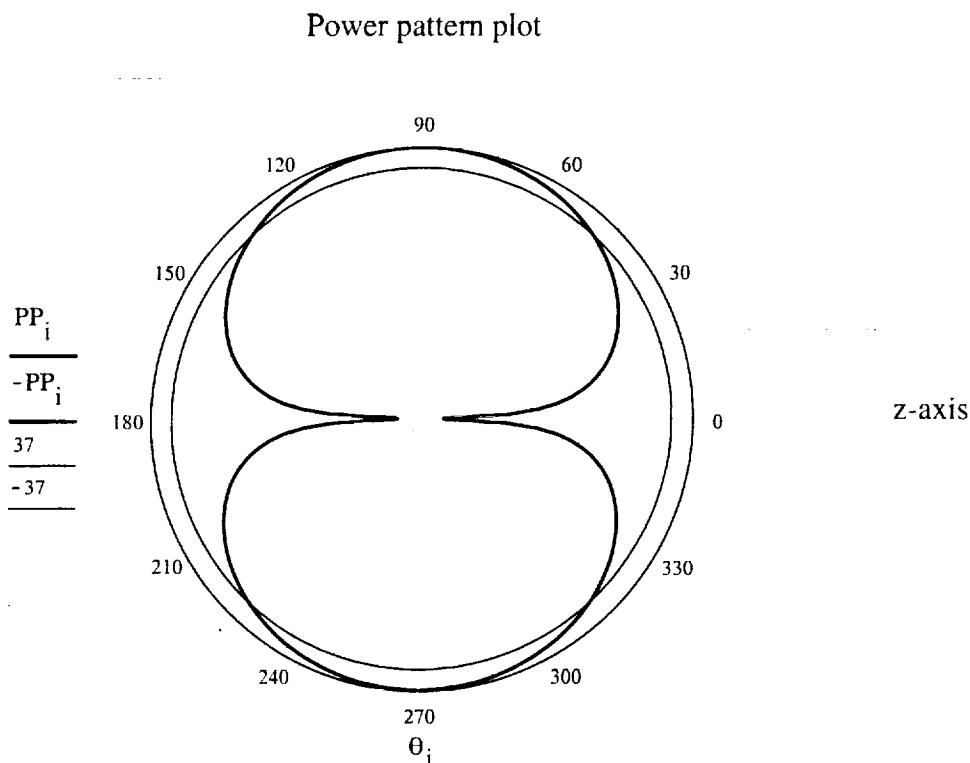
Normalized field pattern plot



The power pattern plot can be computed by determining the log base10 of the magnitude of the normalized field pattern multiplied by 20.

$$P_i := \text{if}(20 \cdot \log(|F_i|) > -40, 20 \cdot \log(|F_i|), -40)$$

$$PP_i := P_i + 40$$



In both plots, we can see that the approximate half power beam width is 87 degrees.

In order to compute the gain of the antenna, we find solve for the beam solid angle of the antenna. Using the beam solid angle, we can determine the directivity of the antenna which is proportional to the gain.

$$\Omega := \int_0^{2 \cdot \pi} \int_0^{\pi} (|E(\beta_1, L_1, \theta)|)^2 \cdot \sin(\theta) \, d\theta \, d\phi$$

The directivity of the antenna is:

$$D := 4 \cdot \frac{\pi}{\Omega} \quad D = 1.539$$

The efficiency of the antenna is approximately 99%.

$$G := 0.99 \cdot D \quad G = 1.524$$

$$G_{\text{dB}} := 10 \cdot \log(G) \quad G_{\text{dB}} = 1.83 \quad \text{dB}$$

We will design the UHF antenna with the same procedure as the VHF antenna. The only difference between the design will be the frequency. We will set the frequency, f_1 , to equal 450 MHz.

$$\text{Frequency :} \quad f_1 := 450 \cdot 10^6$$

$$\text{Length of the antenna:} \quad L_1 := 3 \cdot \frac{10^8}{f_1 \cdot 4} \quad L_1 = 0.167 \quad \text{m}$$

$$\text{Conversion of meters to inches:} \quad L_{\text{inches}} := L_1 \cdot \frac{100}{2.54} \quad L_{\text{inches}} = 6.562 \quad \text{in}$$

In order to plot the normalized field pattern of the antenna, we must compute the magnitude of the E-field divided by the maximum value of the field.

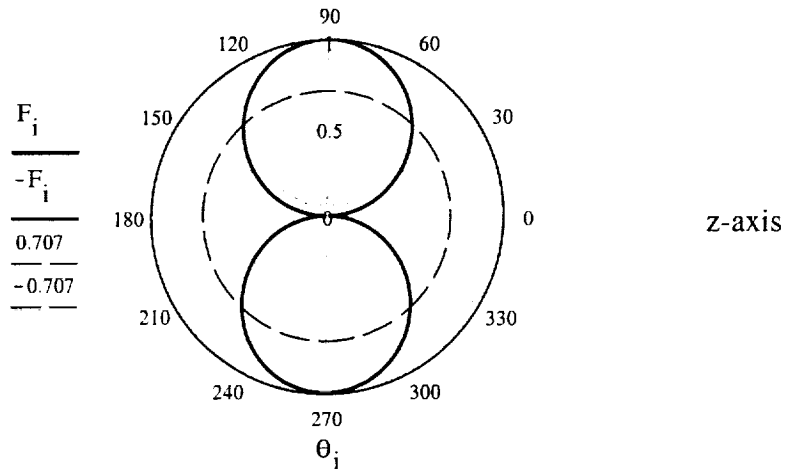
$$\text{Phase constant:} \quad \beta_1 := \beta(f_1)$$

$$\text{Magnitude of the E-field:} \quad f\theta_1 := \left| E(\beta_1, L_1, \theta_1) \right|$$

$$\text{Maximum value:} \quad \text{max}_f := 1$$

$$\text{Normalized field pattern:} \quad F_i := \left(\frac{f\theta_1}{\text{max}_f} \right)$$

Normalized field pattern plot

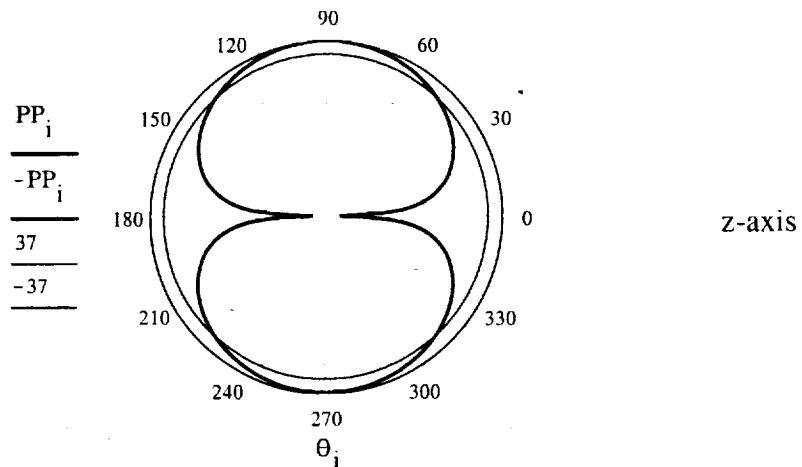


The power pattern plot can be computed by determining the log base10 of the magnitude of the normalized field pattern multiplied by 20.

$$P_i := \text{if}(20 \cdot \log(|F_i|) > -40, 20 \cdot \log(|F_i|), -40)$$

$$PP_i := P_i + 40$$

Power pattern plot



In both plots, we can see that the approximate half power beam width is 87 degrees.

In order to compute the gain of the antenna, we find solve for the beam solid angle of the antenna. Using the beam solid angle, we can determine the directivity of the antenna which is proportional to the gain.

$$\Omega := \int_0^{2 \cdot \pi} \int_0^{\pi} (|E(\beta_1, L_1, \theta)|)^2 \cdot \sin(\theta) \, d\theta \, d\phi$$

The directivity of the antenna is:

$$D := 4 \cdot \frac{\pi}{\Omega} \quad D = 1.539$$

The efficiency of the antenna is approximately 99%.

$$G := 0.99 \cdot D \quad G = 1.524$$

$$G_{\text{dB}} := 10 \cdot \log(G) \quad G_{\text{dB}} = 1.83 \quad \text{dB}$$

We will analyze the VHF antenna for the crosslink frequency. We will set the frequency, f1, to equal 144.39 MHz.

$$\text{Frequency :} \quad f_1 := 137 \cdot 10^6$$

$$\text{Length of the antenna:} \quad L_1 := 3 \cdot \frac{10^8}{f_1 \cdot 4} \quad L_1 = 0.547 \quad \text{m}$$

$$\text{Conversion of meters to inches:} \quad L_{\text{inches}} := L_1 \cdot \frac{100}{2.54} \quad L_{\text{inches}} = 21.553 \quad \text{in}$$

In order to plot the normalized field pattern of the antenna, we must compute the magnitude of the E-field divided by the maximum value of the field.

Crosslink frequency: $f1 := 144.39 \cdot 10^6$

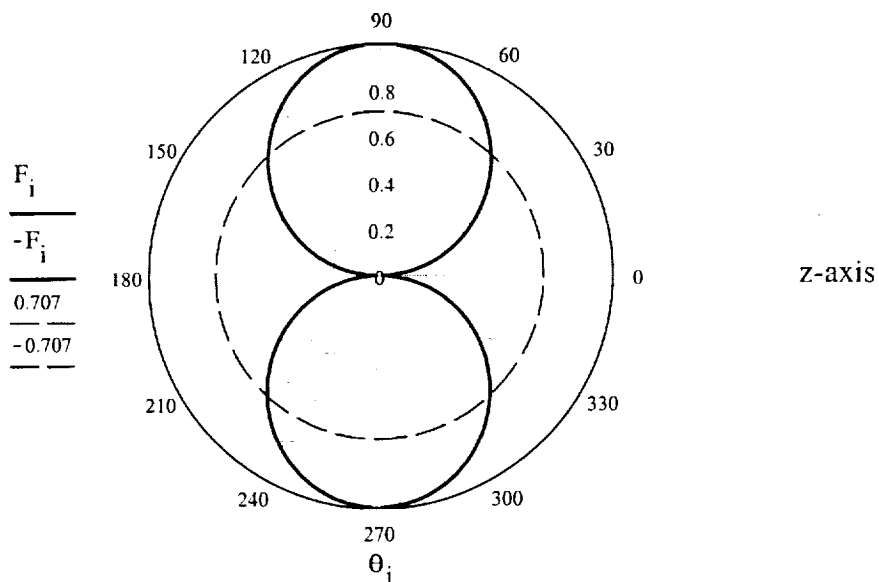
Phase constant: $\beta1 := \beta(f1)$

Magnitude of the E-field: $f\theta_i := |E(\beta1, L1, \theta_i)|$

Maximum value: $\max_f := \max(f\theta)$

Normalized field pattern: $F_i := \left(\frac{f\theta_i}{\max_f} \right)$

Normalized field pattern plot

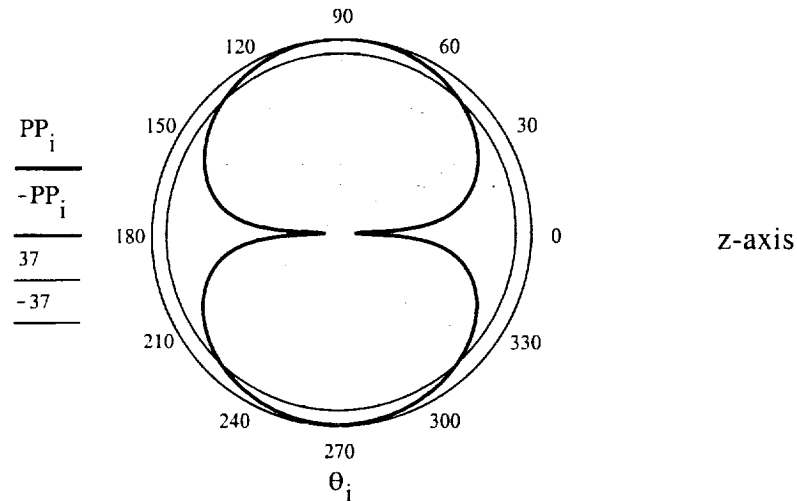


The power pattern plot can be computed by determining the log base 10 of the magnitude of the normalized field pattern multiplied by 20.

$$P_i := \text{if}(20 \cdot \log(|F_i|) > -40, 20 \cdot \log(|F_i|), -40)$$

$$PP_i := P_i + 40$$

Power pattern plot



In both plots, we can see that the approximate half power beam width is 85 degrees.

In order to compute the gain of the antenna, we find solve for the beam solid angle of the antenna. Using the beam solid angle, we can determine the directivity of the antenna which is proportional to the gain.

$$\Omega := \int_0^{2\pi} \int_0^{\pi} \left(\left| \frac{E(\beta_1, L_1, \theta)}{\max_f} \right| \right)^2 \cdot \sin(\theta) \, d\theta \, d\phi$$

The directivity of the antenna is:

$$D := 4 \cdot \frac{\pi}{\Omega} \quad D = 1.547$$

The efficiency of the antenna is approximately 99%.

$$G := 0.99 \cdot D$$

$$G = 1.532$$

$$G_{\text{dB}} := 10 \cdot \log(G)$$

$$G_{\text{dB}} = 1.853 \quad \text{dB}$$

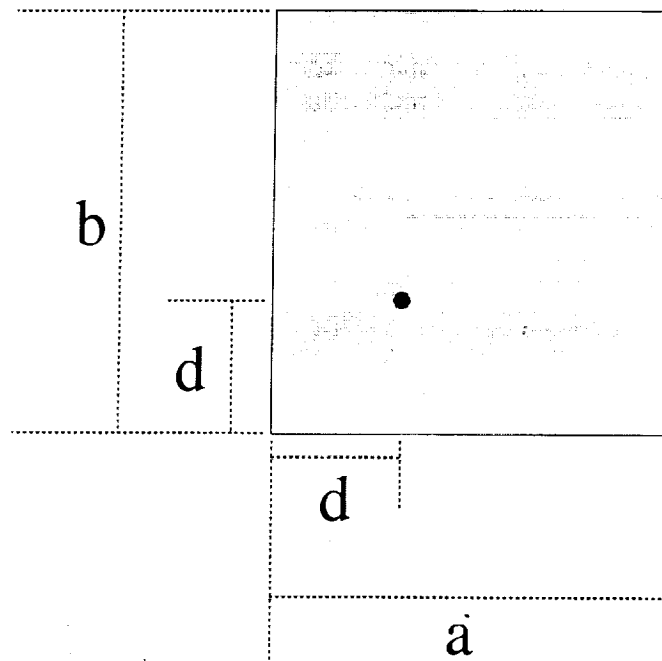


D. S-BAND PATCH ANTENNA DESIGN AND ANALYSIS

TRANSMISSION-LINE MODEL OF CP PATCH ANTENNA 17 Feb 2000

Russell P. Jedlicka, PhD
 Electromagnetics Laboratory
 Klipsch School of Electrical & Computer Engineering
 New Mexico State University
 Las Cruces, New Mexico
 (505) 646-4821

A nominal dimension is chosen for a nearly square patch and then a small amount is added to one side, removed from the other to tune for CP, "equal amplitude" currents in phase quadrature.



Describe the patch geometry and electrical parameters.

$\epsilon_r := 2.45$	Relative dielectric constant		
$dim := 0.0427$	Square Patch dimensions (m)		
$\Delta := 0.016 \cdot dim$	Trim increment		
$a := dim - \Delta$	Length of patch (m)	$a = 0.0420168$	meters
$b := dim + \Delta$	Height of patch (m)	$b = 0.0433832$	meters
$h := .001524$	Substrate thickness (m)		

$d := 0.014$ Feed point inset distance (m). Assume symmetrically displaced from corner.

$t := .00003556$ Conductor thickness

$l_{x1} := d \cdot \left(1 - \frac{\Delta}{\text{dim}}\right)$ Distance from feed point to radiating edge 1 (m)

$l_{x2} := a - l_{x1}$ Distance from feed point to radiating edge 2 (m)

$l_{y1} := d \cdot \left(1 + \frac{\Delta}{\text{dim}}\right)$ Distance from feed point to radiating edge 1 (m)

$l_{y2} := b - l_{y1}$ Distance from feed point to radiating edge 2 (m)

An analysis of the above geometry is performed below. Synthesis of a microstrip patch to operate at a specific frequency can be performed by iteratively using the analysis equations below.

The speed of light in free space (m/s). $c := 3 \cdot 10^8$ $j := \sqrt{-1}$

The relative permittivity and permeability of free space.

$\epsilon_0 := 8.854 \cdot 10^{-12}$ F/m $\mu_0 := 4 \cdot \pi \cdot 10^{-7}$ H/m

The wave impedance in free space. $\eta_0 := \sqrt{\frac{\mu_0}{\epsilon_0}}$ W/square

Analyze the geometry over the range of frequencies:

$f := 2100, 2101 \dots 2300$ MHz $\lambda_0(f) := \frac{c}{f} \cdot 10^{-6}$ meters

Microstrip is an open transmission structure which has an effective dielectric constant (Gupta, et al, 1981). Since a and b are not finalized but will both be close to dim , we will use it to determine the effective dielectric constant. Any changes to a and b will only have a second order effect.

$$Q := (\epsilon_r - 1) \frac{\frac{t}{h}}{4.6 \cdot \sqrt{\frac{\text{dim}}{h}}} \quad F := \left(1 + 10 \cdot \frac{h}{\text{dim}}\right)^{-.5}$$

Effective Dielectric Constant

$$\epsilon_{\text{eff}} := \frac{\epsilon_r + 1}{2} + \frac{\epsilon_r - 1}{2} \cdot F - Q \quad \epsilon_{\text{eff}} = 2.346$$

The corresponding free space and dielectric wavenumbers (phase constant) are:

$$k_0(f) := \frac{2 \cdot \pi}{\lambda_0(f)} \text{ rad/m} \quad k_d(f) := 2 \cdot \pi \cdot \frac{\sqrt{\epsilon_{\text{eff}}}}{\lambda_0(f)} \text{ rad/m}$$

The slot is represented by the admittance of a slot in a ground plane (Harrington, 1961).

$$G_x(f) := \left(\frac{\pi \cdot b}{\lambda_0(f) \cdot \eta_0} \right) \text{ Conductance}$$

$$B_x(f) := G_x(f) \cdot (1 - .636 \cdot \ln(k_0(f) \cdot h)) \text{ Susceptance}$$

Y1 is the admittance of edge 1

$$Y_{x1}(f) := G_x(f) + j \cdot B_x(f)$$

Y2 is the admittance of edge 2

$$Y_{x2}(f) := Y_{x1}(f)$$

$$G_y(f) := \left(\frac{\pi \cdot a}{\lambda_0(f) \cdot \eta_0} \right) \text{ Conductance}$$

$$B_y(f) := G_y(f) \cdot (1 - .636 \cdot \ln(k_0(f) \cdot h)) \text{ Susceptance}$$

Y1 is the admittance of edge 1

$$Y_{y1}(f) := G_y(f) + j \cdot B_y(f)$$

Y2 is the admittance of edge 2

$$Y_{y2}(f) := Y_{y1}(f)$$

Y0 is the approximate admittance of the microstrip line between the two edges (reciprocal of Z0).

$$Y_0 := \frac{\text{dim} \cdot \sqrt{\epsilon_{\text{eff}}}}{h \cdot \eta_0} \quad Y_0 = 0.114 \quad \text{mhos}$$

The x edge 1 admittance is transformed to the feed point

$$Y_{xtrans1}(f) := Y_0 \frac{Y_{x1}(f) + j \cdot Y_0 \cdot \tan(k_d(f) \cdot l_{x1})}{Y_0 + j \cdot Y_{x1}(f) \cdot \tan(k_d(f) \cdot l_{x1})}$$

The x edge 2 admittance is transformed to the feed point

$$Y_{xtrans2}(f) := Y_0 \frac{Y_{x2}(f) + j \cdot Y_0 \cdot \tan(k_d(f) \cdot l_{x2})}{Y_0 + j \cdot Y_{x2}(f) \cdot \tan(k_d(f) \cdot l_{x2})}$$

The y edge 1 admittance is transformed to the feed point

$$Y_{ytrans1}(f) := Y_0 \frac{Y_{y1}(f) + j \cdot Y_0 \cdot \tan(k_d(f) \cdot l_{y1})}{Y_0 + j \cdot Y_{y1}(f) \cdot \tan(k_d(f) \cdot l_{y1})}$$

The y edge 2 admittance is transformed to the feed point

$$Y_{ytrans2}(f) := Y_0 \frac{Y_{y2}(f) + j \cdot Y_0 \cdot \tan(k_d(f) \cdot l_{y2})}{Y_0 + j \cdot Y_{y2}(f) \cdot \tan(k_d(f) \cdot l_{y2})}$$

The total input admittances are calculated

$$\text{Across x dimension} \quad Y_{inputx}(f) := Y_{xtrans1}(f) + Y_{xtrans2}(f)$$

$$\text{Across y dimension} \quad Y_{inputy}(f) := Y_{ytrans1}(f) + Y_{ytrans2}(f)$$

$$Z_{inputx}(f) := \frac{1}{Y_{inputx}(f)} \quad Z_{inputy}(f) := \frac{1}{Y_{inputy}(f)}$$

The total input admittance is the series combination.

$$Z_{input}(f) := Z_{inputx}(f) + Z_{inputy}(f) \quad \frac{j \cdot 376}{\sqrt{\epsilon_r}} \cdot \tan\left(\frac{2 \cdot \pi \cdot h}{\lambda_o(f)}\right)$$

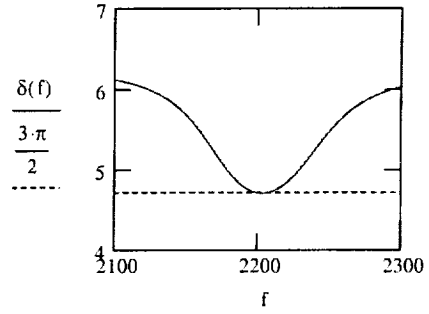
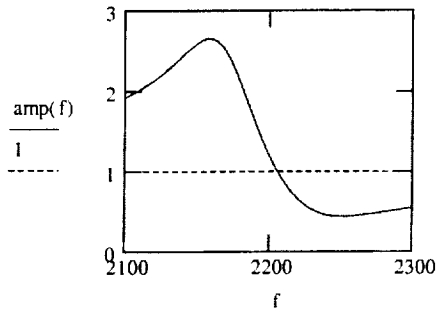
Now determine the amplitude and phase split. First, the amplitude split E_y to E_x .

$$\text{amp}(f) := \left| \frac{Z_{inputy}(f)}{Z_{inputx}(f)} \right|$$

Now the phase of E_y w.r.t. E_x .

$$\delta(f) := \text{angle} \left(\text{Re} \left(\frac{Z_{inputy}(f)}{Z_{inputx}(f)} \right), \text{Im} \left(\frac{Z_{inputy}(f)}{Z_{inputx}(f)} \right) \right)$$

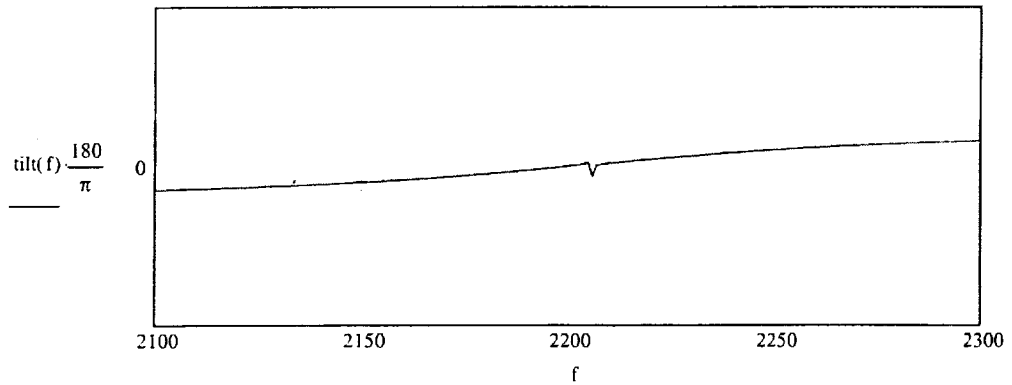
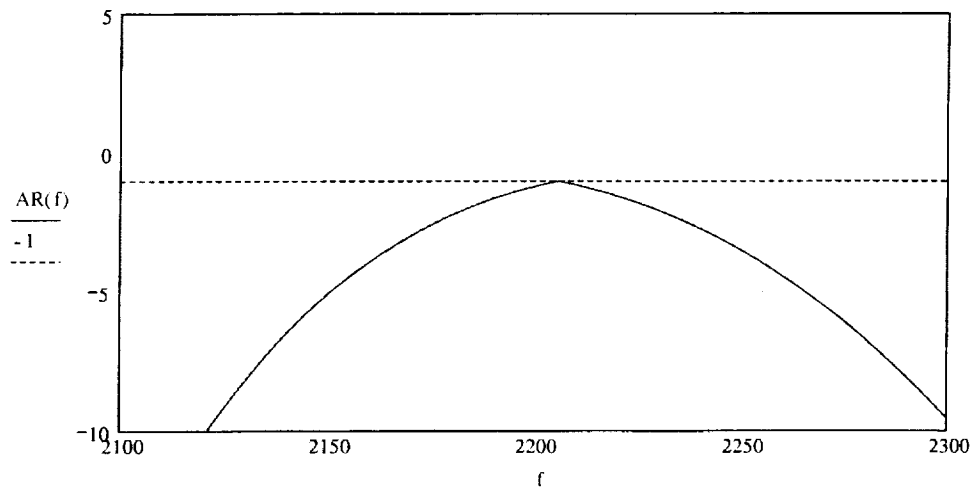
Plot the results.



Now determine the polarization state.

$$\gamma(f) := \text{atan}(\text{amp}(f)) \quad \text{eps}(f) := \frac{1}{2} \cdot \text{asin}(\sin(2 \cdot \gamma(f)) \cdot \sin(\delta(f))) \quad \text{tilt}(f) := \frac{1}{2} \cdot \text{atan}(\tan(2 \cdot \gamma(f)) \cdot \cos(\delta(f)))$$

$$\text{AR}(f) := \cot(\text{eps}(f))$$



The reflection coefficient is now calculated

$$Z_{\text{coax}} := 50 \quad \Omega$$

$$\Gamma_{\text{in}}(f) := \frac{Z_{\text{input}}(f) - Z_{\text{coax}}}{Z_{\text{input}}(f) + Z_{\text{coax}}}$$

The magnitude of the reflection coefficient and VSWR are now calculated

$$M\Gamma(f) := |\Gamma_{\text{in}}(f)| \quad \text{vswr}(f) := \frac{1 + M\Gamma(f)}{1 - M\Gamma(f)}$$

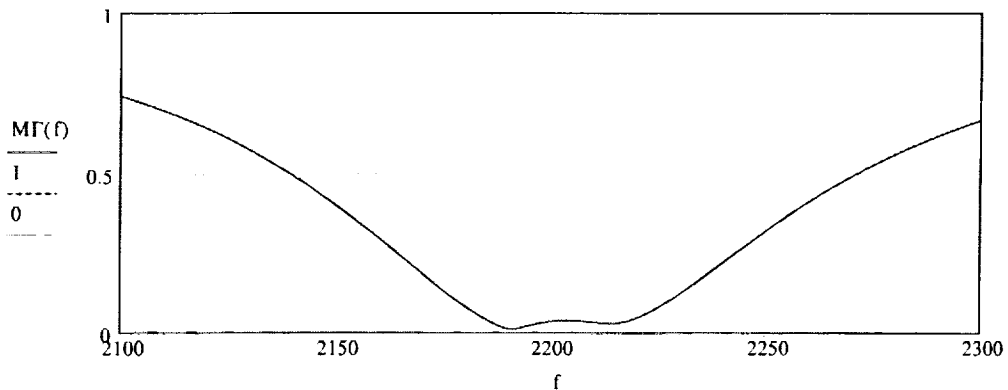
Determine the real and imaginary parts and plot on the complex reflection coefficient plane.

$$M\Re(f) := \text{Re}(\Gamma_{\text{in}}(f)) \quad M\Im(f) := \text{Im}(\Gamma_{\text{in}}(f))$$

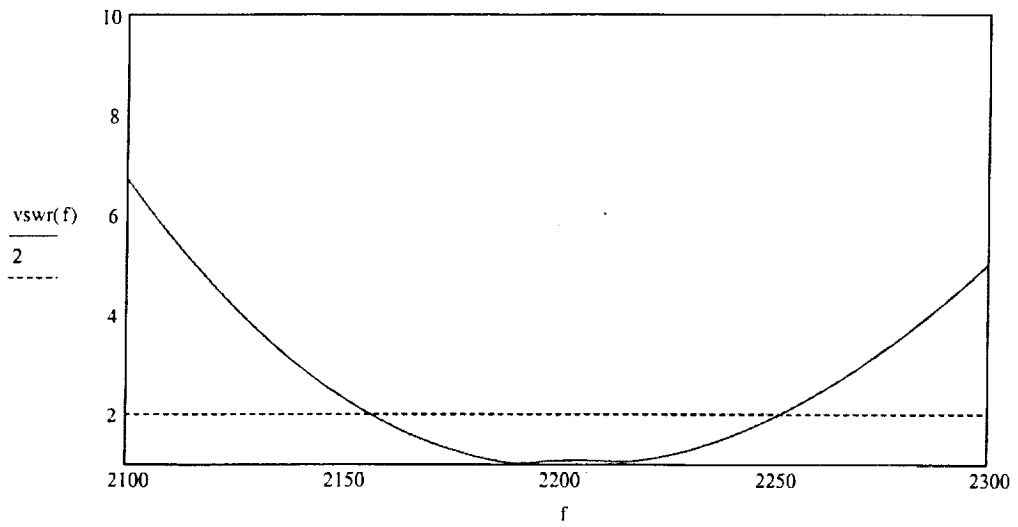
PATCH GEOMETRY AND MATERIAL PROPERTIES

Patch length	b = 0.0434 m	Substrate thickness	h = 1.524 · 10 ⁻³
Patch width	a = 0.042 m	Dielectric constant	ε _r = 2.45
Inset distance (feed point)	d = 0.014 m	Effective ε _r	ε _{eff} = 2.346

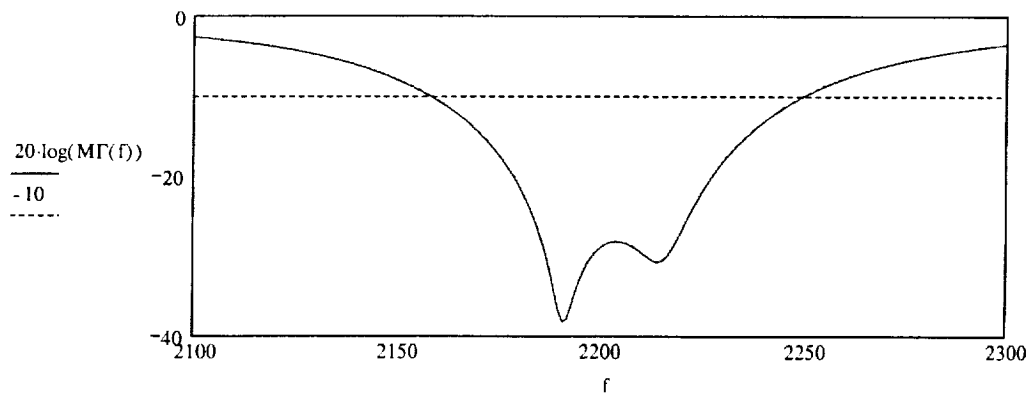
Plot the magnitude of the reflection coefficient.

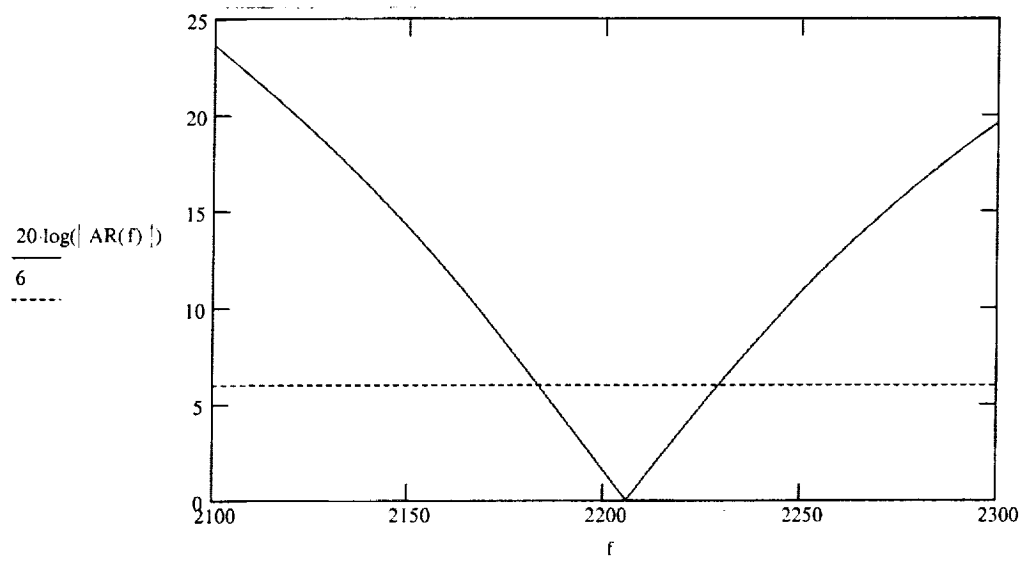


The corresponding VSWR on the coaxial cable is



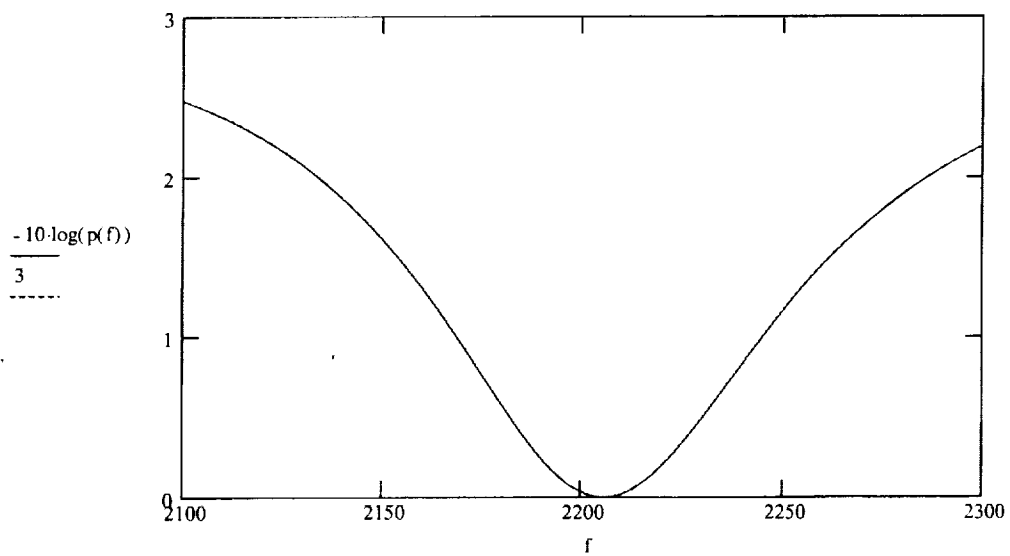
S_{11} (dB), the negative of the Return Loss (dB)





Compute the PML to RHCP

$$p(f) := \left[\cos(\gamma(f)) \cdot \cos\left(\frac{\pi}{4}\right) + \sin(\gamma(f)) \cdot \sin\left(\frac{\pi}{4}\right) \cdot e^{j\left(\frac{-\pi}{2} - \delta(f)\right)} \right]^2$$



The patterns of a circularly-polarized, microstrip patch will be based upon the assumption that the field along each radiating edge is uniform. That is, across the dimension a the field is constant. Furthermore, from the transmission line model we know that the fields at the two edges are about one-half wavelength apart on the microstrip, or parallel-plate, transmission line. This makes the fields in the "equivalent" slots in the same direction. We proceed as follows:

Determine the pattern of a single slot

Compute the array factor for pairs of slots (along x and y)

Compute the pattern of the array of two slots

We obtain the pattern of a slot (dimensions a x h) by the ELECTRIC VECTOR POTENTIAL METHOD. This is simply a two-dimensional Fourier Transform. Assuming uniform fields along the a and h dimensions, we find for a single slot

$$g_{ax}(f_p, \theta, \phi, b, h) := \frac{\sin\left(k_0(f_p) \frac{h}{2} \cdot \sin(\theta) \cdot \cos(\phi)\right) \sin\left(k_0(f_p) \frac{b}{2} \cdot \sin(\theta) \cdot \sin(\phi)\right)}{\left(k_0(f_p) \frac{h}{2} \cdot \sin(\theta) \cdot \cos(\phi)\right) \left(k_0(f_p) \frac{b}{2} \cdot \sin(\theta) \cdot \sin(\phi)\right)}$$

$$g_{ay}(f_p, \theta, \phi, a, h) := \frac{\sin\left(k_0(f_p) \frac{a}{2} \cdot \sin(\theta) \cdot \cos(\phi)\right) \sin\left(k_0(f_p) \frac{h}{2} \cdot \sin(\theta) \cdot \sin(\phi)\right)}{\left(k_0(f_p) \frac{a}{2} \cdot \sin(\theta) \cdot \cos(\phi)\right) \left(k_0(f_p) \frac{h}{2} \cdot \sin(\theta) \cdot \sin(\phi)\right)}$$

$$f_p := 2.200 \cdot 10^3$$

The array factor of the two slots separated by the distance b is given by.

$$F_{\theta}(f_p, \theta, \phi, a, b, h) := \left(\frac{1 + \cos(\theta)}{2} \right) \cdot \left[\cos(\phi) \cdot \left[\left(g_{ax}(f_p, \theta, \phi, b, h) \right) \frac{\sin\left[k_0(f_p) \cdot (a + h) \cdot \sin(\theta) \cdot \cos(\phi) \right]}{2 \cdot \sin\left(k_0(f_p) \frac{a + h}{2} \cdot \sin(\theta) \cdot \cos(\phi) \right)} \right] \dots \right. \\ \left. + \sin(\phi) \cdot \left[\left(g_{ay}(f_p, \theta, \phi, a, h) \right) \frac{\sin\left[k_0(f_p) \cdot (b + h) \cdot \sin(\theta) \cdot \sin(\phi) \right]}{2 \cdot \sin\left(k_0(f_p) \frac{b + h}{2} \cdot \sin(\theta) \cdot \sin(\phi) \right)} \right] \right]$$

$$F_{\phi}(f_p, \theta, \phi, a, b, h) := \left(\frac{1 + \cos(\theta)}{2} \right) \cdot \left[\cos(\phi) \cdot \left[(g_{ay}(f_p, \theta, \phi, a, h)) \cdot \frac{\sin[k_0(f_p) \cdot (b+h) \cdot \sin(\theta) \cdot \sin(\phi)]}{2 \cdot \sin\left(k_0(f_p) \cdot \frac{b+h}{2} \cdot \sin(\theta) \cdot \sin(\phi)\right)} \right] \dots \right. \\ \left. + \sin(\phi) \cdot \left[(g_{ax}(f_p, \theta, \phi, b, h)) \cdot \frac{\sin[k_0(f_p) \cdot (a+h) \cdot \sin(\theta) \cdot \cos(\phi)]}{2 \cdot \sin\left(k_0(f_p) \cdot \frac{a+h}{2} \cdot \sin(\theta) \cdot \cos(\phi)\right)} \right] \right]$$

$$P_{\theta}(f_p, \theta, \phi, a, b, h) := \frac{\left(F_{\theta}(f_p, \theta + 10^{-4}, \phi + 10^{-4}, a, b, h) \right)^2}{\left(F_{\theta}(f_p, 10^{-4}, 10^{-4}, a, b, h) \right)^2 + \left(F_{\phi}(f_p, 10^{-4}, 10^{-4}, a, b, h) \right)^2}$$

$$P_{\phi}(f_p, \theta, \phi, a, b, h) := \frac{\left(F_{\phi}(f_p, \theta + 10^{-4}, \phi + 10^{-4}, a, b, h) \right)^2}{\left(F_{\theta}(f_p, 10^{-4}, 10^{-4}, a, b, h) \right)^2 + \left(F_{\phi}(f_p, 10^{-4}, 10^{-4}, a, b, h) \right)^2}$$

$$\Omega_A := \int_0^{2\pi} \int_0^{\pi} \left[(P_{\theta}(f_p, \theta_c, \phi_c, a, b, h)) + P_{\phi}(f_p, \theta_c, \phi_c, a, b, h) \right] \cdot \sin(\theta_c) d\theta_c d\phi_c$$

$$D := \frac{4 \cdot \pi}{\Omega_A} \quad D = 4.477 \quad 10 \cdot \log(D) = 6.51 \quad \text{dBi} \quad \text{FSG} := 10 \cdot \log(D)$$

Power Pattern

$$P_{\theta\text{dB}}(f_p, \theta, \phi, a, b, h) := \text{if}(P_{\theta}(f_p, \theta, \phi, a, b, h) > 10^{-4}, 10 \cdot \log(P_{\theta}(f_p, \theta, \phi, a, b, h)), -40)$$

$$P_{\phi\text{dB}}(f_p, \theta, \phi, a, b, h) := \text{if}(P_{\phi}(f_p, \theta, \phi, a, b, h) > 10^{-4}, 10 \cdot \log(P_{\phi}(f_p, \theta, \phi, a, b, h)), -40)$$

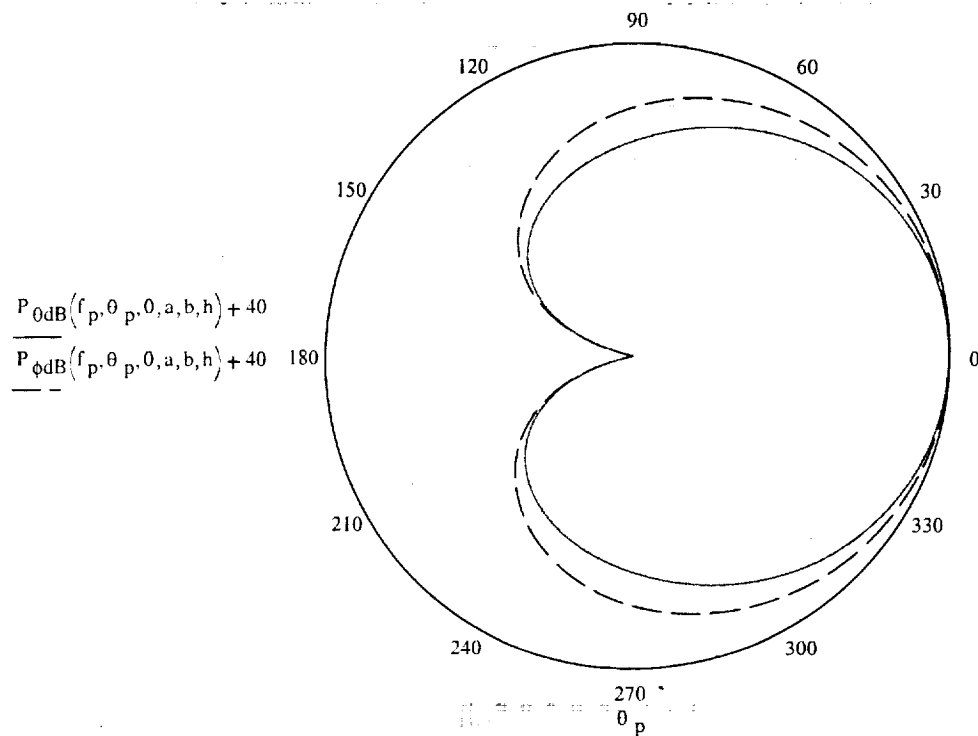
$$P_{\text{totdB}}(f_p, \theta, \phi, a, b, h) := \text{if}\left(\begin{matrix} P_{\theta}(f_p, \theta, \phi, a, b, h) \dots > 10^{-4} \\ + P_{\phi}(f_p, \theta, \phi, a, b, h) \end{matrix} , 10 \cdot \log\left(\begin{matrix} P_{\theta}(f_p, \theta, \phi, a, b, h) \dots \\ + P_{\phi}(f_p, \theta, \phi, a, b, h) \end{matrix} \right), -40 \right)$$

$$N_{\text{pat}} := 181 \quad i := 1..N_{\text{pat}}$$

$$\theta_{\text{plot}_i} := (i - 1) \cdot \left(\frac{2 \cdot \pi}{N_{\text{pat}} - 1} \right) - \pi$$

Polar Log Plot -- F is already normalized to the range 0 to -40 dB, for plotting purposes simply add 40 dB so that the built-in polar plot (non-negative values only) will work.

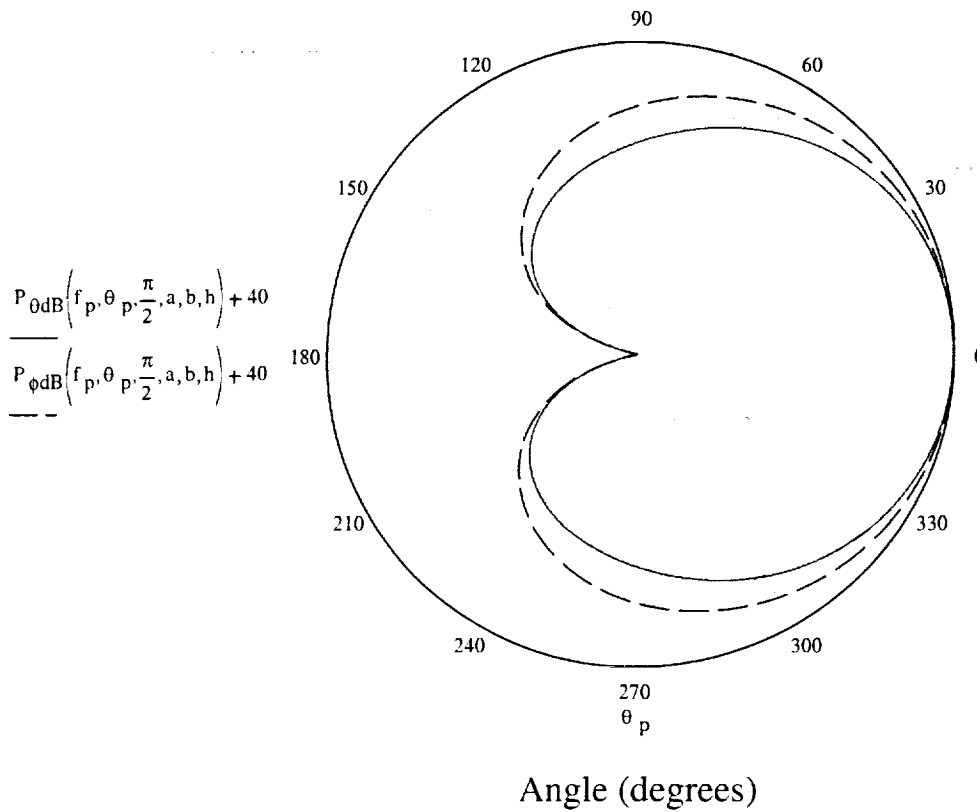
$$\text{dB}_i := 37$$



Angle (degrees)

Full Scale Gain is FSG = 6.5 dB_i

10 dB/division



Full Scale Gain is FSG = 6.5 dB;
10 dB/division

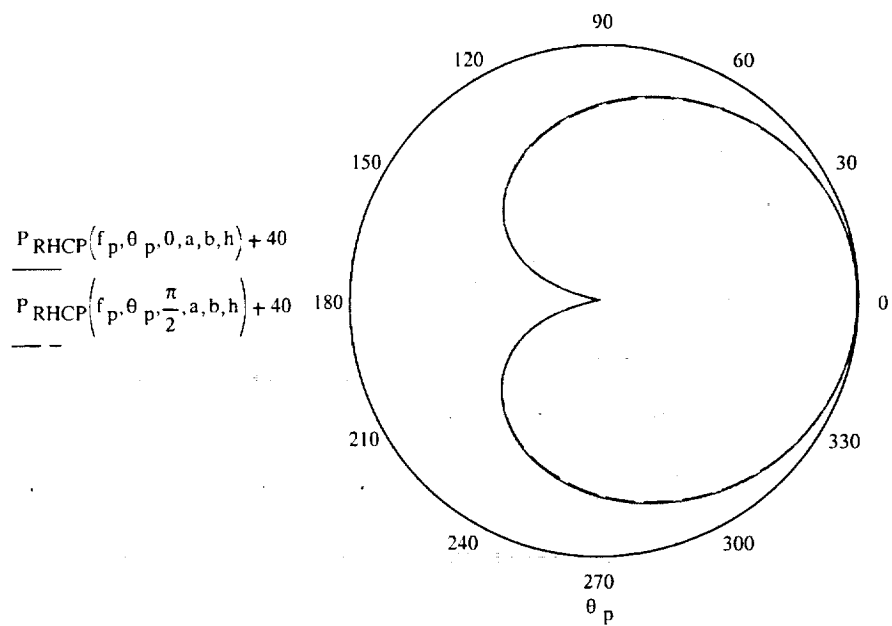
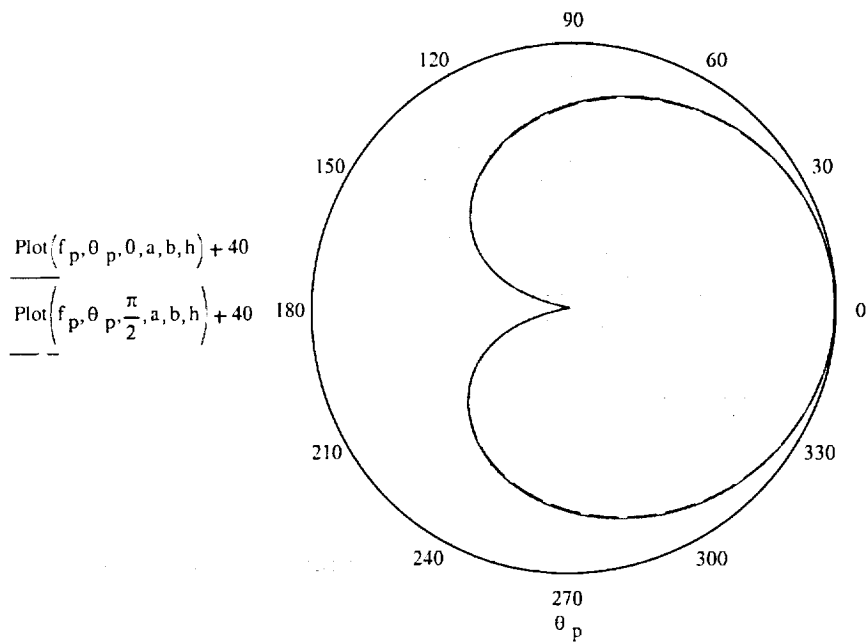
$$\gamma_p(f_p, \theta, \phi, a, b, h) := \text{atan} \left(\frac{\sqrt{P_\phi(f_p, \theta, \phi, a, b, h)}}{\sqrt{P_\theta(f_p, \theta, \phi, a, b, h)}} \right)$$

$$\varepsilon(f_p, \theta, \phi, a, b, h) := \frac{1}{2} \cdot \text{asin} \left(\sin \left(2 \cdot \gamma_p(f_p, \theta, \phi, a, b, h) \right) \cdot \sin \left(\delta(f_p) \right) \right)$$

$$\text{PML}_p(f_p, \theta, \phi, a, b, h) := -20 \cdot \log \left[\cos \left[\frac{-\pi - (2 \cdot \varepsilon(f_p, \theta, \phi, a, b, h))}{2} \right] \right]$$

$$P_{RHCP}(f_p, \theta, \phi, a, b, h) := P_{\text{totdB}}(f_p, \theta, \phi, a, b, h) - PML_p(f_p, \theta, \phi, a, b, h)$$

$$\text{Plot}(f_p, \theta, \phi, a, b, h) := \text{if}(P_{RHCP}(f_p, \theta, \phi, a, b, h) > -40, P_{RHCP}(f_p, \theta, \phi, a, b, h), -40)$$



REFERENCES

- [1] Anderson, B. and Horan, S., "Three Corner Sat Constellation – New Mexico State University: Communications, LEO Telecommunications Services, Intersatellite Communications, and Ground Stations and Network," SSC99-VI-7, 13th Annual AIAA/USU Conference on Small Satellites, August 1999.
- [2] Hansen, E., et al., "Three Corner Sat Constellation – University of Colorado: Commands & Data Handling, Distributed Operations, Stereoscopic Imaging, Science Operations, and Spacecraft Operations," SSC99-IV-1, 13th Annual AIAA/USU Conference on Small Satellites, August 1999.
- [3] Underhill, B., et al., "Three Corner Sat Constellation – Arizona State University: Management; Electrical Power System; Structures, Mechanisms, Thermal, and Radiation; Attitude/Orbit Determination and Control; Micropropulsion Experiment; and Integration," SSC99-III-1, 13th Annual AIAA/USU Conference on Small Satellites, August 1999.
- [4] National Telecommunications and Information Administration, U.S. Department of Commerce, "Manual of Regulations and Procedures for Federal Radio Frequency Management," September 1995.
- [5] Unisys Corporation Defense Systems, "Data Link Basics: The Link Budget," May 1987.
- [6] Kenwood, "TH-D7 Software," CD-ROM, 1999.
- [7] Hilgraeve Inc., "Hyper Terminal," Developed for Microsoft, 1998.
- [8] Kenwood, "TH-D7 In-Depth Manual," CD-ROM, 1999.
- [9] LabVIEW, "LabVIEW User Manual," National Instruments, January 1996.
- [10] Stutzman, W. L. and Thiele G. A., "Antenna Theory and Design," John Wiley & Sons, Inc., 1998.
- [11] Mathsoft, Inc., "MathCad 8 Professional," Mathsoft, Inc. 1998.
- [12] Kenwood, "TH-D7 A/E Service Manual," Kenwood Corporation, 1998.
- [13] MX-COM, Inc., "CMX589A High Speed GMSK Modem," October 1999.
Retrieved March 10, 2000 from the World Wide Web:
http://208.242.41.183/prod_info/pi589A-2.htm

[14] Jedlicka, R. "Transmission-Line Model of CP Patch Antenna," EE 491 Class Notes, New Mexico State University, February 17, 2000.

